

25195402



e #:~



This is to certify that the

dissertation entitled

The Photo-Oxidation Of Organic Substrates
By Use Of The Hexanuclear Molybdenum And
Tungsten(II) Halide Clusters

presented by

Julie Ann Jackson

has been accepted towards fulfillment of the requirements for

Ph.D. degree in Chemistry

Major prote

Date 6 Dec. 1989

MSU is an Affirmative Action/Equal Opportunity Institution

O-12771

PLACE IN RETURN BOX to remove this checkout from your record. TO AVOID FINES return on or before date due.

DATE DUE	DATE DUE	DATE DUE
CCT \$1 2007		

MSU Is An Affirmative Action/Equal Opportunity Institution

THE PHOTO-OXIDATION OF ORGANIC SUBSTRATES BY USE OF THE HEXANUCLEAR MOLYBDENUM AND TUNGSTEN(II) HALIDE CLUSTERS

By

Julie Ann Jackson

A DISSERTATION

Submitted to
Michigan State University
in partial fulfillment of the requirements
for the degree of

DOCTOR OF PHILOSOPHY

Department of Chemistry

1989

ABSTRACT

THE PHOTO-OXIDATION OF ORGANIC SUBSTRATES BY THE USE OF HEXANUCLEAR MOLYBDENUM AND TUNGSTEN(II) HALIDE CLUSTERS

By

Julie Ann Jackson

The photo-oxidation of organic substrates by use of the hexanuclear molybdenum and tungsten(II) halide clusters has been investigated. Indirect and direct oxidation via singlet oxygen and electron transfer pathways, respectively, have been achieved. In regard to the former, trapping experiments, quantum yield measurements, and transient absorption studies have revealed that electronically excited $[\mathrm{M_6X_8}]\mathrm{Y_6}^{2-}$ ions react with oxygen exclusively by energy transfer to produce singlet oxygen. Generation of singlet oxygen by electron transfer between one-electron oxidized cluster and the superoxide ion is efficiently circumvented by the competitive energy transfer process despite the high free energy driving forces associated with the former pathway. That the quenching rates of the $[M_6X_8]Y_6^{2-}$ (M = Mo, W; X = Cl, Br) ions are small and similar $(k_q^{obs} = 8.1)$ (3.7) x 10⁷ M⁻¹ s⁻¹), as determined by Stern-Volmer analysis of emission intensity and lifetime data, is entirely consistent with a highly nonadiabatic exchange resulting from poor overlap of the oxygen acceptor orbitals with the sterically shielded frontier orbitals of the metal core and the facebridging halides.

The M_6X_{12} core has been immobilized on polymers containing pendant nucleophilic groups and the reactions of these clusters as heterogeneous singlet oxygen catalysts have also been studied. The cluster modified polymer (P- M_6X_{12}) retains all of the energy transfer properties of homogeneous $M_6X_{12}^{2-}$ ions, but the rate of quenching of P- M_6X_{12} by oxygen is slower than in solution owing to smaller diffusion coefficients of oxygen in the polymer matrix. The rate of oxygen diffusion can be controlled by adjusting the physical structure of the polymer matrix with choice of solvent and pH. Biexponential lifetime behavior has been exhibited by the polymer bound cluster derivatives (P- M_6X_{12}) in solid and solution environments which can be attributed to binding of the *cis* and *trans* isomers of M_6X_{12} to the nucleophilic sites on the polymer.

The suitability of these clusters for the direct photo-oxidation of organic substrates, alcohols in particular, has been elucidated. The $[M_6X_8]Y_6^{2-*}$ excited state undergoes oxidative quenching with electron accepting molecules to yield $[M_6X_8]Y_6^{-}$, which oxidizes alcohols by direct electron transfer. The mechanism for organic substrate oxidation by $[M_6X_8]Y_6^{-}$ ions has been studied electrochemically. It is most probable that alcohol oxidation occurs by two successive hydrogen atom abstraction reactions. Alcohol oxidation is accompanied by the formation of chlorinated products, resulting from the nucleophilic attack of halide on a carbonium ion produced by reaction of the protons liberated in the hydrogen atom abstraction steps with the alcohol. On the basis of this mechanism, potential photochemical pathways were explored.

In Memory of My Dad, Who Possessed the
Ability to Keep Life in Perspective

ACKNOWLEDGEMENTS

I would like to express my appreciation to the past and present members of the group for their friendship, encouragement, chemical discussions, and occasional harassment. (In what other environment could "bitch" be meant with such warmth and compassion!)

I would like also to thank Dr. Daniel G. Nocera for not allowing my experience in graduate school to be a passive one. Under his guidance, I have definitely learned the difference between "good" and "bad" chemistry.

Finally, my gratitude goes to my family and my husband, Dan, for their steadfast love and support.

TABLE OF CONTENTS

				P	age
LIST	OF TA	BLES	•••••		ix
LIST	OF FI	GURE	s	••••••	xiii
I.	INTR	ODUC	CTION		1
	A.	Overv	view-T	he Nature of Oxidation	1
	B.	The T	Cherma	al Oxidation of Organic Substrates	3
		1.	Auto-	Oxidation	3
			a.	Radical Catalysis of Auto-Oxidation	
				Reactions	3
			b.	Transition Metal Catalysis of	
				Auto-Oxidation Reactions	5
				i. Homolytic Oxidation of	
				Organic Substrates	5
				ii. Heterolytic Oxidation of	
				Organic Substrates	8
		2.	Oxida	ation of Organic Substrates by Metal	
			Comp	olexes Activated by Molecular Oxygen	11
		3.	Direc	t Homolytic Oxidation of Organic	
			Subst	trates by Metal Complexes	18
		4.	Direc	t Oxidation of Organic Substrates by	
			Oxo-I	Metal Reagents	22
		5.	Activ	ation of Organic Substrates by Direct	
			Coord	lination to Transition Metal Complexes	35
	C.	The F	Photo-C	Oxidation of Organic Substrates	37
		1.	Indir	ect Oxidation of Organic Substrates	37
		2.	Direc	t Oxidation of Organic Substrates	49

			P	age
		3.	The Hexanuclear Molybdenum and Tungsten(II)	
			Halide Clusters: Potential Indirect and Direct	
			Photo-Oxidation Catalysts	56
II.	EXP	ERIM	ENTAL	69
	A.	Mate	erials	69
		1.	Preparation of Hexanuclear Molybdenum	
			Clusters	69
		2.	Preparation of Hexanuclear Tungsten Clusters	70
		3.	Preparation of Polymer Bound	
			Cluster Derivatives	7 2
		4.	Preparation of Polymer Bound Rose Bengal	73
		5 .	Singlet Oxygen Trapping and Inhibiting Reagents .	74
		6.	Quenchers	7 5
		7.	Reagents Used in Direct Oxidation Studies	7 5
		8.	Supporting Electrolyte	75
		9.	Solvents	76
	B.	Expe	erimental Methods	76
		1.	Quenching Experiments	76
		2.	Photolysis Experiments	78
			a. Apparatus	78
			b. ¹ O ₂ Photo-Oxidation Studies	78
			c. Direct Photo-Oxidation Studies	82
		3.	Transient Absorption Studies	82
		4.	Electrochemical Methods	83
			a. Cyclic Voltammetry	83
			b. Bulk Electrolysis	84

				rage
III.	INDI	RECI	PHOTO-OXIDATION OF ORGANIC SUBSTRATES	
	BY U	SE O	F SINGLET OXYGEN CHEMISTRY	89
	A.	Back	kground	89
	B.	Hom	nogeneous Reactions	91
		1.	Background	91
		2.	Results	98
		3.	Discussion	114
		4.	Conclusion	137
	C.	Hete	erogeneous Reaction	138
		1.	Background	138
		2.	Results and Discussion	145
		3.	Conclusion	159
IV.	DIRE	CT P	HOTO-OXIDATION OF ORGANIC SUBSTRATES	164
	A.	Back	kground	164
	B.	Resu	ılts and Discussion	166
		1.	Electrochemical Studies	166
		2.	Photochemical Studies	182
	C.	Con	clusion	190
v	REFE	CREN	CES	192

LIST OF TABLES

	ł	'age
1	Electrocatalytic Oxidation of Selected Organic Substrates	
	By Use of Mono-Oxo Ru(IV) Complexes	34
2	Products of the Photoreaction of Polyoxometallates (POM)	
	with Organic Substrates	54
3	Emission, Spectroscopic and Electrochemical Data of the	
	(NBu ₄) ₂ M ₆ X ₁₄ Clusters	65
4	Cluster Lifetime and Oxygen Quenching Rate Constants	99
5	Electronic Origin of Lowest Energy Excited State, Reduction	
	Potentials, and Energy and Electron Transfer Driving Forces	101
6	Effect of DABCO on Oxidation Reactions via $^1\mathrm{O}_2$	104
7	Effect of 2,6-Di-tert-Butyl Phenol (DTBP) on Oxidation	
	Reactions via O ₂ ⁻	105
8	Products of Reaction of 1-Methylcyclohexene 7, and 1,2-	
	Dimethylcyclohexene 8, with Oxygen under Photosensitized	
	and Radical Oxidation Conditions	111

	I	Page
9	Quantum Yields for the [M ₆ X ₈]Y ₆ ²⁻ -Sensitized Photo-Oxidation	
	of 2,3-Diphenyl-p-Dioxene 2 in Acetone	115
10	Energy Transfer Quenching Reactions of Transition Metal	
	Complexes which Exhibit Low Pre-Exponential Factors	134
11	Swelling Properties of Reillex 402 TM (Data Courtesy of Reilly Tar	
	and Coal Company)	144
12	Photo-Oxidation of 2,3-Diphenyl- p -Dioxene 2 with P-Mo $_6\mathrm{Cl}_{12}$	
	in Acetonitrile	146
13	Products of Reaction of 1-Methylcyclohexene 7, and 1,2-	
	Dimethylcyclohexene 8, with Oxygen under Photosensitized	
	and Radical Oxidation Conditions using Polymer Bound	
	Sensitizers	148
14	Solid State Emission Lifetimes of Cluster-Incorporated	
	Polyvinylpyridine Polymers	150
15	Solid State Emission Lifetimes of Cluster-Incorporated	
	Polyvinylpyridine Polymers Synthesized under Different	
	Reaction Conditions	151
16	Solution Emission Lifetimes of Cluster-Incorporated	
	Polyvinylpyridine Polymers in Various Solvents	152

	r	age
17	Solid State Emission Lifetimes of Relevant Cluster Derivatives	153
10		
18	Rate Date for the Quenching of P-Mo ₆ Cl ₁₂ in MeOH by Molecular Oxygen	156
19	pH Studies of the Solution Emission Lifetimes of Cluster-	
	Incorporated Polyvinylpyridine Polymers	158
20	The Photo-Sensitized Oxygenation of 2,3-Diphenyl-p-Dioxene 2,	
	Using P-Mo ₆ Cl ₁₂ in Methanol, Acetone and Toluene	160
21	Electrochemical Data of the $(NBu_4)_2M_4X_{14}$ Clusters in CH_2Cl_2	165
22	Product Characterization for the Oxidation of Benzyl Alcohol by	
	Electrogenerated M ₆ X ₁₄	177
23	Rates for the Oxidation of Alcohols by Transition Metal	
	Complexes	181
24	Quenching Rate Data for Mo ₆ Cl ₁₄ ^{2-*} with Various Electron Transfer Quenchers	183
25	Quenching Rate Data for Mo ₆ Br ₁₄ ^{2-*} and W ₆ C ₁₄ ^{2-*} with Various	10.
	Electron Transfer Quenchers	184

	P	age
26	Photochemical Systems for the Oxidation of Alcohols in	
	CH ₃ CN	188

LIST OF FIGURES

	P	age
1	Oxygenated complexes of transition metals, where M = transition metal	13
		20
2	Peroxymetallation in selective oxidative processes	17
3	The oxidation of olefins by CrO_2Cl_2 at low temperatures	28
4	The hydroxylation of alkanes by use of iron oxo complexes.	
	(After Chang, C. K.; Dolphin, D. in Bioorganic Chemistry;	
	van Talen, E., Ed.; Academic Press: New York, 1978;	
	Vol. 4, pg. 62)	31
5	Potential energy curves for molecular oxygen. (After	
	Hertzberg, G. Molecular Spectra and Molecular Structure.	
	I. Spectra of Diatomic Molecules; 2nd ed., Van Nostrand:	
	New York, 1950)	39
6	Molecular orbital description of the triplet sensitized	
	generation of singlet oxygen. (After Turro, N. J. Modern	
	Molecular Photochemistry; Benjamin/Cummings: Menlo Park,	
	CA, 1978, Chapter 14)	42

	P	age
7	Representations of various intermediates postulated for the	
	mechanism of epoxidation of dienes by singlet oxygen via	
	the 1,2-cycloaddition reaction. (After Bloodworth, A. J.;	
	Eggelte, H. J. in Singlet Oxygen; Frimer, A. A., Ed.;	
	CRC: Boca Raton, FL, 1985; Vol. 2, pg. 100)	48
8	Photochemical pathway for the oxidation of organic	
	substrates by use of $Pt_2(\mu-P_2O_5H_2)_4^{4-}$	52
9	Idealized structure of the $[M_6X_8]Y_6^{2-}$ ions	58
10	Electronic absorption and emission spectra of the	
	tetrabutylammonium salts of $[M_6X_8]Y_6^{2-}$ ions, in acetonitrile	
	at room temperature: (a) () $Mo_6Cl_{14}^{2-}$; (····) $Mo_6Br_{14}^{2-}$;	
	(b) () $W_6Cl_{14}^{2-}$; (····) $W_6Br_{14}^{2-}$; (—) $W_6I_{14}^{2-}$. (From	
	Newsham, M. D. Ph. D. Dissertation, Michigan State	
	University, 1988)	61
11	Molecular orbital diagram of the $[M_6X_8]Y_6^{2-}$ ions	63
12	Modified Latimer diagram of (NBu ₄)Mo ₆ Cl ₁₄ in acetonitrile	
	at room temperature (electrode potentials in V vs. SCE, excited	
	state energy in eV)	67
13	Potential reaction pathways for reaction between excited state	
	sensitizer (S*), organic substrate, and oxygen	95

	Page
14	Pathways for the reaction of ¹ O ₂ with 1-methylcyclohexene 7 107
15	Pathways for the reaction of ${}^{1}O_{2}$ with
	1,2-dimethylcyclohexene 8 109
16	The tetrabutylammonium salt of Mo ₆ Cl ₁₄ ²⁻ -photosensitized
	conversion of 2,3-diphenyl-p-dioxene 2 to ethylene glycol
	dibenzoate 3 in d_6 -acetone as monitored by $^1\mathrm{H}$ nmr spectroscopy
	at various irradiation $\lambda_{exc} \ge 436$ nm)time intervals. Upon
	photosensitized reaction, the 4.4 ppm resonance of the
	methylene protons of 2 are shifted to 4.9 ppm for 3 and the phenyl
	ring proton resonance located at 7.3 ppm in 2 is split and shifted
	downfield in 3. Peaks arising from the tetrabutylammonium cation
	and the solvent lie between 0.9 and 3.5 ppm 113
17	Plot of k_BT ln k_q^{obs} , where ln k_q^{obs} is the logarithm of the
	observed quenching rate constant, vs. the free energy driving
	force, ΔG_{et} , for electron transfer from electronically
	excited $[M_6X_8]Y_6^{2-}$ to oxygen, eq (122). Values of ΔG_{et} are
	given in Table 5. The numbering scheme for different
	clusters is given in Tables 4 and 5

18	Plot of the logarithm of the observed quenching rate constant	
	vs. the free energy driving force, ΔG_{en} , for energy transfer	
	from electronically excited $[M_6X_8]Y_6^{2-}$ to oxygen, eq (121).	
	Values of ΔG_{en} are given in Table 5. The numbering	
	scheme for different clusters is given in Tables 4 and 5	121
19	Free energy dependence of the rate constant for energy	
	transfer, calculated by evaluating eq (132) with	
	$k_d = 1.0 \times 10^{10} M^{-1} s^{-1}, k_{-d} = 1.2 \times 10^{10} M^{-1} s^{-1}, k_{en}^{0} = 9.4 \times 10^7 s^{-1},$	
	T = 298 K, and $\Delta G_{en}^{\dagger}(0)$ values of (a) 0.10 eV, (b) 0.15 eV, and	
	(c) 0.20 eV. The solid line is the theoretical fit to the	
	experimental data (O). The numbering scheme for different	
	clusters is given in Tables 4 and 5	126
20	Transient difference spectra for $W_6I_{14}^{2-}$ in deoxygenated	
	CH ₃ CN (O), W ₆ I ₁₄ ^{2−} /TCNE in deoxygenated CH ₃ CN (□),	
	and $W_6I_{14}^{2-}$ in oxygenated CH_3CN (\triangle), recorded with	
	355-nm excitation. All difference spectra were recorded 50 ns	
	after the excitation pulse. The concentration of $W_6I_{14}^{2-}$ in	
	CH ₃ CN was 8 x 10 ⁻⁴ M and that of TCNE (tetracyanoethylene)	
	was 4×10^{-3} M. Deoxygenated and oxygen saturated solutions	
	were prepared by bubbling with N_2 and O_2 , respectively	131
21	Depiction of the e_g and a_{2g} metal based cluster orbitals	136

Page

	F	age
22	Model depicting $\mathrm{Mo_6Cl_{14}}^{2-}$ electrostatically bound to methylated	
	polyvinylpyridine	142
23	Model depicting Mo ₆ Cl ₁₂ covalently bound to	
	4-polyvinylpyridine (Reillex TM 402)	162
24	Cyclic voltammogram of the $ m Mo_6Cl_{14}^{-/2-}$ couple in $ m C_2H_4Cl_2$	
	(0.1 M NBu ₄ PF ₆ at room temperature)	168
25	Gas chromatogram of the oxidation products of the ${ m Mo_6Cl_{14}}^{2-}/$	
	benzyl alcohol system, where peak (A) is benzaldehyde and	
	peak (B) is benzyl chloride	171
26	Mass spectra of the oxidation products of the ${ m Mo_6Cl_{14}}^{2-}$ /	
	benzyl alcohol system, where (A) is benzaldehyde spectrum	
	and (B) is the benzyl chloride spectrum. ([P] denotes the	
	parent ion peak)	174
27	Proposed photochemical pathway for the oxidation of organic	
	substrates by use of the $M_6X_{14}^{2-}$ clusters	186

CHAPTER I

Introduction

A. Overview-The Nature of Oxidation

The process of oxidation, the gain of oxygen or loss of hydrogen from a molecule, is a fundamental chemical phenomenon. Atmospheric oxygen is the most universally prevalent, as well as economically important oxidizing agent. It's action may be beneficial or deleterious depending on the conditions under which it occurs. Control of oxidation reactions has resulted not only in the inhibition of the oxygenation of organic materials, 1 such as the deterioration of rubber, gasoline, plastics, lubricating oil, natural oils and fats, but also in promoting selective oxidation of petroleum feedstocks to a variety of industrial chemicals. Today, we are in the age of petroleum, with 90% of organic chemicals being derived from crude oil.² Some of the most significant catalytic oxidation processes that have been developed over the years include the Wacker Process³ for acetaldehyde formation, the Amoco process⁴ for production of terephthalic acid, and numerous processes for the epoxidation of olefins. While the majority of these reactions exhibit good selectivity and efficiency, there are some inherent disadvantages to the use of hydrocarbon feedstocks and fuels, including spiralling prices for materials, high energy requirements, and the need to develop cleaner processes in an effort to reduce pollutants. Thus, interest has turned to a wide variety of oxidation methodologies including direct and indirect photo-oxidation processes.

Two different types of photochemical technologies have developed in the field of oxidation chemistry. In photo-assisted catalysis, a reactive intermediate generated photochemically catalyzes a spontaneous (exoergic) oxygen activation reaction. In the second application, photochemical catalysis, a chemical reaction is driven in the nonspontaneous or endoergic direction by using light as a stoichiometric reagent to produce an

excited state, which drives the oxidation reaction. In either of these technologies, the system must absorb light, convert it to chemical energy and in principle catalyze the net reaction. Advantages of photochemical over thermal activation include much milder reaction conditions since light can produce non-Boltzman distributions of the reactants; the generation of unique intermediates that are inaccessible to thermal pathways, and the facile production of catalytic sites in unusual media, at surfaces, or at interfaces.

Although photo-oxidation reactions may proceed via very different mechanisms, the common denominator in all of these reactions is the majority of oxidizing agents are inorganic compounds. The principal reason that transition metal complexes have become an essential ingredient in such a wide range of systems is their versatility in binding substrate, their ability to access a variety of oxidation states, and a diverse coordination geometry.⁷

In an effort to keep this overview of oxidation chemistry to a manageable length, the ensuing discussion will emphasize homogeneous reactions, particularly those catalytic in nature, which result in the incorporation of one or more oxygen atoms into an organic substrate. Topics such as oxidative coupling, isomerization, and polymerization will not be discussed. The mechanisms of these oxidation reactions will be presented in subsequent sections according to the nature of the interaction between the organic substrate and oxidizing agent.

B. The Thermal Oxidation of Organic Substrates

B.1. Auto-Oxidation

B.1.a. Radical Catalysis of Auto-Oxidation Reactions

Auto-oxidation is defined¹ as the direct oxidation of C-H bonds effected by oxygen, or the production of free radicals that are capable of directly combining with free oxygen. These reactions typically proceed via a free radical chain mechanism⁸ as follows:

Initiation:
$$In_2 \longrightarrow 2In^{\bullet}$$
 (1)

$$In^{\bullet} + RH \longrightarrow InH + R^{\bullet}$$
 (2)

Propagation:
$$R \cdot + O_2 \longrightarrow RO_2 \cdot$$
 (3)

$$RO_{2} \cdot + RH \xrightarrow{k_{p}} RO_{2}H + R \cdot \tag{4}$$

Termination:
$$R^{\bullet} + RO_2^{\bullet} \longrightarrow RO_2 R$$
 (5)

$$2RO_2 \cdot \xrightarrow{k_t} RO_4 R \xrightarrow{} Prod. + O_2$$
 (6)

Although initiation by direct reaction of most hydrocarbons with molecular oxygen (i.e. $RH + O_2 \longrightarrow R^{\bullet} + HO_2^{\bullet}$) is kinetically and thermodynamically unfavorable, it has been observed in the auto-oxidation of indene, tetralin, and 4a,4b-dihydrophenanthrenes. Chain initiation can be accomplished most easily by a compound that yields free radicals upon thermal decomposition at typical temperatures between 50 °C and 150 °C. Typical initiators include aliphatic azo compounds, peroxides, dialkyl peroxides, and peroxyesters. Irradiation with UV light may also initiate the auto-oxidation by homolytic cleavage of certain peroxides. 11

The reaction of alkyl radical R• with oxygen in eq (3) is usually diffusion controlled and the rate controlling propagation step at partial pressures above 100 torr of oxygen is principally hydrogen atom transfer from substrate to the alkyl radical (eq (4)). Other reactions such as addition to unsaturated systems, radical displacement and oxygen atom transfer occur, ¹² but to a lesser degree and will not be discussed here. The rate constants for hydrogen transfer from similar compounds can be correlated to the driving force of eq (4). Alkyl peroxy radicals, being resonance stabilized and relatively inactive, are quite selective and preferentially abstract only the most weakly bound hydrogen atoms. Although the R-H bond strength is the dominant factor in determining the rate constant for hydrogen atom abstraction, steric and polar factors also play a significant role. ^{11a,12} Relative rates of attack at primary, secondary and tertiary C-H bonds of 2-methylpentane increase from 1:30:300. ¹³

At reasonable oxygen pressures, eq (5) is negligible and the termination step occurs exclusively by mutual destruction of two alkyl peroxy radicals, eq (6). The mode of tetraoxide decomposition depends upon the structure of the alkyl group. ¹⁴ In general, that the chain termination rate constants increase along the series, tertiary peroxy < secondary peroxy < primary peroxy, reflects the differences in the activation energies for tetraoxide decomposition. Thus, the overall rate of auto-oxidation of a substrate depends on both the rates of chain propagation, k_p , and termination, k_{\downarrow} .

In general, the ease of auto-oxidation is reflected by the resonance stabilization of the initial radicals. Therefore, saturated hydrocarbons are much more resistant to auto-oxidation than olefins. Among hydrocarbons, tertiary C-H bonds are most easily oxidized, while CH₃ groups are the most

difficult to oxidize. Ethers are quite susceptible to auto-oxidation, while aldehydes are more easily attacked than ketones. Aliphatic alcohols are not easily oxidized, and in fact sometimes serve as excellent chain terminators.

B.1.b. Transition Metal Catalysis of Auto-Oxidation Reactions

In principle, a metal catalyst may intervene in eqs (1) - (6). In practice, the key role of transition metal complexes is to enhance or catalyze the decomposition of hydroperoxide and alkyl hydroperoxide intermediates in liquid phase auto-oxidations thereby reducing the induction period. Reactions of peroxides mediated by metal ions can be divided into two types of fundamentally different mechanisms.² The first class involves homolytic one electron processes in which free radicals are intermediates. The second group involves heterolytic, two electron processes in which the function of the metal complex is to increase the electrophilicity of the hydroperoxide.

B.1.b.i. Homolytic Oxidation of Organic Substrates

Homolytic oxidation reactions of organic substrates with metal species proceed by a one equivalent change in oxidation state of the metal and free radicals are generated as intermediates. Subsequent reaction of the free radical with the metal complex can be classified as outer-sphere electron transfer (eq (7)) or inner-sphere ligand transfer (eq (8)) processes. ¹⁵

$$R^{\bullet} + M^{n+} \longrightarrow R^{+} + M^{(n-1)+}$$
 (7)

$$R^{\bullet} + M^{n+}X \longrightarrow RX + M^{(n-1)+}$$
 (8)

Competition between these two pathways depends to a large extent on the nature of ligand X. Hard ligands favor electron transfer, and soft ligands favor ligand transfer. ¹⁶

Whereas a number of metal complexes have been shown to decompose hydrogen peroxide, ¹⁷ the most studied reactions of the metal catalyzed homolytic oxidation of organic substrates involve complexes of copper ¹⁸ and iron. ¹⁹ The best known example is Fenton's reagent, ²⁰ which consists of ferrous salts and hydrogen peroxide. The iron (II) catalyzed decomposition of peroxide proceeds via a free radical chain process involving hydroxyl radicals ²¹ as transient intermediates.

$$Fe(II) + H_2O_2 \longrightarrow Fe(III) + OH^- + HO^{\bullet}$$
 (9)

$$Fe(III) + H2O2 \longrightarrow Fe(II) + HO2 + H+$$
 (10)

$$Fe(II) + HO - Fe(III)OH$$
 (11)

$$Fe(III) + HO_{2} \cdot \longrightarrow Fe(II) + O_{2} + H^{+}$$
 (12)

$$HO^{\bullet} + H_2O_2 \longrightarrow H_2O + HO_2^{\bullet}$$
 (13)

In the presence of organic substrates, the hydroxyl radicals produce free radicals, which can undergo a variety of reactions.

$$RH + HO^{\bullet} \longrightarrow R^{\bullet} + H_{o}O$$
 (14)

$$R^{\bullet} + R^{\bullet} \longrightarrow R_2$$
 (15)

$$R^{\bullet} + Fe(III) \longrightarrow [R^{+}] + Fe(II) \longrightarrow Prod.$$
 (16)

$$R^{\bullet} + Fe(II) \longrightarrow [R^{-}] + Fe(III) \xrightarrow{H_2O} RH$$
 (17)

As evidenced by the rhs of eqs (14) - (17), the use of transition metal catalysts introduces a variety of products. The hydroxyl radical reacts

relatively indiscriminately^{21a} with the organic substrates of eq (14), possibly resulting in the formation of several types of alkyl radicals. Aliphatic esters, ethers, nitriles and carboxylic acid radicals undergo efficient dimerization reactions via eq (15). Radicals which form stable carbenium ions exhibit the reaction shown in eq (16). Thus, these reactions result in low yields of oxidation products, thereby limiting the synthetic utility of this technique. This is especially true for water immiscible substrates, since the production of the hydroxyl radical occurs in the aqueous phase. Most of the interest in this area is a result of the implications of these systems in biological oxidation processes, as well as their use as initiators in polymerization.²²

In auto-oxidation reactions not only peroxides form, but hydroperoxides as well. The elementary steps in homolytic metal catalyzed hydroperoxide decomposition in hydrocarbon solutions occur in a manner similar to that of aqueous peroxide decomposition,

Reduction:
$$RO_2H + M^{(n-1)+} \longrightarrow RO^{\bullet} + M^{n+} + OH^-$$
 (18)

Oxidation:
$$RO_2H + M^{n+} \longrightarrow RO_2^{\bullet} + M^{(n-1)+} + H^+$$
 (19)

The relative rates of eqs (18) and (19) are roughly correlated to the redox potential of the particular $M^{n+}/M^{(n-1)+}$ couple. If a given metal ion is capable of effecting only one of these reactions, then stoichiometric rather than catalytic decomposition of hydroperoxide occurs unless a means of returning the metal ion to its original oxidation state is available.

Since alkyl hydroperoxides are fairly strong oxidants, eq (18) is generally faster than eq (19). When a metal is a strong reducing agent, such as Ti(III), V(II), Fe(II), Cu(I), or Cr(II), decomposition occurs via eq

(18), while with strong oxidants, such as Pb(IV)²³ and Ce(IV)²⁴, eq (19) predominates. When the metal has two oxidation states of comparable stability, eqs (18) and (19) occur concurrently. Rhodium,²⁵ iridium,²⁵ cobalt,²⁶ and manganese²⁷ complexes are able to induce catalytic decomposition of alkylhydroperoxides into alkoxy and alkylperoxy radicals,

$$RO_{9}H + Co(II) \longrightarrow RO + Co(III)OH$$
 (20)

$$RO_2H + Co(III) \longrightarrow RO_2 + Co(II) + H^+$$
 (21)

The oxy radicals may then undergo several subsequent reactions, including hydrogen abstraction or addition to unsaturated substrates.²⁸ Alkyl peroxy radicals may be introduced into olefins, ethers, and alkyl aromatics via the peroxyester reaction.²⁸

Selectivity or multiple product formation is one of the major problems generally encountered in homolytic oxidation reactions. Since catalyst participation in such systems is essentially limited to the hydroperoxide decomposition step, selectivity improvements based on tailoring catalyst are restrictive. Greater success in this direction might be anticipated with metal catalyzed oxidation reactions in which the metal remains closely associated with the substrate or oxidant. Such types of oxidation reactions are not likely to involve free radical intermediates and fall under heterolytic oxidation.

B.1.b.ii. Heterolytic Oxidation of Organic Substrates

Many acidic metal oxides of the early transition metals such as MoO_3 , WO_3 , V_2O_5 , TiO_2 and SeO_2 catalyze reactions of peroxides with organic substrates heterolytically through the formation of inorganic

peracids.²⁴ These reagents closely resemble organic peracids and readily undergo heterolysis at the O-O bond with nucleophiles. Although peroxide is a relatively weak electrophile, substitution of hydrogen by an electron withdrawing oxo metal group renders the peroxidic oxygens more electrophilic. These peracids are all hydroxy hydroperoxides that are formed via a general reaction involving addition of hydrogen peroxide to an M=O group.

$$M=O + H_2O_2 \longrightarrow M OOH$$
 (22)

These reagents are used extensively in the epoxidation of olefins under basic or neutral conditions³⁰ and will also catalyze other reactions that are characteristic of organic peracids, such as the oxidation of tertiary amines to amine oxides and sulfides to sulfoxides.³¹

In heterolytic metal catalyzed oxidation processes, the organic substrate and/or oxygen containing reactant is activated by coordination to the metal center with oxidation changes occuring in two electron steps. Thus free radicals are not involved as intermediates, and the metal remains closely associated with the substrate/reactant during most of the chemical transformations. On the basis of electrophilic properties, H_2O_2 and RO_2H function similarly as epoxidation reagents, but the combination of RO_2H to the metal catalyst is far superior to that of H_2O_2 owing to the presence of water in the H_2O_2 systems, 31 which retards the rate of reaction. Furthermore, water can also have a deleterious effect on selectivity. Metal- RO_2H reagents have greater synthetic utility than the analogous metal- H_2O_2 reagents owing to their solubility in nonpolar solvents such as

hydrocarbons. The production of epoxides by reaction of olefin with alkyl peroxides in the presence of soluble compounds of Mo, V, W, Ti and other metals has been developed into a commercial process for the manufacturing of propylene oxide. The reaction scheme is outlined below for molybdenum catalysis: 34

$$Mo(VI) + RO_2H \longleftrightarrow [Mo(VI)RO_2H]$$
 (23)

$$[Mo(VI)RO_2H] + C=C \xrightarrow{k_e} C-C + Mo(VI) + ROH$$
 (24)

$$Mo(VI) + RO_2H \xrightarrow{k_d} Mo(V) + RO_2 + H^+$$
 (25)

$$Mo(V) + RO_2H \xrightarrow{fast} Mo(VI)OH + RO$$
 (26)

O¹⁸ experiments indicate the presence of an intact alkyl hydroperoxide complex eq (23).³⁵ This is consistent with the observation that polar solvents, particularly alcohols and water, greatly retard the reaction by competing with the hydroperoxide for coordination sites on the metal.^{31,36}

Epoxide selectivity is directly related to k_e/k_d . The rate of homolytic oxidation (k_d) increases with redox potential of the metal, but the rate of heterolysis, k_e , is related to Lewis acidity. Selectivity is maximized by using metals with low oxidation potentials and high Lewis acidity. Thus the following order of activity Mo > W > Ti, V is observed for soluble transition metal catalysts. Selectivity is also influenced by electronic properties of coordinated ligands, however the ligand affect may only be observed in initial stages of oxidation because of the rapid destruction of ligands under

oxidizing conditions. For these reasons, the observed rates of Mo catalyzed epoxidation of olefins are generally independent of added Mo catalyst. ^{31,37} Although several mechanisms ³⁵⁻³⁸ have been proposed for the process of epoxidation in eqs (23) - (26), there is general agreement that due to the high yields of epoxide and the stereo-specificity of the reaction, epoxidation must occur only via a heterolytic mechanism.

In all of the metal catalyzed oxidation reactions considered thus far, the actual oxidizing species is a hydroperoxide. Another possible route involves direct oxygen activation, where the energy of activation for direct reaction with the substrate is lowered by complexation of molecular oxygen.

B.2. Oxidation of Organic Substrates by Metal Complexes Activated by Molecular Oxygen

The use of molecular oxygen as a selective oxidant is severely limited due to its biradical nature. Since dioxygen has a triplet ground state, its direct combination with organic molecules is a spin-forbidden process. Transition metals displaying multiple spin and states of oxidation can readily interact with dioxygen even to the extent of forming isolable oxygen adducts.^{2,38} The metal acts as a reducing agent by adding electrons to the antibonding orbitals of dioxygen, thus increasing the O-O distance and facilitating bond cleavage. Through the ability of the metal to simultaneously bind oxygen and the substrate, favorable entropic conditions are created for selective substrate oxidation.

Figure 1 schematically represents the different oxygenated species, which can form upon interaction of oxygen with reduced transition metal complexes.³⁸ The first step shows the formation of the dioxygen adduct MO₂, which can have either the superoxo structure if the metal is a one

Figure 1

Oxygenated complexes of transition metals, where M = transition metal.

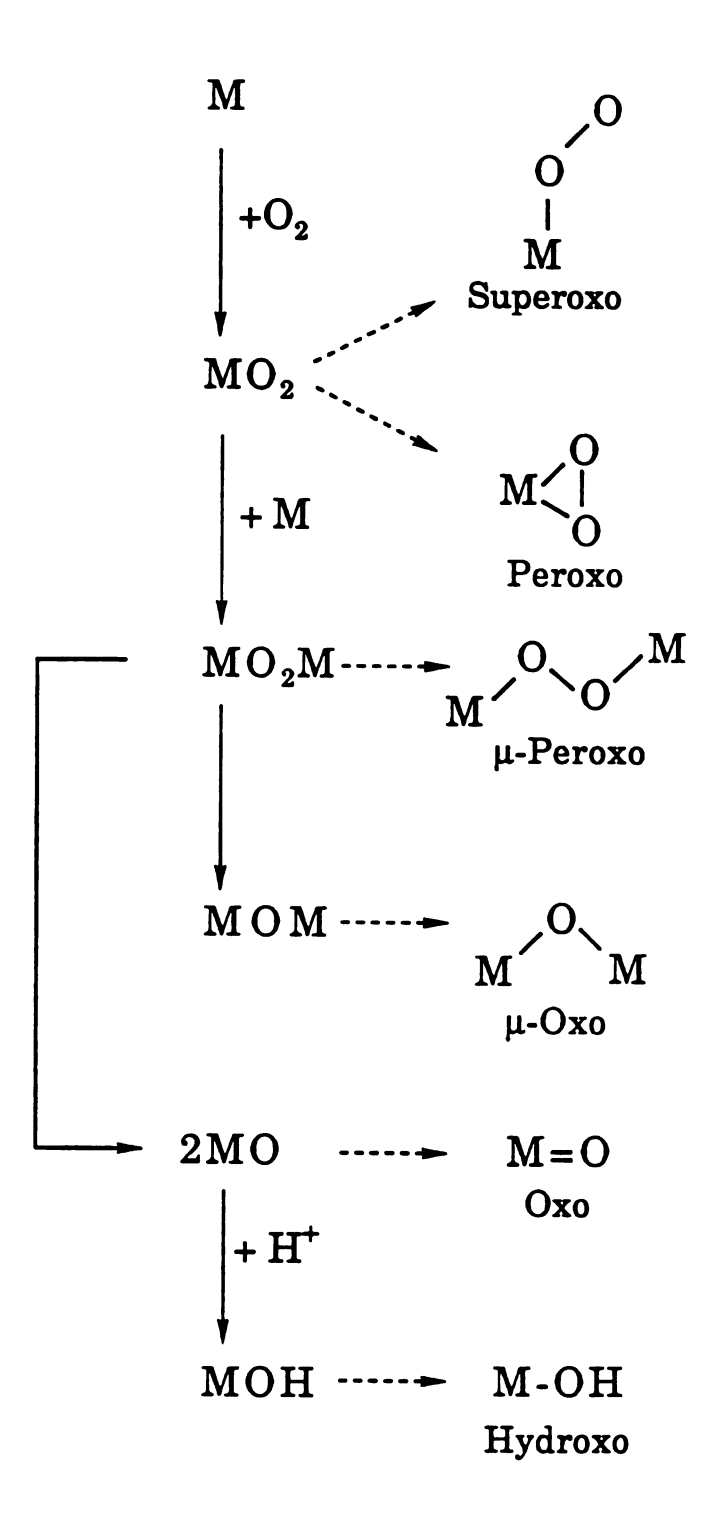


Figure 1

electron donor, or the peroxo structure, if the metal is a two electron donor. These dioxygen adducts may further react with a second metal to produce the μ -peroxo species, with subsequent transformation either by cleavage of the O-O bond into the oxo species M=O, or by loss of one oxygen atom to form the μ -oxo species M-O-M. The hydroxy species M-O-H are obtained upon hydrolysis of the oxo complex. While all six of these compounds are potential oxygen sources for substrates, discussion will be limited to the initial complexes formed upon oxygen activation.

Peroxo complexes, also referred to as side-bonded or π bonded dioxygen complexes are generally diamagnetic and can be obtained by two methods.³⁸ The first method occurs by reaction of hydrogen peroxide with oxo-metal complexes in a higher oxidation state. Typically, the transition metals are from Group IV, V, and VI (eg. Mo(VI) and W(VI)). In this case, dioxygen is already reduced and of peroxidic nature. The electrophilic nature of the peroxo complex arises from the inability of the d⁰ metal to provide electrons.² The second method of obtaining peroxo complexes is the direct interaction of oxygen with reduced two electron donor metal complexes, (usually from Group VIII) which results in nucleophilic peroxo complexes.² Despite the different modes of preparation and differences in the metal environment, the peroxidic nature of these two kinds of complexes is very similar. These compounds have a limited existence in dipolar, protic solvents owing to the rapid displacement of the peroxo ligands by the solvent.

Transfer of coordinated oxygen from these transition metal peroxo complexes to organic substrate occurs by insertion of the substrate, usually an olefin or ketone, into the metal-peroxide bond leading to the formation of a five membered peroxo-metallic adduct.³⁸ The nature of the products.

which result from the decomposition of the peroxometallocycle, depends on the electrophilicity of the metal and the nature of the substrate. In the case of olefins, molybdenum, which is more electrophilic, orients the electron transfer towards the alkyl carbon bond affording epoxide, while rhodium which is much less electrophilic, orients the electron transfer towards the β carbon atom, from which β hydride elimination affords the methyl ketone. These processes are summarized in Figure 2. Epoxidation (eq (27)) can be made catalytic by using excess H_2O_2 to regenerate the peroxo complex. ^{38,39} Catalysts have been used for Baeyer-Villiger oxidation of cyclic ketones to lactones, secondary alcohols to ketones (eq (28))^{2,38} and terminal olefins to methyl ketones (eq (29)). ^{2,38,40}

Whereas the oxidation of organic substrates using transition metal complexes activated by molecular oxygen results in several selective oxidations, the emphasis in this area of oxygen activation lies in the applications of this chemistry to biological systems. Many metalloenzymes responsible for the utilization of molecular oxygen in biological systems, proceed through μ -peroxo and superoxo complexes. These compounds are primarily oxygen adducts containing one or more redox couples from the Cu(I)/Cu(II) (hemocyanin), Fe(II)/Fe(III) (hemoglobin and myoglobin), Mn(II)/Mn(III) (photosynthesis) and Co(II)/Co(III) (Vitamin B₁₂) groups. Although the model systems of these biological reactions may be capable of effecting mild selective oxidations of organic substrates, most studies of these systems are in the context of their relevance to enzymatic oxidation mechanisms.

Peroxymetallation in selective oxidative processes.

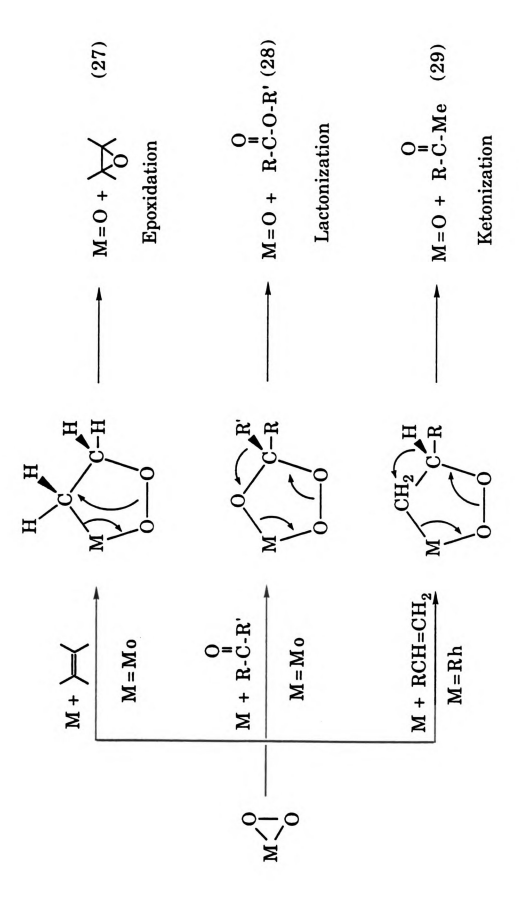


Figure 2

B.3. Direct Homolytic Oxidation of Organic Substrates by

Metal Complexes

The direct interaction of strong metal oxidants with organic substrates can lead to the production of radical intermediates by two distinct pathways: electron transfer and electrophilic substitution. Both processes are depicted below for the reaction of a metal triacetate with a hydrocarbon.

Electron Transfer

$$M(OAc)_3 + RH \longrightarrow RH^{\ddagger} + M(OAc)_3^-$$
 (30)

$$RH^{\ddagger} \longrightarrow R \cdot + H^{+}$$
 (31)

Electrophilic Substitution

$$RH + M(OAc)_3 \longrightarrow RM(OAc)_2 + HOAc$$
 (32)

$$RM(OAc)_2 \longrightarrow R \cdot + M(OAc)_2$$
 (33)

The net result is the one-electron reduction of the metal oxidant with concomitant formation of the substrate radical (R.). The ease of electron transfer oxidation to produce the cation-radical (RH.) is related to the ionization potential of the hydrocarbon. Electrophilic substitution is also expected to parallel the electron transfer pathway and the distinction between these two processes based on structure-reactivity relationships alone is often difficult to make. The two processes are used as the mechanistic basis for the following discussion of redox reactions of various organic substrates with metal complexes.

Terephthalic acid, the product obtained by oxidizing both of the methyl groups of p-xylene is used in the formation of the dimethyl ester to make polyester fiber, which comprises 41.5% of the total synthetic

fiber market.²⁴ Most processes for terephthalic acid production (the Amoco and Mobil processes) involve the use of air or oxygen as the oxidant in the presence of homogeneous cobalt or manganese catalysts.⁴ Generally, the oxidations are carried out in acetic acid using either Co(III) or Mn(III) as the catalyst. Typical operating conditions involve temperatures between 100 °C and 200 °C and pressures in the range of 15 to 30 atm. The first stage of oxidation, p-xylene to p-toluic acid, occurs quite readily in the presence of small amounts of cobalt or manganese salts, with the formation of the diacid necessitating the presence of higher catalyst concentration and/or promoters.

Alkyl aromatic oxidations involving Co(III) catalysts appear to proceed almost exclusively via an electron transfer mechanism.² Most of the experimental data are consistent with the initial formation of a radical cation via electron transfer oxidation of the methyl-aromatic by Co(III), followed by proton loss from the radical cation to give the benzyl radical, which in the presence of oxygen forms the peroxy species. The peroxy radical goes on to give normal oxidation products, as depicted below.^{2,41}

$$ArCH_3 + Co(III) \longrightarrow [ArCH_3]^{\ddagger} + Co(II)$$
 (35)

$$[ArCH3]^{\dagger} \longrightarrow ArCH2 + H^{\dagger}$$
 (36)

$$ArCH_2 \cdot + O_2 \longrightarrow ArCH_2O_2 \cdot \longrightarrow Products$$
 (37)

The cobalt (III) species can be regenerated by a number of methods,

$$ArCH_2O_2 \cdot + Co(II) \longrightarrow ArCHO + Co(III) + OH^-$$
 (38)

$$ArCH_2O_2H + Co(II) \longrightarrow ArCHO + Co(III) + OH^-$$
 (39)

$$ArCH_2O_2 \cdot + ArCH_3 \longrightarrow ArCH_2O_2H + ArCH$$
 (40)

Both of the catalyst regeneration reactions lead to the formation of aromatic aldehydes, which are the primary products of the oxidation of methylbenzenes. The corresponding aromatic acids are produced by subsequent aldehyde oxidation via a peroxy allyl intermediate. The relative rates of oxidation of alkyl benzenes are the reverse of that expected from a classical free radical mechanism. As an example, toluene is oxidized faster than cumene. Similarly, p-ethyltoluene, sec-butyl toluene and 1,1-di-p-tolylethane afford products mainly from oxidation of the methyl groups, which can be accounted for by proton loss from the intermediate cation-radical as governed by stereoelectronic considerations and not by the thermodynamic stability of the radical formed. The loss of any one of the hydrogens on the methyl group is not conformationally restricted owing to the low barrier of rotation.

As mentioned previously, promoters are frequently added to the cobalt catalyzed oxidation of p-xylene. Inorganic or organic bromide has a **Pronounced synergistic** effect on the auto-oxidation of alkyl aromatic hydrocarbons.⁴² The promoting effect of bromide is ascribed to the

formation of bromine atoms via electron transfer oxidation by Co (III). The active catalyst is considered to be acetatobromocobalt(II). The bromine

$$Co(OAc)_2 + NaBr \longrightarrow Co(OAc)Br + NaOAc$$
 (41)

atom is an extremely efficient hydrogen abstractor, which can rapidly form the benzyl radical thus initiating the auto-oxidation sequence shown in eqs (42) - (44),

$$(AcO)Co(III)Br \longrightarrow (AcO)Co(II) + Br \cdot$$
 (42)

$$ArCH_3 + Br \cdot \longrightarrow ArCH_2 \cdot + HBr$$
 (43)

$$ArCH_2 \cdot + O_2 \longrightarrow ArCH_2O_2 \cdot etc.$$
 (44)

The cobalt (III) species is regenerated via either eq (38) or (39) and the concurrently formed hydroxide ion or cobalt hydroxy species can regenerate the bromide ion as follows,

$$Co(III)(OH) + HBr \longrightarrow Co(III)Br + H_2O$$
 (45)

Additives such as methyl ethyl ketone and Zr(IV) and Hf(IV) acetates have also been observed to promote complete oxidation to terephthalic acid.⁴³ In contrast to the situation found with cobalt catalyzed auto-oxidations carried out in the absence of bromide, there is no evidence for the intermediacy of radical cations, and no apparent direct reaction between the Co(II) complex and the hydrocarbon substrate. Conversely, manganic acetate is also capable of oxidizing alkyl aromatic compounds in a direct reaction. However, Mn(III) is a weaker oxidant than Co(III) and an electron transfer mechanism is only observed with aromatic compounds having an

ionization potential of less than 8 eV. With less reactive benzene and toluene, the products result from the reaction of radicals generated from the thermolysis of Mn(III) acetate.

While the oxidation of aromatics and alkanes⁴⁴ are two of the most widely used processes industrially, the direct homolytic oxidation of other types of substrates has been quite successful. The direct oxidation of alkenes by hard metal oxidants (Co(III),⁴⁵ Mn(III)⁴⁶) proceeds by cation-radical intermediates, while use of soft metal oxidants (Pb(IV),⁴⁸ Tl(III),⁴⁸ Hg(II)⁴⁹), occurs by organometallic intermediates or oxymetallation. Depending upon reaction conditions, a variety of products may be formed (aldehydes, ketones, epoxides, glycols, etc.). In the presence of metal catalysts, such as Mn(II), Co(II), and Fe(II), linear aldehydes are easily converted to linear carboxylic acids.⁵⁰ The oxidation of primary and secondary alcohols produces carbonyl compounds with cobalt and manganese salts, but not as readily as olefins or aldehydes due to the homolytic cleavage of metal alkoxides.⁵¹

B.4. Direct Oxidation of Organic Substrates by Oxo-Metal Reagents

The oxidation of organic substrates by oxometal (M=O) reagents such as permanganate, 52 chromic acid and chromyl compounds, 53 SeO₂, 54 OsO₄, 55 RuO₄ 56 and MnO₂ 57 are well known to chemists. These reagents have played an important role in organic reactions owing to their capacity for selective oxygen transfer to a wide variety of substrates under mild conditions. These reactions are shown below where L = trialkylphosphine, trialkylamine, or dialkylsulfide.

Similarly, dioxo-metal reagents can also promote oxidative transformations.

$$O = M^{n+} - C = C$$

$$O = M^{n+} - C = C$$

$$O = M^{n+} - C = C$$

$$O = M^{(n-4)+} + C = C$$

$$O = M^{(n-4)+} + C = C$$

$$O = M^{(n-2)+} + C = C + C = C$$

$$O = M^{(n-2)+} + C = C + C =$$

As shown in eq (46) - (52), oxo-metal reagents are capable of oxidatively transforming a variety of substrates. The essential mechanistic feature that is common to all of these reactions is the participation of one or more M=O groups.

The O=Mⁿ⁺ functional groups constitute one example of a general class of high valent XMⁿ⁺ species comprised of various metal vlides, shown below, which are capable of transferring the group X to various substrates,

$$O=M^{n+}$$
 $RN=M^{n+}$ $(R)_2C=M^{n+}$ $(Cl)_2M^{n+}$

especially olefins. The mechanisms by which such transformations occur are subject to the same ambiguities as those in the previous section. Thus, electron transfer processes involving radical intermediates, as well as electrophilic mechanisms involving organometallic intermediates, as exemplified by the oxidation of hydrocarbons are possible.

Electron Transfer

O

$$\parallel$$

 $HO-M^{n+} + R \cdot O=M^{(n-2)+} + ROH$ (54)

Electrophilic Substitution⁵⁸

$$HO - M^{(n-2)+} - O = M^{(n-2)+} + ROH$$
 (56)

The interaction of olefins with oxo-metal reagents can involve reaction either at the double bond or the allylic C-H bond. In general, it appears that allylic oxidation stems from moderately strong oxidants (electrophiles) such as Se(IV) and Mo(V). For example, SeO₂ is the most commonly used reagent for the allylic oxidation of olefins.⁵⁴ The mechanism involves an initial ene addition of Se=O to produce an organoselenium intermediate⁵⁹ followed by oxidative elimination to carbonyl compounds or hydrolysis to alcohols as shown below.

Attack at the carbon-carbon double bond is typical of strong oxidants (electrophiles), such as osmium and ruthenium tetraoxides, permanganate, and chromium (VI). The first three reagents are considered to effect oxidation by way of cyclic esters which are hydrolyzed to glycols or undergo C-C bond cleavage to carbonyl.

Alternatively, the interaction of olefins with chromyl compounds [Cr(VI)O₂X₂] is notorious for producing complex mixtures of products. Oxidation of olefins at low temperatures with $\text{CrO}_2\text{Cl}_2^{58,60}$ yields the three primary products; epoxide, chlorohydrin, and vicinal dichloride, which arise from cis addition processes. 58 These results can be explained with the scheme in Figure 3 involving attack of the substrate at the chromium center to produce an organometallic intermediate. The decomposition of the initially formed π complex by Pathways A and B leads to alkyl chromium(VI) intermediates upon insertion of the olefin into a O=Cr(VI) or Cl-Cr (VI) group, respectively. The intermediate metallocycle can decompose to give the epoxide (pathway C) or a Cr(IV) complex (pathway D), which constitutes reductive elimination of carbon and chlorine ligands. Similarly, Pathway F also involves reductive elimination to form vicinal dichlorides. Pathway E represents a carbon to oxygen migration of the metal with concomitant two electron reduction of the metal. The literature now abounds with examples of stable high-valent organometallic derivatives of Cr, 61 Nb, 62 Ta, 62 W, 63 and Re. 64 The concept of [2+2]

The oxidation of olefins by ${\rm CrO_2Cl_2}$ at low temperatures.

Figure 3

addition to oxo-metal functions can be extended to the reactions of other useful reagents such as OsO_4^{65} with olefins.

In addition to the simple oxides, heme containing oxygenases typified by the cytochrome c P-450 enzymes catalyze the hydroxylation and epoxidation of a wide variety of organic substrates in biological systems by reactions that are very similar to stoichiometric oxidation with oxometal reagents such as the chromyl compounds. 66 In these enzymatic systems, oxo-iron(V) species are the active oxidants formed by the reductive activation of dioxygen. 67 Two electrons are supplied by the cofactor and the overall stoichiometry of oxygen activation is consistent with steps B - D in the catalytyic cycle in Figure 4, which illustrates the hydroxylation of an alcohol. Support for the intermediacy of oxo-iron(V) is derived from the observations that the combination of molecular oxygen and hydrogen donor can be replaced in vivo by a variey of single oxygen donors such as hydroperoxides and peroxyacids.⁶⁸ The oxidation of alkanes and olefins have been studied using model metal porphyrin catalysts (biomimetic oxidations). Active oxidants have been generated by two-electron oxidation of the porphyrin complexes of Cr(III).⁶⁹ Mn(III)⁷⁰ and Fe(III).⁷¹ Both homolytic and heterolytic pathways have been observed in reaction systems with C-H bonds and π systems. ^{70a,b}

The oxidation of hydrocarbons with oxo-metal reagents often presents problems such as the insolubility of the substrate in water and the difficulty of finding a solvent that is not attacked by the oxidant. These reactions are often characterized by low yields and/or requirements for significantly greater than stoichiometric amounts of oxidant. Recently, phase transfer catalysis techniques have been used increasingly to effect solubilization⁷² of these oxidants in relatively nonpolar solvents such as benzene, methylene

The hydroxylation of alkanes by use of iron oxo complexes. (After Chang, C. K.; Dolphin, D. in *Bioorganic Chemistry*; van Talen, E., Ed.; Academic Press: New York, 1978; Vol.4, pg. 62).

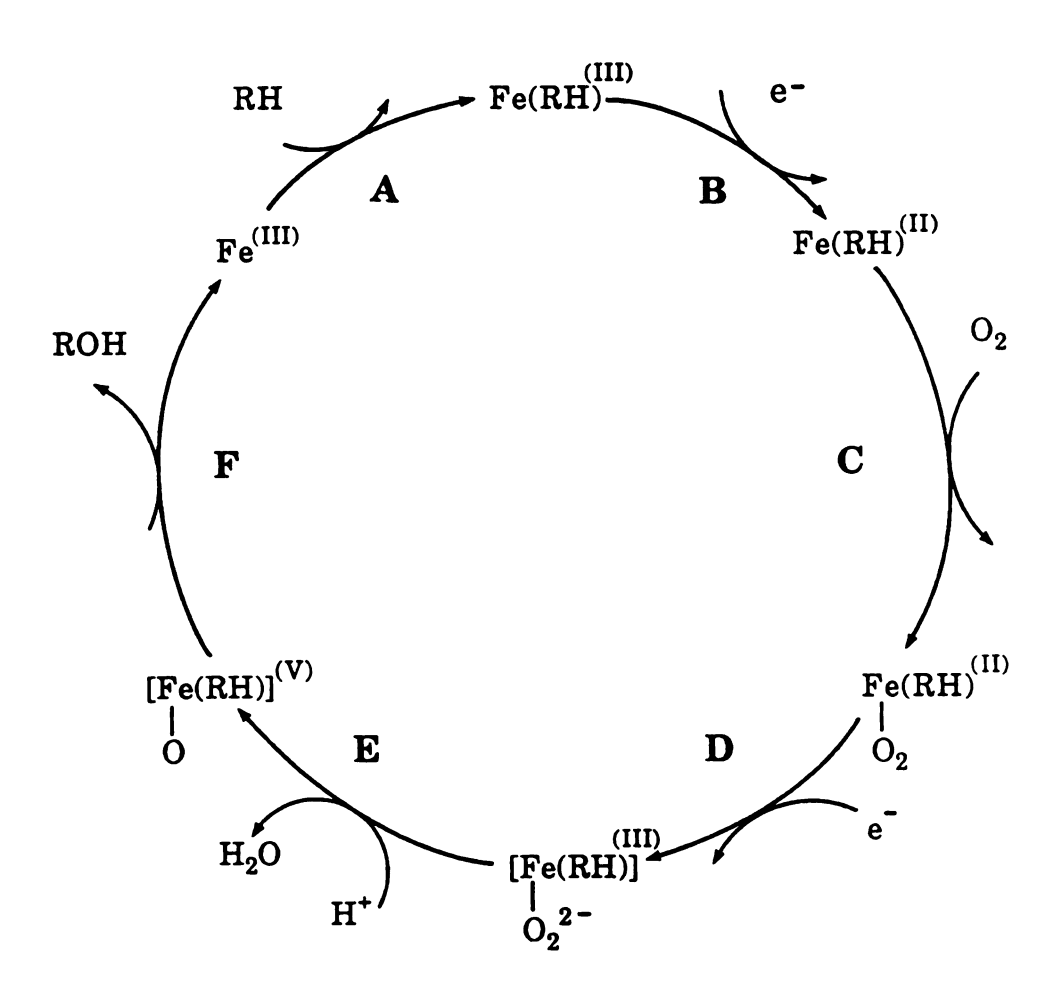


Figure 4

chloride and chloroform. This technique has achieved considerable success in promoting selective oxidations of a variety of organic substrates under mild conditions. Both stoichiometric and catalytic amounts of phase transfer reagents, such as tetraalkyl phosphonium and tetraalkyl ammonium salts and crown ethers have been used to promote the solubilization of a variety of oxo-metal anion reagents such as KMnO₄,⁷³ K₂Cr₂O₇,⁷⁴ and K₂CrO₄.⁷⁵ In the presence of phase transfer agents, the oxo-metal anion is transported into the organic phase as the tetraalkyl ammonium or phosphonium salt or as the crown ether complex.

An alternative approach to these stoichiometric oxidations is the electrochemical generation of the metal oxidant.⁷⁶ The similarity between the chemical oxidation of alkenes, arenes, and alkanes (in general) by electron transfer oxidants and electrochemical oxidations of the same substrates is noteworthy, since the anodic processes are known to involve successive one electron transfers and cation-radicals as intermediates.⁷⁷

This alternative involves the use of a surface attached catalyst where the redox chemistry occurs at the catalyst and the role of the electrode is to provide a source of oxidizing or reducing equivalents at a controlled potential. There is an extensive and growing coordination chemistry of the higher oxidation states of ruthenium and osmium based on metal-oxo formation. Included in this chemistry is a series of polypyridyl complexes of ruthenium and osmium, which have proven to be versatile catalytic oxidants toward a variety of inorganic and organic substrates. The polypyridyl complexes are coordinatively well defined and chemically stable. It is on the basis of their coordinative stability that these compounds can be made catalytic by oxidative regeneration of Ru(IV)=O intermediates

according to the following electron transfer scheme where py = pyridine and bpy = bipyridine.

$$[(bpy)_{2}(py)Ru(II)(OH_{2})]^{2+} \xrightarrow{-e^{-}} [(bpy)_{2}(py)Ru(III)(HO)]^{2+}$$

$$\xrightarrow{-e^{-}} [(bpy)_{2}(py)Ru(IV)=O]^{2+}$$
(63)

As shown in Table 1, $[(bpy)_2(py)Ru(IV)(O)]^{2+}$ is capable of oxidizing a variety of substrates. The key to these oxidations is the loss of protons upon oxidation and stabilization of the higher oxidation states by electron donation from bound hydroxo or oxo ligands. Mechanistic studies suggest that the Ru=O compounds promote oxidations along different pathways including O-atom transfer, H-atom transfer, and hydride transfer. These electrocatalytic oxidations can be carried out under mild conditions, compared to other oxidants, and exhibit good selectivity (Table 1) particularly for aromatic substrates containing multiple functional groups.

The direct interaction of organic substrates with high-valent metal complexes and oxo reagents plays a key role in the oxidations presented in Sections 3 and 4. These metal oxidants are generally strong electrophiles, which react with organic substrates via electrophilic attack or one electron transfer. In the next section, another group of oxidative processes will be discussed which involve metal complexes containing "soft" metals such as Pd(II) in low oxidation states and hence not particularly strong electrophiles.

Table 1

Electrocatalytic Oxidation of Selected Organic Substrates

By Use of Mono-Oxo Ru(IV) Complexes

Catalyst System	Substrate	Products	Mochanism	Ref
$[(bpy)_2(py)Ru(II)(OH_2)]^{2+/}$	Dimethyl Sulfide	DMSO	O - Atom Transfer	20
$[(\mathrm{bpy})_2(\mathrm{py})\mathrm{Ru}(\mathrm{IV})(\mathrm{O})]^{2+\;\mathbf{a}}$	Phenol	Quinone	O - Atom Transfer	83
ı	Styrene	Styrene Oxide	O - Atom Transfer	81
	trans-Stilbene	trans-StilbeneOxide	O - Atom Transfer	81
	Formate Ion	CO	Hydride Transfer	83
	Formic Acid	CO	Hydride Transfer	83
	$ m H_2O_2$	0	H - Atom Transfer	88
	PPh_3	$OPPh_3$	O - Atom Transfer	88
$[(trpy)(bpy)Ru(II)(OH_2)]^{2+}$	2-Propanol	Acetone	Hydride Transfer	22
$[(trpy)(bpy)Ru(IV)(O)]^{2+b}$	Acetaldehyde	Acetate Ion	Hydride Transfer	84
	4-Methyl Benzoate Ion	Terephthalate Ion	Hydride Transfer	8 8
	Toluene	Benzoate Ion	Hydride Transfer	84
	Crotonic Acid	Fumarate Ion	Hydride Transfer	84
	p-Xylene	Terephthalate Dianion	Hydride Transfer	84
	p-Phthlate	Terephthalate Ion	Hydride Transfer	87
a hny = hinyridina b trny =	. 9 9' 9" ternamidine			

bpy = bipyridine. " trpy = 2, 2', 2"- terpyridine.

B.5. Activation of Organic Substrates by Direct Coordination to Transition Metal Complexes

In 1894, F. C. Phillips reported that aqueous palladium chloride was reduced to palladium metal by ethene with concurrent formation of ethanal.⁸⁸ This reaction, which amounts to the stoichiometric oxidation of ethene by palladium attracted little industrial interest until the late 1950's, when a group working for Wacker Chemie reported that the palladium metal could be readily reoxidized to palladium chloride in the presence of certain oxidants such as cupric or ferric chloride.³ The overall reaction is now known to constitute a palladium catalyzed oxidation of ethylene to acetaldehyde, with molecular oxygen as the terminal oxidant. The following sequence of reactions has been proposed.⁸⁹

$$C_2H_4 + PdCl_2 + H_2O \longrightarrow CH_3CHO + Pd + 2HCl$$
 (64)

$$Pd + 2CuCl_2 \longrightarrow PdCl_2 + Cu_2Cl_2$$
 (65)

$$Cu_2Cl_2 + 2HCl + O_2 \longrightarrow 2CuCl_2 + H_2O$$
 (66)

Acetaldehyde is formed in ~95% yield and the side products include acetic acid (~2%), CO₂ (~1%), and chlorinated products (~1%).⁹⁰ Propylene is oxidized under similar conditions to acetone in 90% yield and 1-butene affords methyl ethyl ketone in ~85% yield.⁹¹ Yields vary considerably with the higher olefins⁹¹ with mixtures often being obtained as a result of olefin isomerization. Aqueous solutions of other Group VIII metal salts, such as those of Pt(II), Ir(III), Ru(III) and Rh(III) oxidize olefins in an analogous manner, but much less effectively than Pd(II).⁹¹

The kinetics and mechanism of the Pd(II) catalyzed oxidations of olefins have been studied extensively and are the subject of continuing

debate. A mechanism with the following basic steps is consistent with experimental data.⁸⁹

$$PdCl_{4}^{2-} + C_{2}H_{4} \longrightarrow [PdCl_{3}C_{2}H_{4}]^{-} + Cl^{-} \qquad (67)$$

$$[PdCl_{3}C_{2}H_{4}]^{-} + H_{2}O \longrightarrow [PdCl_{2}(H_{2}O)C_{2}H_{4}] + Cl^{-} \qquad (68)$$

$$[PdCl_{2}(H_{2}O)C_{2}H_{4}] + H_{2}O \longrightarrow [HOCH_{2}CH_{2}PdCl_{2}(H_{2}O)]^{-} + H^{+} (69)$$

$$[HOCH_{2}CH_{2}PdCl_{2}(H_{2}O)]^{-} \longrightarrow HOCH_{2}CH_{2}PdCl(H_{2}O) + Cl^{-} (70)$$

$$HOCH_{2}CH_{2}PdCl(H_{2}O) \longrightarrow CH_{3}CHO + Pd + HCl + H_{2}O \qquad (71)$$

In the first step, the reduction of electron density at the double bond by π -complexation renders it susceptible to nucleophilic attack by water or hydroxide. π -coordination of ethene involves concurrent loss of Cl⁻ to form the 16 electron Pd(II) anion which undergoes ligand replacement to yield the neutral Pd(II) aquo species. In accordance with a nucleophilic process, the rate decreases with increasing alkyl substitution at the double bond. Pd(II) catalyzes the nucleophilic attack on olefins more readily than Pt(II)⁹² because Pd(II)-olefin complexes are formed more rapidly than those of Pt(II) and back-donation is less for Pd than for Pt resulting in lower electron density around olefinic complexes of the former. Also, the Pdolefin bond is weaker than the Pt-olefin bond leading to a lower activation energy for $\sigma - \pi$ rearrangement and Pd(II) can readily expand its coordination sphere to accept a fifth or sixth ligand.

In industrial Wacker processes, $CuCl_2$ is almost universally used as the palladium oxidant since the resulting Cu_2Cl_2 can be readily reoxidized in air or oxygen. The role of copper as the cocatalyst in these reactions is still not completely resolved. In commercial processes, since the

concentration of copper far exceeds that of palladium, it is likely that copper chloride is involved in more than just the reoxidation of the palladium.

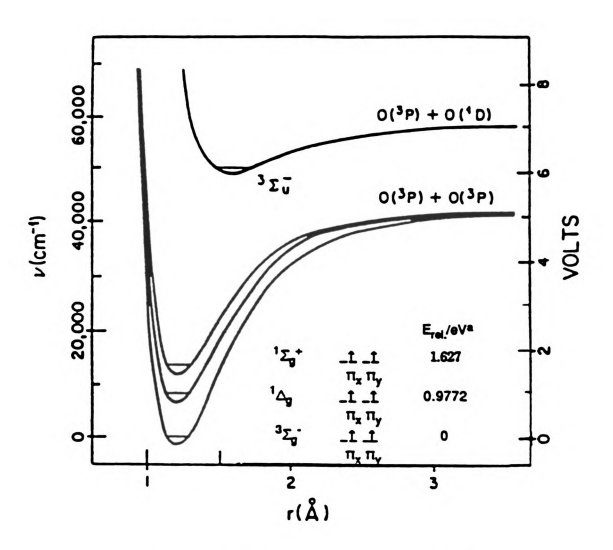
C. The Photo-Oxidation of Organic Substrates

The photocatalytic oxidation of organic substrates involves chemical reactions that are driven in the nonspontaneous or endoergic direction using light as a stoichiometric reagent. These types of reactions offer unique alternatives for substrate oxidations that are not accessible via conventional thermal reaction pathways. Photo-oxidation reactions may occur via direct or indirect reaction between the photochemically active transition metal complex and the substrate.

C.1. Indirect Photo-Oxidation of Organic Substrates

The use of molecular oxygen, as a selective thermal oxidant, is severely hampered by its biradical nature. Since dioxygen has a triplet ground state, its direct combination with organic molecules is a spin forbidden process. In part, this problem has been overcome by the activation of molecular oxygen by transition metal complexes (as previously discussed in this chapter), but these reactions pose different challenges. For example, many of these reactions still proceed via radical pathways, and therefore selectivity is still a problem. Also, release of the product from the metal complex is a significant issue, since it determines the catalytic ability of the system. An alternative method of oxidation, which exhibits high reactivity and selectivity, is the oxidation of organic substrates by excited state or singlet oxygen, ${}^{1}O_{2}$. There are two low lying excited states of oxygen, the ${}^{1}\Delta_{g}$ and the ${}^{1}\Sigma_{g}$ states shown in Figure 5. Rapid deactivation of the ${}^{1}\Sigma_{g}$ state to the ${}^{1}\Delta_{g}$ state results in the short lifetime of the ${}^{1}\Sigma_{g}$ state (1

Potential energy curves for molecular oxygen. (After Hertzberg, G. Molecular Spectra and Molecular Structure. I. Spectra of Diatomic Molecules; 2nd ed., Van Nostrand: New York, 1950.)



^a λ_{emis} ($^{1}\Sigma_{\text{g}}^{+}$) = 761.6 nm, λ_{emis} ($^{1}\Delta_{\text{g}}$) = 1,269 nm.

Figure 5

= 10^{-9} sec in water).⁹³ Thus the term $^{1}O_{2}$ refers to the $^{1}\Delta_{g}$ state and the vast majority of $^{1}O_{2}$ chemistry exclusively occurs from the $^{1}\Delta_{g}$ state.

Although singlet oxygen may be produced by a variety of methods⁹⁴ such as by gaseous discharge, 94 the decomposition of hydrogen peroxide and the thermal decomposition of organic ozonides and photoperoxides.94 the most efficient production of singlet oxygen has been by the photosensitization of transition metal compounds.⁹⁴ These photosensitized oxidations are initiated by absorption of a photon by the sensitizer, to produce a short lived singlet (¹S*) which often undergoes intersystem crossing to the longer-lived triplet (3S*). Collisional energy transfer between the sensitizer excited state and ground state molecular oxygen occurs to form $^{1}\mathrm{O}_{2}$ via the energy exchange mechanism depicted in Figure 6. This exchange occurs via electronic overlap of the orbitals of the excited state sensitizer and oxygen, thereby requiring physical contact between the interacting partners. In this exchange interaction, a double electron substitution reaction occurs where an electron on ${}^3S^*$ jumps to O_2 simultaneously with the movement of an electron from O_2 to ${}^3S^*$, resulting in the formation of ground state sensitizer and ¹O₂. As shown below, the oxidation of the organic substrate (A) by singlet oxygen is photocatalytic in the transition metal sensitizer.

$$S + hv \longrightarrow {}^{1}S^{*} \longrightarrow {}^{3}S$$
 (72)

$$^{3}S^{*} + O_{2} \longrightarrow S + ^{1}O_{2}$$
 (73)

$$^{1}O_{2} + A \longrightarrow AO_{2}$$
 (74)

¹O₂ reactions with organic substrates are set apart from autooxidation reactions by the high degree of stereo- and regio-specificity. The

Molecular orbital description of the triplet sensitized generation of singlet oxygen. (After Turro, N. J. Modern Molecular Photochemistry; Benjamin/Cummings: Menlo Park, CA, 1978, Chapter 14.)

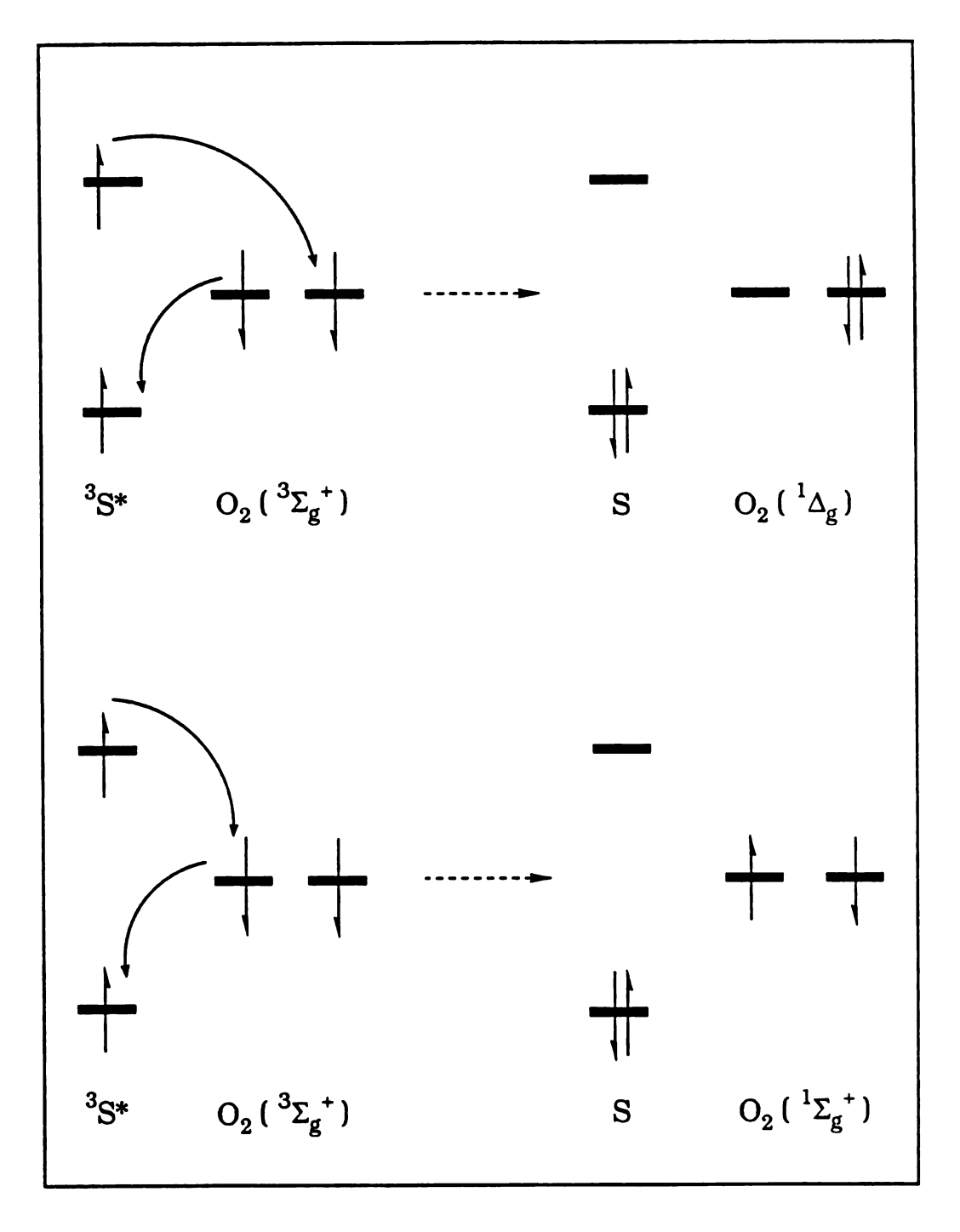


Figure 6

eration of hemistry;

three modes in which $^{1}O_{2}$ adds to olefins are highly specific: (i) the "ene" reaction; (ii) dioxetane formation; or (iii) Diels-Alder addition to form the endoperoxide. In the $^{1}O_{2}$ "ene" reaction (eq (75)), 95 olefins containing allylic hydrogens are oxidized to the corresponding allylic hydroperoxides in which the olefinic linkage has shifted to a position adjacent to the original double bond. Silyloxy-olefins also undergo an ene type reaction with $^{1}O_{2}$, 96 producing silylperoxy ketones eq (76). The trimethyl silyl group takes the place of the allylic hydrogen, while the ether oxygen replaces the allylic carbon.

$$\begin{bmatrix} + & 0 \\ H & 0 \end{bmatrix} \longrightarrow \begin{bmatrix} 1 & 0 \\ H & 0 \end{bmatrix}$$
 (75)

Over the past forty years of research on the $^{1}O_{2}$ ene reaction, a variety of factors which characterize allylic hydroperoxidation reactions have been uncovered. $^{97-99}$ The $^{1}O_{2}$ ene reaction proceeds stereospecifically in a suprafacial manner in reference to the ene unit such that oxygen attack and hydrogen removal occur from the same side of the olefins. 97a There is no loss of optical activity in the oxidation of optically active olefins, 97b making the $^{1}O_{2}$ route to allylic funtionalization attractive to synthetic chemists. 97c $^{1}O_{2}$ is quite sensitive to steric factors 97d and approaches the substrate predominantly from the less hindered side. This leads to

preferential abstraction of those allylic hydrogens which are perpendicular to the plane of the double bond in the low energy conformations of the olefins. Because of the low activation energies (1 - 5 kcal) for singlet oxygen processes, little dependence of the rate on the temperature is observed. Solvent, too, has little effect on the rate of the ene reaction. The relative reactivity of various sites on polyenes toward $^{1}O_{2}$ is generally related to the ionization potential. Attack preferentially occurs at the more highly substituted double bond, which is usually the double bond of lowest ionization potential. The exact mechanism for the ene reaction remains unclear, but it is generally accepted that these reactions involve at least one irreversibly formed intermediate with perepoxide-like geometry. Solution of the intermediate precludes this issue.

If the ene reaction is precluded by a lack of allylic hydrogen sites or for steric reasons, singlet oxygen will add over the double bond forming 1,2-dioxetanes (four membered cyclic peroxides), as shown in eq (77). Singlet oxygen undergoes cycloaddition to enol ethers, enamines and certain

electron rich alkenes. In most cases, 1,2-cycloaddition of singlet oxygen to olefins requires the presence of electron-donating groups in the alkene, such as $-NR_2$, -OR and -SR. Although the characteristic reaction of dioxetanes 101 is the chemiluminescent thermal decomposition to carbonyl fragments, some dioxetanes may be isolated by irradiating the substrate in the presence of oxygen and sensitizer at $^{-78}$ °C. These reactions also

exhibit a high degree of specificity, similar to the ene reaction. Two mechanistic extremes are considered to explain the thermal decomposition of the dioxetane that leads to direct production of high yields of carbonyls; diradical (two step) pathway eq (78a) and concerted pathway eq (78b). Most results have been interpreted to support a two-step mechanism. No experimental data to date has required a concerted interpretation.

Alternatively, singlet oxygen acting as a dienophile, may react with conjugated dienes via a Diels-Alder reaction to yield an endoperoxide 103

There are five basic types of conjugated dienes which undergo singlet oxygenation to yield endoperoxides:¹⁰³ nonhomoannular aliphatic dienes, alkenylarene systems, homoannular aliphatic dienes, heterocyclic dienes, and nonheterolytic aromatic dienes. The mechanism of the addition of singlet oxygen to conjugated systems has received little attention in the way of detailed investigation, probably because endoperoxidation bears an obvious resemblance to the formation of cyclohexene rings by the well

known Diels-Alder reaction. Consequently, a concerted mechanism has been more or less assumed. Differences between singlet oxygen and conventional Diels-Alder dienophiles have come to light, suggesting the necessity for an alternative to the concerted pathway is necessary. 103a Various intermediates (B - D) that have been postulated for these cycloaddition reactions are shown in addition to the transition state (A) in Figure 7. The reactivity and regions electivity of the dienes are more complex than substrates containing a single double bond due to the competition of the ene and cycloaddition reactions with the Diels-Alder reaction. 103a

In theory, any transition metal complex which is photochemically active possessing an excited state of higher energy than that of ${}^{1}O_{2}$ (${}^{1}\Delta_{g}$) and is sufficiently long-lived 104 may function as a photosensitizer in these oxidation reactions. While Ru(bpy)₃^{2+ 105} has been the prototype for these systems since the early 1970's, complexes of Os(II), 106 Ir(III), 106 Re(I), 107 Cr(III), 108 metalloporphyrins, 109 Pt(II), 110 Pd(II), 111 and other Ru(II) derivatives 105 have been shown to be efficient producers of $^{1}O_{2}$. Thus, $^{1}O_{2}$ chemistry utilizes a wide range of transition metal complexes as sensitizers and exhibits a high degree of specificity in the catalytic reactions with olefinic substrates or compounds containing carbon heteroatom double bonds. While the reactivity between singlet oxygen and organic substrates is fairly well documented, the mechanism of transition metal sensitized singlet oxygen generation has become quite controversial. Recently, conflicting evidence has been reported in the literature regarding the presence of alternative pathways for the generation of ¹O₂ by excited state electron transfer pathways. 112

Representations of various intermediates postulated for the mechanism of epoxidation of dienes by singlet oxygen via the 1,2-cycloaddition reaction. (After Bloodworth, A. J.; Eggelte, H. J. in *Singlet Oxygen*; Frimer, A. A., Ed.; CRC: Boca Raton, FL, 1985; Vol. 2, pg. 100.)

C.2. Direct Photo-oxidation of Organic Substrates

During the past 15 years, the photocatalytic properties and the photochemical behavior of transition metal complexes have attracted much attention. A careful examination of the literature for processes catalyzed by transition metal compounds under the action of UV or visible irradiation shows no obvious correlation between the systems studied and an almost complete casualness in the choice of the systems which have been investigated. Numerous studies have demonstrated the propensity of electronically excited metal complexes to exchange electrons, 114-115 but most of this work has been directed toward solar energy and the development of alternative energy supplies, particularly the splitting of water. As a result, the redox photochemistry of small molecules other than water, 116a including the direct photochemical oxidation of organic substrates by use of excited state transition metal complexes, has been virtually unexplored.

The binuclear d^8 - d^8 platinum(II) complex $Pt_2(\mu-P_2O_5H_2)_4^{4-}$ (abbreviated $Pt_2(POP)_4$), where $P_2O_5H_2$ = pyrophosphite bridging ligands, exhibits rich excited-state chemistry. The $Pt_2(POP)_4$ excited state $(^3A_{2u})$ is formed by a transition between metal centered orbitals $(d\sigma^* \to p\sigma)$. This triplet state is a viable chemical reagent in part because of its long lifetime at ambient temperature $(9 \ \mu s)$ and its high quantum yield of formation $(\Phi = 0.50)$. Triplet $Pt_2(POP)_4^*$, with its $d\sigma^*$ electron localized at an axial coordination site, is electronically similar to the methyl radical or $Mn(CO)_5$. The finding that $Pt_2(POP)_4^*$ abstracts halogen atoms from halocarbons and hydrogen atoms from aromatic hydrocarbons supports this analogy. 118 Redox reactions may occur at the vacant axial-ligand Pt site via an innersphere pathway.

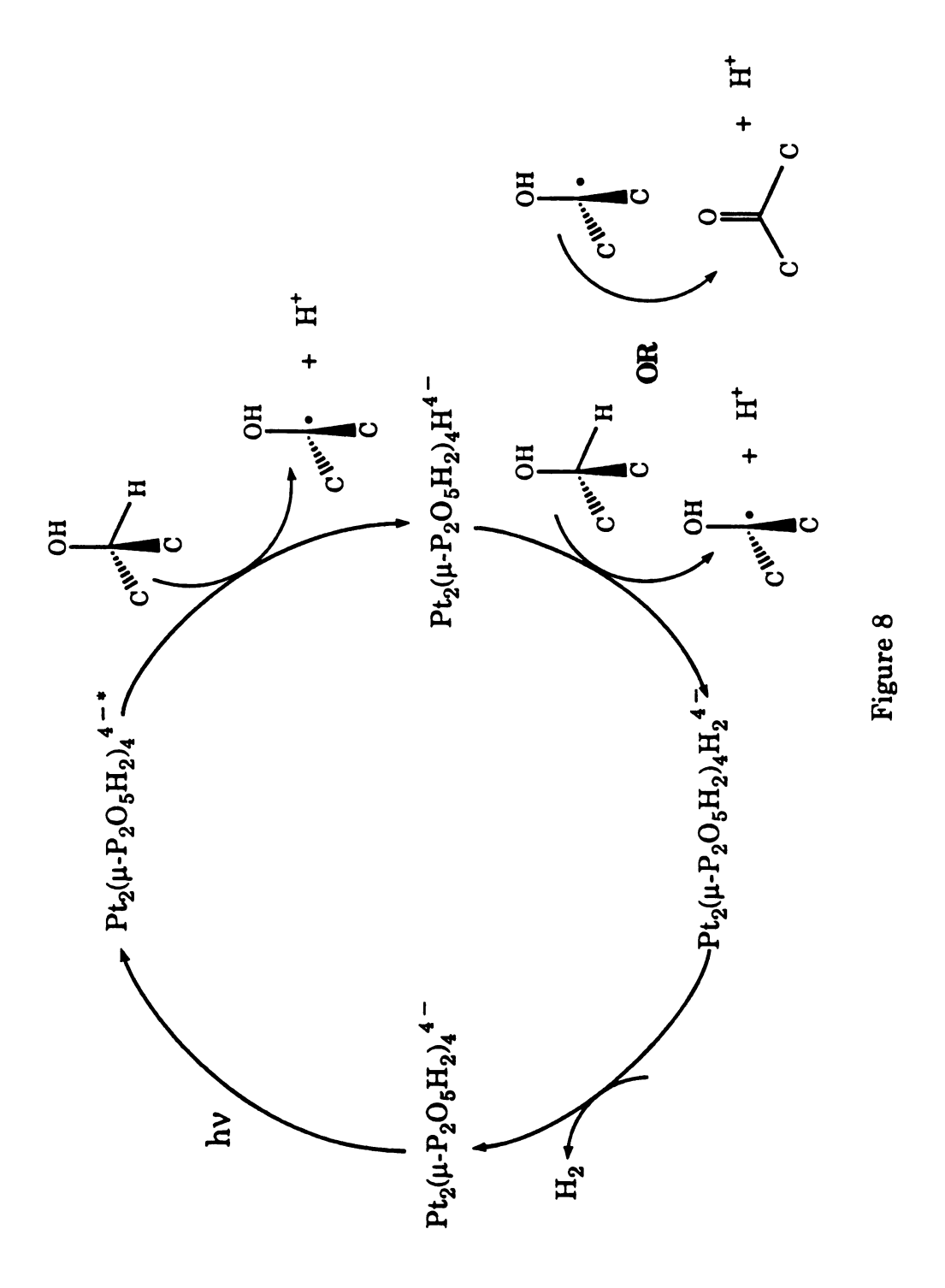
The first example of C-H bond cleavage by Pt₂(POP)₄* is the photochemical conversion of isopropyl alcohol to acetone and hydrogen. ¹¹⁹ The photoinduced reaction is catalytic in Pt₂(POP)₄, as shown in Figure 8, and involves the ³A_{2u} state as a reactive intermediate. The first step is hydrogen-atom abstraction of the methine hydrogen to give the radical pair Pt₂(POP)₄H and (CH₃)₂COH, followed by propagation steps leading to Pt₂(POP)₄H₂ and acetone. In probing the chemical reactivity of these intermediate platinum hydride complexes, it has been found that Pt₂(POP)₄ is a photochemical catalyst for the conversion of ethanol to hydrogen and acetaldehyde¹²⁰ and for the formation of acetone from isopropanol by the transfer hydrogenation of cyclohexene and cyclopentene with isopropanol. ¹²¹

$$C_nH_{2n-2} + (CH_3)_2CHOH \xrightarrow{Pt_2(POP)_4^*} C_nH_{2n} + (CH_3)_2CO$$
 (80)

The dihydride reacts with HCl to generate hydrogen and rapidly with oxygen to give $Pt_2(POP)_4$. The oxygen chemistry indicates that the complex can be viewed as $(Pt^{2+})_2(H\bullet)_2$. This free radical reactivity of $Pt_2(POP)_4^*$ is reflected in atom-transfer reactions that occur with no prior electron transfer step.

 $Pt_2(POP)_4^*$ has the potential to be more selective than other radicals in atom abstractions due to the presence of μ -pyrophosphite ligands, that present a fairly bulky, hydrophilic axial site interaction surface to an incoming substrate. Work to date suggests that allylic C-H bonds of substituted olefins and benzylic C-H bonds of aromatic hydrocarbons are homolytically cleaved quite rapidly by $Pt_2(POP)_4^*$. A platinum complex of analogous structure, $Pt_2(pcp)_4^{4-}$, where pcp is the

Photochemical pathway for the oxidation of organic substrates $by~use~of~Pt_2(\mu\text{-}P_2O_5H_2)_4^{\mbox{4-}}.$



μ-methylenebis(phosphinito) ligand, exhibits very similar reactivity to Pt₂(pop)₄⁴. ^{118a}

Besides these Pt_2 complexes, the inorganic complexes that have received perhaps the most attention in recent years in the area of photo-oxidation chemistry are the polyoxometallates or polyoxoanions. The general formula for heteropolycomplexes (HPC's) and isopoly electrolytes may be represented as $[M_mO_y]^{p-}$ for isopolyanions and $[X_xM_mO_y]^{q-}$ for heteropolyions. M is usually Mo or W and to a lesser extent V, Nb, or Ta. The heteroatom X can be one of 64 elements, belonging to various groups of the periodic table with the exception of the noble gases. The metals are in high oxidation states (d^0,d^1) . Typical examples are the molybdates and tungstates with x/m values of 1/12 and 2/18 designated as $X_xM_m^{q-}$ (i.e. $PW_{12}O_{40}^{3-}$). The 1:12 anions can be considered spherical with a diameter of about 1.2 nm and the 2:18 anions can be considered as ellipsoids with axes of 1.2 nm and 1.7 nm.

Although these complexes have been well-known for over a century, it has only been since 1977 that the polyoxometallates have been developed as reagents or catalysts for thermal 124-125 and photochemical 126-132 processes involving organic substrates. With the substantial reactivity of the latter, it is now well documented that polyoxometallates undergo photosensitization upon exposure to near visible and UV light in the presence of a great variety of organic compounds to give rise to the blue species, "the heteropoly blues." This reaction occurs with concomitant oxidation of organic compounds, including alcohols, glycols, hydroxyacids, amines, carboxylic and dicarboxylic acids. 126-127 These oxidations have been reported by a number of groups and are summarized in Table 2.

Table 2

Products of the Photoreaction of Polyoxometallates (POM)

with Organic Substrates

Substrate	POM	Products	Фа	Ref.
Olefins	W ₁₀ O ₃₂ ⁴⁻	Dimers	Relative	128
Benzene	$W_{10}O_{32}^{4}$	Diphenyl	0.10	128
Cyclohexene	$W_{10}O_{32}^{4}$	3,3'-Dicyclohexene	1.0	128
Octene	$W_{10}O_{32}^{4}$	Dicyclooctene	0.60	128
Alkanes	PW ₁₂ O ₄₀ ³ -	Alkenes	Absolute	129
Cyclooctane	$PW_{12}O_{40}^{3}$	Cyclooctene	~0.1	129
2,3-Dimethylbutane	$PW_{12}O_{40}^{3}$	2,3-Dimethylbutene	~0.1	129
Octane	PW ₁₂ O ₄₀ ³⁻	Dicyclooctene	~0.1	129
Alcohols	PW ₁₂ O ₄₀ ³⁻	Aldehyde/Ketone	Absolute	130
MeOH	PW ₁₂ O ₄₀ ³ -	Formaldehyde	0.003	130
1-Propyl	$PW_{12}O_{40}^{3}$	Propanone	0.14	130
Sec-Butyl	PW ₁₂ O ₄₀ ³ -	2-Butanone	0.11	130
Benzylic C-H	PW ₁₂ O ₄₀ ³ -	Oxygenated Products	Relative	130
Benzhydrol	$PW_{12}O_{40}^{3}$	Benzophenone	2.5	130
Benzyl Methyl Ether		Methyl Benzoate	1.0	130
Diphenyl Methane	PW ₁₂ O ₄₀ ³⁻	Benzophenone	4.5	130
Misc. Substrates	PW ₁₂ O ₄₀ 3-	NR ^b	NR b	131
DMF	$PW_{12}O_{40}^{3}$	NR ^b	NR ^b	131
Acetone	PW ₁₂ O ₄₀ ³ -	NR ^b	NR ^b	131
Benaldehyde	PW ₁₂ O ₄₀ ³ -	NR ^b NR ^b		131
Benzonitrile	PW ₁₂ O ₄₀ ³ -	NR ^b NR ^b		131

^a Photochemical quantum yield. ^b Not reported.

Although many different HPC's have been used in these oxidation reactions, the data summarized shows only two HPC's for consistency.

While the general mechanism and the details regarding the routes of activation of the reactions summarized in Table 2 are somewhat obscure, excitation seems to involve oxygen-to-metal charge transfer ($\lambda > 300$ nm) of the HPC. Organic species undergo precomplexation with photo-excited metallates and react mainly by hydrogen atom and/or electron transfer, resulting in the reduction of the polyoxometallates and oxidation of the organic species through the transformation of radicals. It has been claimed that substrate oxidation occurs via a two electron, two proton route with removal of the α hydrogen before the substrate desorbs from the catalyst surface. Desorption of the free radical and diffusive encounter with a second excited state is unlikely as indicated by failure to detect alcohol radicals in flash experiments. One photon may add two electrons in the HPC and oxidize one molecule of organic compound, as shown below for isopropanol. 123

$$M^{n-} \longrightarrow M^{n-*} \tag{81}$$

$$M^{n-*} + (CH_3)_2 CHOH \longrightarrow M^{(n+1)-} + (CH_3)_2 COH + H^+$$
 (82)

$$M^{(n+1)-}+ (CH_3)_2COH \longrightarrow M^{(n+2)-} + (CH_3)_2C=O + H^+$$
 (83)

$$M^{(n+2)-} + M^{n-} \longrightarrow 2M^{(n+1)-}$$
 (84)

The catalyst M^{n-} can be regenerated from eq (84) in the presence of Pt(0), $^{128-130}$ RuO₂, 127 or O₂. 129

While the substrate oxidation appears to be site specific, product selectivity (yield) varies significantly with substrate. The efficiency of these reactions is low as indicated by the quantum yield values in Table 2.

It is postulated that the structural complexity of the photocatalyst can significantly influence the efficiency of the photoinduced electron transfer. This is indicated by the inability of stereochemically hindered olefins such as norbornadiene to undergo dimer formation, 128 and the observation that the efficiency of alcohol oxidation was governed not only by the oxidation potential of the alcohol and the availability of α hydrogens, but also by the tightness of the association with the photocatalyst. 130

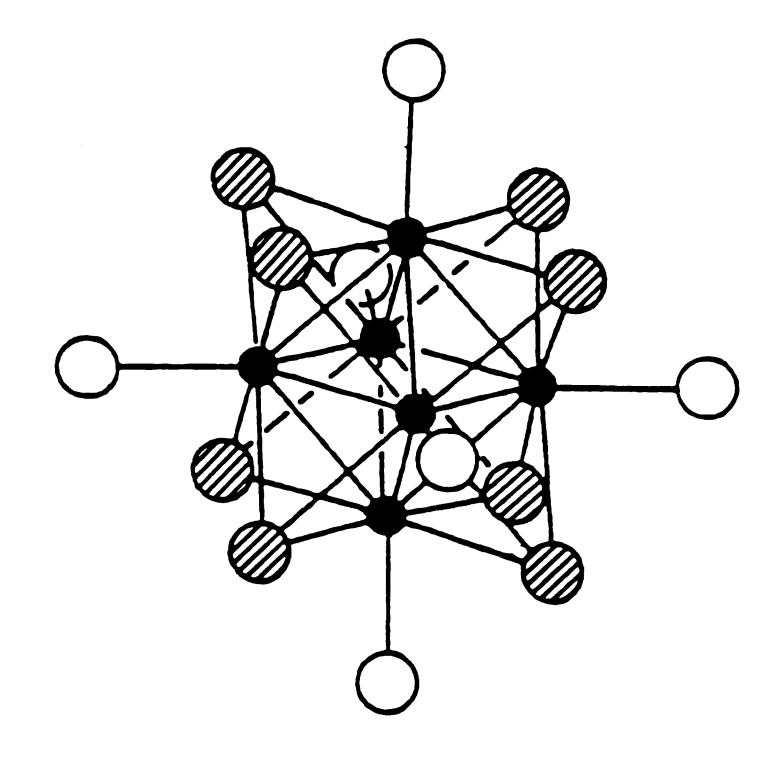
The use of the polyoxometallates for the selective photocatalytic oxidation of organic substrates via electron transfer/atom transfer pathways is somewhat uncertain, given the low efficiencies of these systems. Moreover, extremely weak emission and lifetimes on the nanosecond time scale ¹³⁰ of the HPC's are inconsistent with electron transfer oxidation of substrates. To this end, the polyoxometallates typify the lack of photochemically active inorganic transition metal complexes, with well defined excited states, which allow for the methodical study of photo-oxidation chemistry via both indirect and direct pathways. Described herein is a series of transition metal complexes which are potentially good photo-oxidation reagents ¹³³⁻¹³⁵ via both indirect (singlet oxygen) and direct (redox) pathways due to their unique excited state properties and chemical reactivity: the molybdenum and tungsten (II) halide clusters.

C.3. The Hexanuclear Molybdenum and Tungsten(II) Halide Clusters: Potential Indirect and Direct Photo-Oxidation Catalysts.

The idealized structure of these clusters, shown in Figure 9, consists of eight metal atoms arranged in an octahedral metal core ligated by eight face bridging halides and six axial halides, resulting in the general structure $[M_6X_8]Y_6^{2-}$. The absorption spectra of the molybdenum(II),

Figure 9

Idealized structure of the $[M_6X_8]Y_6^{2-}$ ions.



 $[M_6X_8]Y_6^{2}$

- Mo(II), W(II)
- \bigcirc X = Cl, Br, I
- O Y = Cl, Br, I

Figure 9

 $Mo_6X_{14}^{2-}$ (X = Cl, Br) and tungsten(II) $W_6X_{14}^{2-}$ (X = Cl, Br,I) halide clusters are shown in Figure 10. The absorption spectra exhibit the trend expected for LMCT transitions (absorption energy increases for the clusters along the series I < Br < Cl). Excitation into the broad absorption bands yields intense red and infra-red luminescence, as exhibited by the emission spectra in Figure 10. For the Mo_6 clusters, the emission is halide independent, suggesting that the excited state is metal localized. In the case of the W_6 clusters, the trend of emission energy is opposite that predicted for an LMCT.

This spectroscopic behavior is explained by use of the molecular orbital diagram (Figure 11), obtained from extended Huckel 136 and SCF-X α calculations. 137 The highest energy filled molecular orbitals are metallocalized and the 12 bonds in the octahedral metal core result from the filled a_{1g} , t_{2u} , t_{1u} , t_{2g} , and e_g levels, while the LUMO possesses a_{2g} symmetry. These calculations are supported by EPR spectra of the cluster mono and trianion, 133a as well as the fact that these clusters are diamagnetic. Although excitation involves the promotion of an electron from a low lying ligand-based orbital to the metal based a_{2g} LUMO, this luminescent behavior suggests that ensuing internal conversion and intersystem crossing are extremely efficient and result in the excited state configuration which is primarily metal localized. Thus, luminescence occurs from a spin and LaPorte forbidden metal based triplet excited state. characterization of the cluster excited state has been confirmed experimentally by lifetime and emission measurements. 133,135 The intramolecular excited-state properties of the molybdenum(II) hexanuclear clusters are dependent on the nonradiative decay rates, which obey energy gap law behavior. 133c The deactivating accepting mode is primarily a low

Figure 10

Electronic absorption and emission spectra of the tetrabutylammonium salts of $[M_6X_8]Y_6^{2-}$ ions, in acetonitrile at room temperature: (a) (----) $Mo_6Cl_{14}^{2-}$; (····) $Mo_6Br_{14}^{2-}$; (b) (----) $W_6Cl_{14}^{2-}$; (····) $W_6Br_{14}^{2-}$; (---) $W_6I_{14}^{2-}$. (From Newsham, M. D. Ph. D. Dissertation, Michigan State University, 1988).

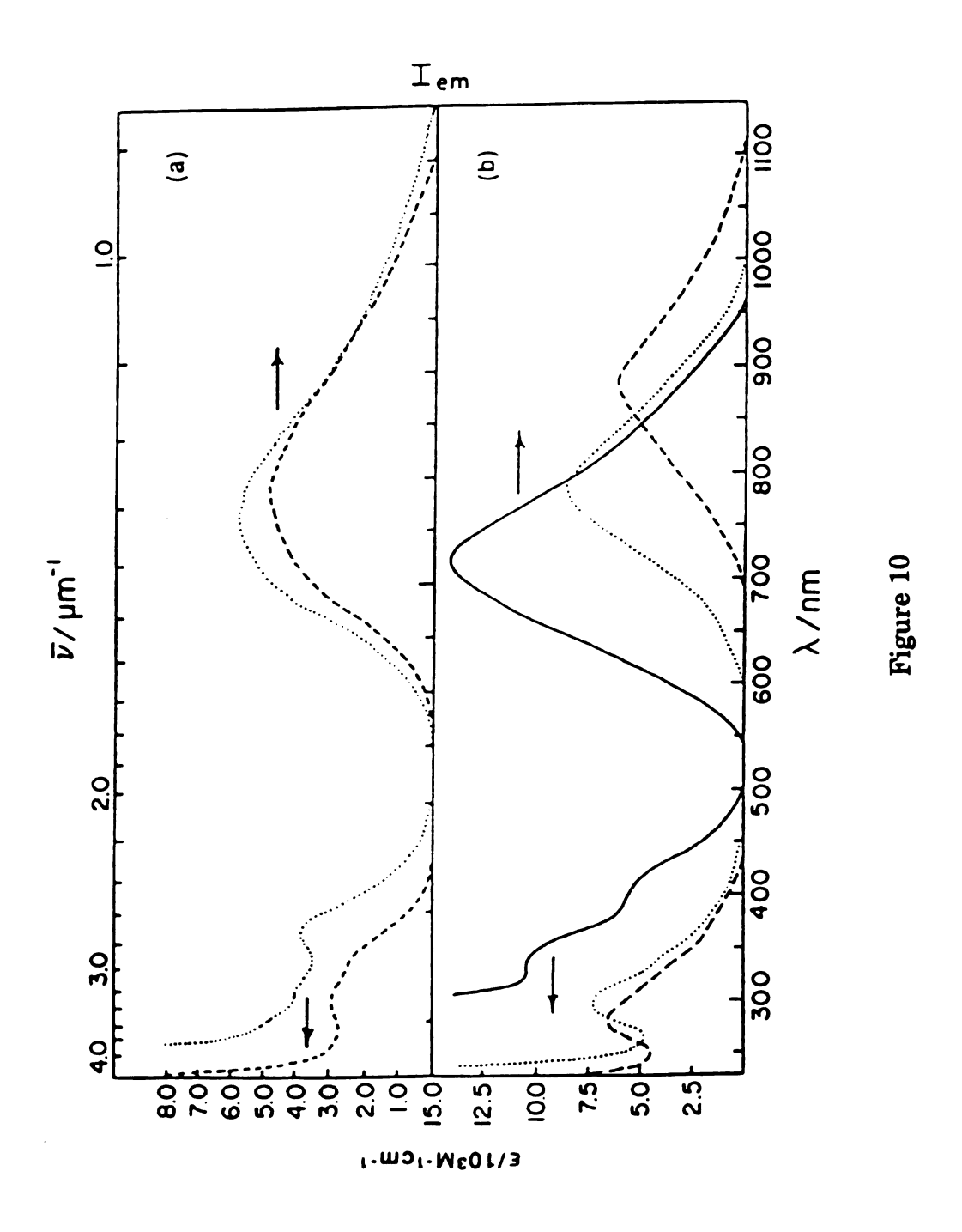
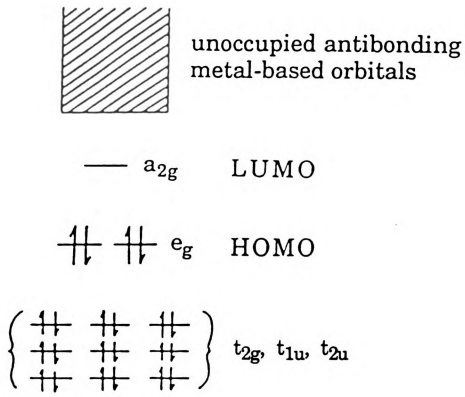


Figure 11

Molecular orbital diagram of the $[\mathrm{M_6X_8}]\mathrm{Y_6}^{2-}$ ions.



 $[M_6X_8]Y_6^2$

a1g

Figure 11

frequency metal-metal core breathing vibration and it is the low energy nature of this accepting mode that is the overriding reason for the long-lived excited states and high emission quantum yields for these cluster systems. The tungsten(II) halide clusters, on the other hand, exhibit more complicated behavior due to the presence of energetically close-lying excited states that mediate nonradiative decay to the ground state. ^{133c}

Thus, the high energy excited triplet state of the clusters is extremely luminescent and exhibits both solution and solid state lifetimes paralleled by few other transition metal complexes. The clusters also undergo facile one electron electrochemical oxidation and reduction, 134 as illustrated by the reduction potentials of the $M_6X_{14}^{-/2-}$ couples in acetone, listed in Table 3. The spectroscopic and electrochemical properties of $Mo_6Cl_{14}^{\ 2-}$ are summarized in the Latimer diagram in Figure 12. From estimates of the 0,0 transition, it is apparent that the clusters are moderately strong oxidants and reductants in the excited state. In addition, these clusters are robust in solution as exhibited by the ability of their excited state properties to be exploited in a variety of environments, 138 such as sol gels and organic polymers. In view of the energy content of the $M_6X_8Y_6^{\ 2-*}$ excited states and the ability to photochemically generate the powerfully oxidizing $M_6X_8Y_6^{\ -}$ ions, these systems are good candidates for photo-oxidation of organic substrates via direct or redox pathways.

The purpose of the investigations described herein is to probe the suitability of the long-lived and redox active hexanuclear Mo(II) and W(II) halide clusters in photo-oxidation reactions. The studies in Chapter Three probe the ability of the clusters to generate $^{1}O_{2}$. Specifically, Section B investigates the pathways by which $^{1}O_{2}$ is produced, with homogeneous clusters in solution. Historically, many compounds have been proven to

Table 3

Emission, Spectroscopic and Electrochemical Data of the $(NBu_4)_2M_6X_{14}$ Clusters

Cluster	E(0,0)/V a	E _{1/2} /V ^b	ф _е с	τ _o /μs ^d (Solid)	τ _o /μs ^e (Acetone)
$\overline{{\rm (NBu_4)_2Mo_6Cl_{14}}}$	1.79	1.46	0.19	118	180
$(\mathrm{NBu_4})_2\mathrm{Mo_6Br_{14}}$	1.79	1.20	0.16	78	120
$(\mathrm{NBu_4})_2\mathrm{W_6Cl_{14}}$	1.83	1.06	0.02	5.4	2.2
$(\mathrm{NBu_4})_2\mathrm{W_6Br_{14}}$	1.91	0.93	0.15	16.4	15.0
$(\mathrm{NBu_4})_2\mathrm{W_6I_{14}}$	2.08	0.67	0.39	29.1	25.0

^a Estimation of the 0-0 energy of the emissive excited state of the $[M_6X_8]Y_6^{2-}$ ions from low temperature (77 K) luminescence spectra. ^b As reduction potentials for the $[M_6X_8]Y_6^{-/2-}$ couple vs. SCE, in acetone. ^c Emission quantum yield. ^d Lifetimes measured with $\lambda_{exc} = 355$ nm (Nd:YAG, fwhm = 8 ns), at room temperature. ^e Lifetimes measured in acetone with $\lambda_{exc} = 355$ nm (Nd:YAG, fwhm = 8 ns), at room temperature.

Figure 12

Modified Latimer diagram of $(NBu_4)Mo_6Cl_{14}$ in acetonitrile at room temperature (electrode potentials in V vs. SCE, excited state energy in eV).

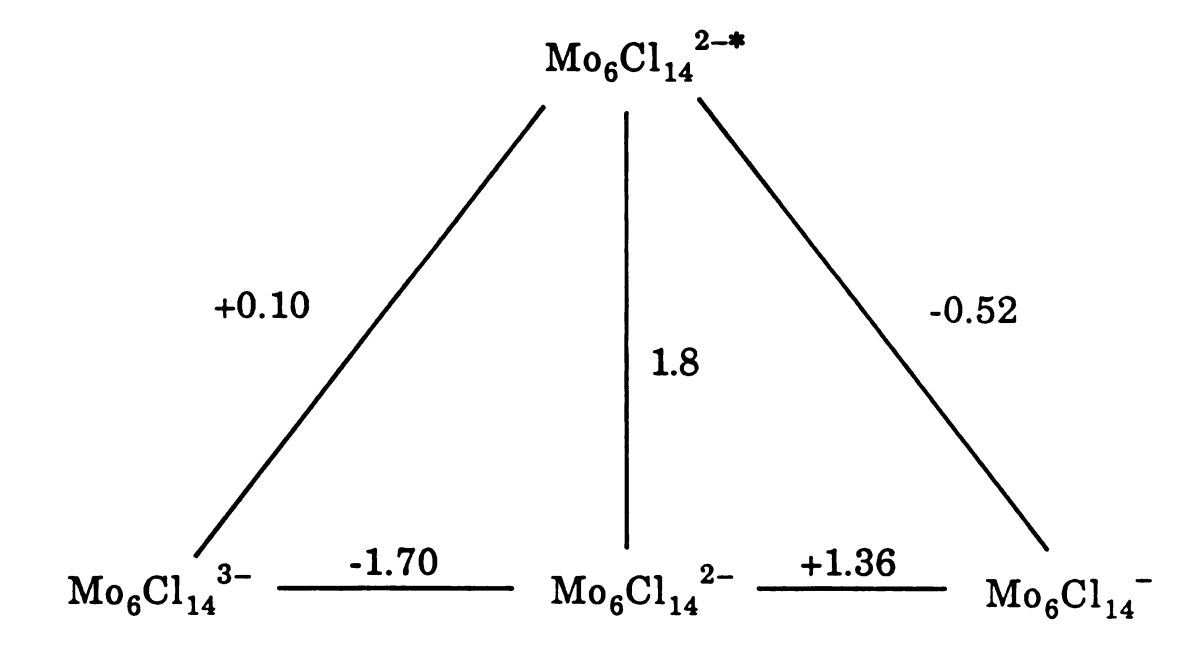


Figure 12

generate $^{1}O_{2}$ via energy transfer pathways, but few complexes (organic or inorganic) such as the clusters, potentially possess both energy and electron transfer routes to $^{1}O_{2}$ formation. In Section C, the generation of singlet oxygen with the $M_{6}X_{12}$ derivatives of the clusters covalently bound to pendant nucleophilic groups on polymeric supports (metallopolymers) is described. In Chapter 4, the suitability of these clusters for the direct photo-oxidation of organic substrates is investigated. The $M_{6}X_{8}Y_{6}^{2-*}$ excited state can undergo oxidative quenching with electron accepting molecules to yield $M_{6}X_{8}Y_{6}^{-}$, which can oxidize alcohols directly. The mechanism for organic substrate oxidation by $M_{6}X_{8}Y_{6}^{-}$ has been studied electrochemically and on this basis, potential photochemical pathways are explored.

CHAPTER II

Experimental

A. Materials

A1. Preparation of Hexanuclear Molybdenum Clusters

 Mo_6Cl_{12} was prepared according to the method of Dorman and McCarley. 139 In a typical reaction, 13.65 g of MoCl₅ (Aldrich), 1.38 g of aluminum, 8.2 g of NaCl, and 13.33 g of AlCl₃ (Alfa) were loaded into a 23 mm x 140 mm quartz tube, with a 150 mm restricted neck, in the dry box. The contents were thoroughly mixed, capped with a rubber septum and removed from the dry box. The tube was then connected to a high vacuum manifold, evacuated for 1 h and flame sealed under dynamic vacuum (~1 x 10⁻⁴ torr). The sealed tube was placed in a 54232 Lindberg tube furnace equipped with a chromel/alumel thermocouple. The temperature was raised to 200 °C and allowed to equilibrate for 6 h. The temperature was then increased over a 3 h period to 450 °C and the reaction was allowed to proceed for 48 h. Upon cooling, the products were removed from the tube under air and added to ~500 ml of 6 M HCl. The solution was heated to boiling in order to dissolve all of the molybdenum chloride product and filtered to remove broken glass and undissolved material. The solution volume was then reduced to ~200 ml and the cluster compound (H₃O)₂Mo₆Cl₁₄ precipitated upon cooling. The cluster was isolated by filtration and recrystallized several times from 6 M HCl. After the final recrystallization, the compound was heated in vacuo for several hours at 100 °C. Mo_6Cl_{12} was obtained by heating the resulting material in vacuo at 200 °C.

 $(\mathrm{NBu_4})_2\mathrm{Mo_6Cl_{14}}$ was prepared by a modification of Sheldon's method. Addition of an excess of $\mathrm{NBu_4Cl}$ to $\mathrm{Mo_6Cl_{12}}$ in 6 M HCl results in precipitation of $(\mathrm{NBu_4})_2\mathrm{Mo_6Cl_{14}}$. The solution was filtered and the precipitate was taken up in $\mathrm{CH_2Cl_2}$. The $\mathrm{CH_2Cl_2}$ solution was filtered in

order to remove insoluble impurities and allowed to evaporate slowly, upon which orange crystals formed. The material was recrystallized several times by evaporation from CH_2Cl_2 . Product purity was determined by electrochemical and lifetime measurements.

 $m Mo_6Br_{12}$ was prepared via a procedure similar to that of $m Mo_6Cl_{12}$, but 14.55 g of NaBr and 26.68 g of AlBr $_3$ (CERAC) were substituted for their chloride counterparts. After cooling the reaction tube, the products were opened to air and leached with 6 M HBr and the solution was filtered. The resulting residue was refluxed for 48 h in a 50/50 (vol/vol) solution of ethanol and HBr. The solution was filtered and reduced in volume. The resulting precipitate was collected by suction filtration, washed with water, and dissolved in hot ethanol. The ethanolic solution was then filtered. Evaporation of the ethanolic filtrate yielded orange solid, $({\rm H_3O)_2Mo_6Br_{14}}$. Solid ${\rm Mo_6Br_{12}}$ was purified by several recrystallizations and dried by using a procedure similar to that for ${\rm Mo_6Cl_{12}}$.

 $(NBu_4)_2Mo_6Br_{14}$ was prepared by addition of an excess of NBu_4Br to Mo_6Br_{12} in ethanol. The recrystallization procedure is identical to that of $(NBu_4)_2Mo_6Cl_{14}$.

Mixed molybdenum halide clusters, $(NBu_4)_2Mo_6X_8Y_6$ (where X, Y = Cl, Br, I) were prepared by Dr. Robert Mussell, using a modified method of Sheldon¹⁴¹ as described elsewhere.¹⁴²

A.2. Preparation of Hexanuclear Tungsten Compounds

Synthesis of hexanuclear tungsten compounds was accomplished by following procedures analogous to those for molybdenum(II) halide preparations. Typically, 19.85 g of WCl₆ (Alfa), 1.81 g of aluminum, 9.00 g of NaCl and 13.33 g of AlCl₃ were loaded into a quartz tube, as described in

Section II.A.1. The reaction tube was heated to 200 °C and the temperature was held constant for 2 h. The temperature was then raised over a 9 h period, including a 6 h pause at 450 °C, to a reaction temperature of 550° C where it was held constant for 24 h. After cooling, the tube was opened and worked-up by procedures similar to those for molybdenum(II) chloride. (NBu₄)₂W₆Br₁₄ was prepared by Dr. Randal King as described in detail elsewhere. ¹⁴³

Tungsten(II) iodide was prepared by the method of Hogue and McCarley, with some modification. 1.00 g of $(NH_4)_2W_6Cl_{14}$, 9.97 g of KI and 3.60 g of LiI were added to a quartz reaction tube in the glove box. The tube was removed from the dry box, placed under vacuum for several hours, and was flame sealed under dynamic vacuum. The reaction tube was placed in a furnace and the temperature was raised to 550 °C over 1.5 h. After holding the temperature at 550 °C for 1 h, the reaction tube was allowed to cool to room temperature and opened under air. The resulting solid was washed with water. The remaining solid was extracted with ethanol and filtered. Evaporation of the ethanolic solution yielded W_6I_{12} . $(NBu_4)_2W_6I_{14}$ was obtained by addition of excess NBu_4I to the ethanolic solution of W_6I_{12} . $(NBu_4)_2W_6I_{14}$ was isolated by filtration and recrystallized several times from CH_4CN .

Mixed tungsten halide clusters, $(NBu_4)_2W_6X_8Y_6$ (where X, Y = Cl, Br, I), were prepared by Dr. Robert Mussell, using the modified procedure of Hogue and McCarley. A detailed description of these syntheses are previously described. A

A.3. Preparation of Polymer Bound Cluster Derivatives

ReillexTM 402 (Aldrich), 4-polyvinylpyridine that is 2% crosslinked with divinylbenzene, was modified with ${\rm Mo_6Cl_{12}}$ as follows. The polymer was dried at 120 °C for several days in an oven and 100 mg of dried polymer was added to refluxing methanol or ethanol solution under argon and allowed to stir for several hours. To the polymer solution, various concentrations of ${\rm Mo_6Cl_{12}}$ were added in the appropriate alcohol. The solution was allowed to reflux for several hours. The resulting polymer bound cluster material was filtered under air and washed with copious amounts of alcohol. The amount of cluster covalently bound to the polymer was determined by monitoring the absorbance at 340 nm of the cluster solution before and after polymer addition. The maximum amount of cluster that has been bound to the polymer by this method is 2 x 10^{-3} moles cluster/gram of polymer. By allowing the polymer/cluster solution to reflux at least 12 h, the amount of cluster bound to the polymer increases to 3.5 x 10^{-3} moles of cluster/gram of polymer.

 ${
m Mo}_6{
m Cl}_{12}$ was covalently bound to 2% and 20% crosslinked styrene-divinylbenzene copolymer derivatized with triphenylphosphine (Aldrich) by the following method: 0.5 g of polymer and 0.3 g of ${
m Mo}_6{
m Cl}_{12}$ were added to 10 ml of ethanol and the solution was allowed to reflux for several hours. The polymer bound cluster material was filtered and washed with copious amounts of ethanol. The amount of cluster bound to the polymer (determined by the same procedure for 4-polyvinylpyridine) was 1.1×10^{-4} and 2.6×10^{-4} moles of cluster/gram of polymer for the 2% and 20% crosslinked polymers, respectively.

A.4. Preparation of Polymer Bound Rose Bengal

Rose Bengal 1 ((3',4',5',6'-tetrachloro-2'-(2,4,5,7-tetraiodo-6-hydroxy-3-3*H*-xanthen-9-yl) benzoic acid, disodium salt), Aldrich) was bound to Merrifield's peptide resin (chloromethylated styrene-divinylbenzene copolymer beads, Aldrich) by attachment to the polymer as the carboxylate ester by using a modification of the method of Blossey, Neckers, Thayer, and Schaap. 145 2.0 g of polymer and 2.0 g of Rose Bengal were added to 60

ml of reagent grade DMF and the solution was brought to reflux for 24 h. The polymer material was filtered and washed with ~200 ml of each of the following solvents: benzene, ethanol, ethanol/water (1:1 vol/vol), water, methanol/water (1:1 vol/vol), and methanol. The final filtrate was colorless. The polymer beads were dried in vacuo for several hours.

A.5. Singlet Oxygen Trapping and Inhibiting Reagents

1,2-Dimethylcyclohexene (Wiley Organics) and 1-methylcyclohexene, 1,4-diazabicyclo[2.2.2]octane (DABCO) and 2,6-di-tert-butylphenol (all from Aldrich) were used as received.

2,3-Diphenyl-p-dioxene was prepared by modification of the method of Summerbell and Berger. 146 10.6 g of benzoin and 0.2 g of p-toluenesulfonic acid were added to 130 ml of ethylene glycol, which had been previously dried over sodium metal and vacuum distilled. The solution was refluxed for 17 h under argon. The solution was allowed to cool, diluted with 200 ml of water, and extracted with four 75 ml aliquots of ether. The ether was evaporated and ~200 ml of hot ethanol was added to the residue, followed by subsequent addition of activated charcoal. The solution was filtered and upon cooling, white transparent crystals formed in solution. The solid was recrystallized several times in ethanol and product purity was confirmed by melting point, IR, NMR, and GC/MS.

Ethylene glycol dibenzoate, the singlet oxygen product of the p-dioxene, was synthesized by modification of the method of Bourne, Stacey, Tatlow and Tedder. To 3 g of benzoic acid and 4 ml of warm trifluoroacetic anhydride (50 °C), 1 ml of dry ethylene glycol was added dropwise under argon. The solution was allowed to stir at 80 °C for 30 min. Aqueous NaHCO₃ was added to the solution until bubbling subsided. The solution was extracted with three 10 ml portions of chloroform. The solution was allowed to evaporate to yield white crystals, which were dissolved in 10-20 ml of ethanol. Microcrystalline product was precipitated upon addition of an equal volume of hexanes. Product purity was determined by melting point, IR, NMR and GC/MS.

A.6. Quenchers

4-Cyano-N-methylpyridinium hexaflurophosphate was prepared by dissolving 3 g of 4-cyanopyridine in 50 ml of a 1:1 acetone/ethanol (vol/vol) solution containing 5 ml of CH₃I. The solution was refluxed overnight and filtered. The resulting solid was dissolved in 60 ml of 50/50 acetone/water solution. Upon addition of 5 g NH₄PF₆, solid precipitated which was subsequently recrystallized in acetone/water solution several times. 4-Cyano-N-benzylpyridinium hexafluorophosphate was synthesized by the same procedure, with the substitution of benzyl chloride for CH₃I.

o- and p-Dinitrobenzene (Aldrich) were purified by recrystallizing the solids in hot ethanol and drying the resulting crystals in vacuo at 120°C. TCNE (tetracyanoethylene) and chloranil (tetrachloro-1,4-benzoquinone), both purchased from Aldrich, were purified by recrystallizing the solid in dichlorobenzene and acetonitrile, respectively, followed by vacuum sublimation. The TCNE anion was prepared by the method of Webster, Mahler, and Benson. 148

A.7. Reagents Used in Direct Oxidation Studies

Benzyl alcohol, isopropanol, Na₂CO₃ (Aldrich Gold Label) and 2-methyl-2-propanol (Aldrich HPLC Grade) were used as received. Cumene was distilled from sodium under an argon atmosphere, prior to use. Dicumene, purchased from Pfaltz and Bauer, was used as received.

A.8. Supporting Electrolyte

Tetrabutylammonium hexafluorophosphate (Southwestern Analytical Chemicals) was dissolved in ethyl acetate, dried over MgSO₄,

recrystallized from pentane-ethyl acetate solution and dried in vacuo for 12 h at 60 °C.

A.9. Solvents

Acetonitrile, acetone, and dichloromethane, obtained from Burdick and Jackson Laboratories (distilled-in-glass grade) and dichloroethane obtained from Aldrich (Gold Label) were used as received for electrochemical and photochemical experiments. For spectroscopic studies, these solvents were subjected to seven freeze-pump-thaw cycles and vacuum distilled onto 4 Å molecular sieves (3 Å molecular sieves were used for CH₃CN) contained in a 1-liter flask equipped with a high-vacuum Teflon valve. Acetone storage over 4 Å molecular sieves was avoided to prevent sieve catalyzed decomposition over long periods of time. Methanol and ethanol, used for polymer syntheses, were refluxed over sodium for no less than 6 h and freshly distilled prior to use.

B. Experimental Methods

B.1. Quenching Experiments

Quenching rate constants were determined by using the Stern-Volmer 149 method of luminescence intensities and lifetimes. Steady state and time resolved luminescence spectra were recorded on an emission spectrometer and a DCR-1A Nd:YAG laser ($\lambda_{\rm exc} = 355$ nm, fwhm = 8 ns) instrument previously described. Stern-Volmer experiments were conducted over a quencher concentration range of 10^{-5} - 10^{-2} M in specially constructed high vacuum cells, consisting of a 1 cm quartz cuvette attached to a side-arm terminating with a 10 ml round bottom flask. The cuvette was isolated from the round bottom chamber by a high vacuum teflon valve.

Solid quenchers were added to the round-bottom flask. After the pressure of the round bottom chamber was reduced to $\sim 5 \times 10^{-6}$ torr, the cell was removed from the vacuum line and the cluster solution, isolated in the 1 cm quartz cuvette, was mixed with the quencher.

For oxygen quenching experiments, oxygen was added to the cell, while attached to the cell by high vacuum manipulations. The concentration of oxygen dissolved in acetone, C_g (M) was calculated by using eq (85), as derived from Henry's Law, 151

$$C_{g} = \frac{X_{g} \rho \quad 1000}{M_{1} (1 - X_{g})} \tag{85}$$

where ρ is the density (g/ml) of acetone, M_1 is the molecular weight of acetone, and X_g is the mole fraction solubility of oxygen in acetone, calculated from eq (86).

$$X_{g} = \frac{P_{g}}{K_{H}} \tag{86}$$

 P_g , the pressure (mm) of oxygen added to the system, was determined by mercury manometry. Henry's Law constant, K_H , may be calculated from eqs (87) and (88), 151

$$K_{\rm H} = 760 \text{ mm} + \frac{1.7033 \times 10^7 \,\rho \,\,\text{mm ml mol}^{-1}}{\alpha \,M_1}$$
 (87)

$$\alpha = L (273.15 K/T) \tag{88}$$

where α is the Bunsen coefficient, L is the Ostwald coefficient ¹⁵¹ and T is the temperature of measurement. Henry's Law, eq (87), is shown evaluated for $P_g = 760$ mm. ¹⁵¹

B.2. Photolysis Experiments

B.2.a. Apparatus

The light source used in photolysis studies was a 1000 W Hanovia Hg/Xe lamp (f/3.0 housing). The excitation beam was passed through a 10 mm aperture onto the photolysis reaction cell, which was a standard Schlenk tube equipped with a serum cap for singlet oxygen experiments or a teflon stopcock for samples prepared under vacuum. The cell was thermostatted at 20.0 °C. Excitation wavelengths were isolated using Schott colored glass cutoff filters.

B.2.b. Singlet Oxygen Photo-Oxidation Studies

In the singlet oxygen studies, samples were photolyzed with oxygen continuously saturating the solution through the side arm of a Schlenk tube. Photo-oxidation was monitored by removing 1.00 ml aliquots with a Hamilton syringe during the course of photolysis. Photochemically generated products were identified by GC/MS (Hewlett Packard 5985 GC/MS equipped with a HP5 capillary column) and ¹H nmr spectroscopy (Bruker WM-250). Once the photoproducts were identified, their formation during photolysis reactions was monitored with a 5890 Hewlett Packard GC equipped with a flame ionization detector, a 25 m GB-1 Foxboro capillary column and integrator. Hexadecane was used as an internal standard. ¹⁵² Quantum yields for the cluster (~1 x 10⁻⁴ M) photosensitized oxidation of 2,3-diphenyl-p-dioxene (1.5 x 10⁻² M) were conducted in acetone at room

temperature using 436 nm irradiation. At this wavelength, no species other than the clusters are excited. The excitation wavelength was isolated with 10 cm CuSO₄ and NaNO₂ solution filters or an Oriel 56450 narrow band-pass interference filter. In conducting quantum yield measurements, the excitation procedures for standard and unknown reactions must be identical. Thus a photolysis train was assembled ensuring adequate experiment reproducibility. The sample holder was designed to allow withdrawal of aliquots during photolysis without changing the area illuminated by the excitation beam.

Absolute quantum yields were determined with the following expression. 153

$$\Phi(\lambda) = [n_p / t] / [I_0 (\lambda)(1-10^{-A})]$$
 (89)

where n_p is the number of product molecules formed during photolysis, $I_o(\lambda)$ is the intensity of the exciting light at 436 nm (photons per second), (1-10^{-A}) is the fraction of light absorbed by the solution, A is the absorbance of the solution and t is the time of irradiation (seconds). $I_o(\lambda)$, was determined using ferrioxalate actinometry, ^{153,154}

$$[Fe(C_2O_4)_3]^{3-*}$$
 \longrightarrow $[Fe(C_2O_4)_3]^{2-} + 2CO_2$ (90)

from the following expression,

$$I_o(\lambda) = \frac{n_{Fe(II)}}{[(1-10^{-A}) \times \Phi \times t]}$$
(91)

where A is the absorbance of ferrioxalate at 436 nm, Φ is the quantum yield of the actinometer at 436 nm (using 0.15 M $K_3 Fe(C_2O_4)_3$, $\Phi_{Fe(II)} = 1.01$), t is the irradiation time and $n_{Fe(II)}$ is the number of Fe(II) ions formed. Since the actinometer solution is optically dense, (1-10^{-A}) approaches unity. Analysis of Fe(II) ions is easily accomplished by complexing the ion with 1,10-phenanthroline; complexed Fe(II) absorbs strongly at 510 nm (ϵ = 1.11 x 10^4 M⁻¹cm⁻¹) in acidic aqueous solution. $n_{Fe(II)}$ is calculated from 155

$$n_{Fe(II)} = \frac{6.023 \times 10^{23} V_1 V_3 A_{Fe(II)}}{V_2 \varepsilon_{Fe(II)} L}$$
(92)

where $V_1(ml)$ is the volume of the actinometer solution irradiated, $V_2(ml)$ is the volume of the aliquot taken for analysis, $V_3(ml)$ is the final volume to which the aliquot V_2 is diluted, $A_{Fe(II)}$ is the solution absorbance of the $Fe(phen)_3^{2+}$ complex at 510 nm, $E_{Fe(II)}$ is the molar absorptivity coefficient, and L is the pathlength of the spectrometer cell used (1 cm).

The quantum yields of the photo-oxidation of 2,3-diphenyl-p-dioxene were computed using eq (93),

$$\Phi = \frac{[6.023 \times 10^{23} \times m/t]}{I_0(\lambda) \times (1-10^{-A})}$$
(93)

where m is the number of moles of product formed. The solvent was removed from the samples and the analyte redissolved in toluene, thus allowing analysis of the 2,3-diphenyl-p-dioxene solution by gas chromatography. $I_o(\lambda)$ was typically 2 x 10^{17} photons sec⁻¹. The relatively small molar absorptivity of many of the clusters at 436 nm ($\epsilon \sim 1,000$ -6,000 M^{-1} cm⁻¹), did not permit the preparation of optically dense solutions [i.e. (1- 10^{-A}) < 1]. In these cases, the absorbances of the solutions were

monitored during the course of the reaction by absorption spectroscopy in order to determine the constancy of the solution absorption during the course of the experiment as well as the quantity (1-10^{-A}) from eq (93). The lamp intensity was determined before and after each oxidation solution by ferrioxalate actinometry; variations in lamp intensity during the course of a photolysis reaction were typically less than 10%.

Photo-oxidations of 2,3-diphenyl-p-dioxene (1.5 x 10^{-2} M) were carried out with $(NBu_4)_2W_6Br_8Cl_6$ (4 x 10^{-4} M) and $(NBu_4)_2W_6I_8Br_6$ (2 x 10^{-4} M) as the photosensitizers (λ_{exc} = 436 nm) in acetone and in the presence of the singlet oxygen trap, DABCO (1,4-diazabicyclo[2.2.2] octane, 5 x 10^{-2} M) and the free radical trap, 2,6-di-tert-butylphenol (5 x 10^{-2} M, 2 x 10^{-1} M). In these inhibition studies, the excitation intensity was monitored before and after each photolysis sample. During the course of photolysis, product analysis was by GC.

In the product distribution studies, the photo-oxidations of 1-methylcyclohexene (2 x 10^{-2} M) were carried out with (NBu₄)₂Mo₆Cl₁₄ (1 x 10^{-5} M, $\lambda_{\rm exc}$ ½ 436 nm), (NBu₄)₂W₆I₁₄ (1 x 10^{-5} M, $\lambda_{\rm exc}$ ½ 436nm), and Rose Bengal (1 x 10^{-3} M, $\lambda_{\rm exc}$ ½ 590 nm) as the photosensitizers in acetone and acetonitrile. Photolyzed solutions were treated with excess triphenylphosphine, which reduced the initially formed hydroperoxide to its corresponding alcohol. Products were analyzed by gas chromatography and GC/MS. As had previously been reported for Rose Bengal, 145,156 product analysis could be facilitated by immobilizing the photosensitizers to polymer supports, owing to the ease in which the photosensitizer could be isolated from photolysis solutions. This was particularly useful for the Rose Bengal and (NBu₄)₂Mo₆Cl₁₄ photosensitized oxidations because oils typically formed during the work-up of the photoproducts.

B.2.c. Direct Photo-Oxidation Studies

Typical solutions photolyzed in the electron transfer photo-oxidation of organic substrates by the hexanuclear clusters were prepared under vacuum in Schlenk tubes. These solutions consisted of 5 ml of ${\rm CH_3CN}$ which was 5 M in alcohol (usually isopropanol or benzyl alcohol) of 5 x 10^{-3} M cluster and 1 x 10^{-1} M quencher (TCNE, chloranil, etc.). The samples were irradiated with magnetic stirring at $\lambda_{\rm exc} \geq 405$ nm for ~20 h. The solution, analyzed before and after irradiation, was isolated from the cluster by vacuum distillation, thus facilitating product identification by gas chromatography (a 5890 Hewlett Packard GC equipped with a flame ionization detector, a 15 m Carbowax Foxboro capillary column, and an integrator) and GC/MS (Hewlett Packard 5985 GC/MS equipped with a 15 m Carbowax Foxboro capillary column).

B.3. Transient Absorption Studies

Transient absorption measurements were made with the pulse-probe technique. The excitation source was a Quanta Ray DCR2-A Nd:YAG laser whose fundamental frequency can be doubled or tripled with a Quanta Ray HG-2 harmonic generator. For the experiments described herein, the third harmonic, which was employed as the excitation pulse, was separated from the second harmonic and fundamental frequencies with three ESCO dichroic mirrors. The laser excitation beam intercepted a white light probe beam generated from a 150-W pulsed OSRAM Xe arc lamp (XBO150/S) mounted in a Photon Technology International (PTI) A1000 lamp housing and driven with a PTI LPS1000 power supply. The excitation and probe beams were nearly collinear with an incidence angle of 11°. The probe

beam passed through a Uniblitz 23X mechanical shutter and a Schott WG-360 cutoff filter before it was focused onto the sample (0.2 cm path length) by a f/7.0 lens. The lamp was pulsed (2 Hz repetition rate) to ~12 A for a duration of 5 ms. The triggering of the Nd:YAG laser, pulsing of the lamp, and opening and closing of the shutter were orchestrated by synchronization electronics designed and built by Martin Rabb, Electronics Design Engineer, Chemistry Department, Michigan State University. The light transmitted by the sample was collimated by an f/7.0 lens and focused by a second lens (f/4.0) through a 399 nm (Schott KV-399) cutoff filter onto the entrance slit of a SPEX 1680A monochromator. The signal obtained from a Hamamatsu R928 photomultiplier tube was amplified using a LeCroy 6103 dual amplifier/trigger. The amplifier output was passed into a LeCroy TR8828D transient recorder, and the digitized signal was stored in two MM8104 memory modules arranged in a series configuration. The amplifier, digitizer, memory modules, and a LeCroy 6010 GPIB interface were housed in a LeCroy 8013A minicrate. Data, acquired and processed by a Compaq 386 computer equipped with a 40 megabyte hard disk, were typically averaged over 1000 pulses.

B.4. Electrochemical Methods

B.4.a. Cyclic Voltammetry

Reduction potentials for the clusters and other compounds were obtained by cyclic voltammetry using a Princeton Applied Research (PAR) Model 173 potentiostat, Model 175 programmer, and a Model 179 digital coulometer. The output of the PAR 179 was fed directly into a Houston Instrument Model 2000 X-Y recorder. A three electrode system was used with a standard two compartment H-cell configuration. A Pt button and

gauze were employed as working and auxiliary electrodes, respectively, and a Ag wire served as a reference electrode by using ferrocene as an internal standard. Potentials were related to the SCE reference scale by using a ferrocenium-ferrocene couple of 0.31 V vs. SCE. 157a

B.4.b. Bulk Electrolysis

The direct oxidation of organic substrates, was accomplished with $M_6X_{14}^-$ ions produced by bulk electrolysis of $(NBu_4)_2M_6X_{14}$. Controlled-potential electrolysis experiments were performed in CH_2Cl_2 and $C_2H_4Cl_2$ with the same instrumentation used in cyclic voltammetric studies. A standard three compartment H-cell was used, with a platinum mesh electrode as the working electrode. All experiments were performed at 22 ± 2 °C, in the nitrogen atmosphere of a glove box. Emission experiments, etc., were performed under vacuum in high vacuum electrochemical cells. Solutions typically contained $9 \times 10^{-3} M$ cluster and 0.1 M tetrabutylammonium hexafluorophosphate.

The current of bulk electrolyzed solutions followed exponential decay to greater than 89% of its initial value. The final current was slightly higher than that prior to bulk electrolysis. Normally, bulk electrolysis required 60 - 90 min, depending upon electrode area, stirring efficiency, and the solubility of the cluster. Cyclic voltammograms were obtained before and after bulk electrolysis in order to determine if any side reactions accompanied the electrolysis process. A 10-fold excess of benzyl alcohol (10 µl) or other substrate was added to the stirring $M_6X_{14}^-$ solution in the working electrode compartment using a 10 µl Hamilton syringe. The solution was allowed to react between 30 and 60 min. All analyses were performed immediately after reaction to minimize side reactions. The

solution was vacuum distilled to isolate product from the cluster, thus facilitating sample analysis. Products were identified using GC/MS (Hewlett Packard 5890 J GC modified by JEOL equipped with a 15 m Carbowax Foxboro capillary column coupled to a JMS-AX505H JEOL MS). Once the products were identified, analyses were conducted using a 5890 Hewlett Packard GC equipped with a flame ionization detector, 15 m Carbowax Foxboro capillary column and integrator.

The current efficiency for the production of aldehyde was calculated on the basis of a two electron oxidation of the alcohol. The amount of carbonyl product formed was corrected for values obtained in blank experiments performed in the absence of cluster. The corrected values were then used to calculate the apparent current efficiency (CE) of the oxidation with the relation,

$$CE = \frac{(N) (2F) \times 100\%}{Q - Q'}$$
 (94)

where N = the number of moles of product from electrolysis of the cluster, F = 96,485 C/mol, Q = the charge passed during electrolysis in the presence of the cluster, and Q' = the charge passed during electrolysis in the absence of the cluster.

Rate data for the oxidation of alcohols by $M_6X_{14}^{-}$ ions were obtained using a four electrode rotating ring disk electrode (RRDE) apparatus, as well as conventional spectroscopic methods. The RRDE system consisted of a Pine AFRDE-4 Bipotentiostat to control the potentials of and measure the currents for the ring and disk electrodes (the two working electrodes) vs. the reference electrode (a Ag wire). The potentials and currents at the ring and disk electrodes were simultaneously recorded with a VP-64424 Soltec X-

Y-Y Recorder. The rotation of the RRDE was controlled by the AFMSRX Modulated Speed Control. Rotation rates typically used in our experiments were between 400-5000 rpm. The rotation rate was limited by the size of the electrochemical cell (a three compartment electrolysis cell separated by fine frits). The counter electrode was typically platinum foil. All experiments were performed using CH_2Cl_2 as the solvent and NBu_4PF_6 as the electrolyte.

The benefit of the RRDE system is that the ring electrode can be used to collect an intermediate after it is produced at the disk electrode. The disk is held at a potential E_D at which the oxidation of the cluster occurs $(M_6X_{14}^{\ 2-} \rightarrow M_6X_{14}^{\ -} + e^-)$, resulting in the production of an anodic current. The ring potential is then maintained at a sufficiently negative potential E_R , so that as long as the oxidation product $M_6X_{14}^{\ -}$ reaches the ring, $M_6X_{14}^{\ -}$ will be reduced to $M_6X_{14}^{\ 2-}$. The collection coefficient N of this process is given in eq (95),

$$N = -\frac{i_R}{i_D} \qquad (Cluster only) \qquad (95)$$

where i_R is the ring current and i_D is the disk current. If there is a chemical reaction involved, such as $M_6X_{14}^- + S \rightarrow M_6X_{14}^{2-} + S_{oxid}$ (where S is an organic substrate), RRDE can be used to determine the rate constant as indicated by the scheme below.

$$M_6 X_{14}^{2-} - e^- \xrightarrow{E} M_6 X_{14}^-$$
 (Disk) (96)

$$M_6 X_{14}^- + S \xrightarrow{C} M_6 X_{14}^{2-} + S_{oxid}$$
 (Solution) (97)

$$M_6 X_{14}^- + e^- \xrightarrow{E} M_6 X_{14}^{2-} + S_{oxid}$$
 (Ring) (98)

The collection coefficient for such an ECE process can be determined in the presence of cluster (N) and (N_k) cluster/alcohol. If k_c is fast, the concentration of $M_6X_{14}^-$ reaching the ring electrode will decrease, and the collection coefficient N_k will be smaller than collection coefficient measured in the absence of alcohol, N.

$$N_k = -\frac{i_R}{i_D}$$
 (Alcohol and Cluster) (99)

The expression used for the calculation of the rate constant \mathbf{k}_{c} from the collection coefficient is 157b

$$\kappa = k_c^{1/2} \omega^{-1/2} D^{-1/6} v^{1/6} (0.51)^{-1/3}$$
 (100)

where ω is the scan rate (mv/sec), ν is the kinematic viscosity (cm²/sec), D is the diffusion coefficient, and κ , the dimensionless kinetic parameter for homogeneous reaction, as obtained from eq (101), ^{157b}

$$N_{k} = N - (\beta')^{2/3} (1 - U * A_{1}^{-1}) + 0.5 A_{1}^{-1} A_{2}^{2} \kappa^{2} U * (\beta')^{4/3} - 2 A_{2} \kappa^{2} T_{2}$$
 (101)

where A_1 = 1.288, A_2 =0.643 $D^{1/3}$ $v^{1/6}$, β' = 3 ln (r_2/r_2), U^* = κ^{-1} tanh($A_1\kappa$), T_2 = 0.718 ln(r_2/r_1), and r_1 , r_2 , and r_3 are the radii of the disk, and the inner and outer radius of the ring electrode, respectively. The diffusion coefficient, D, can be determined by use of the rotating disk electrode (RDE) system, from the Levich equation, 157c

$$i_L = 0.62 \text{nFAD}^{2/3} \text{v}^{-1/6} \omega^{1/2} \text{C}^*$$
 (101)

where A is the cross sectional area of the electrode (cm²), C* is the bulk concentration of species j (M), n is the number of electrons per molecule oxidized or reduced, F is Faraday's constant (96,485 C/mol) and i_L is the limiting current (amps).

The $M_6X_{14}^-$ ions were generated by electrochemical oxidation of solutions containing $(NBu_4)_2M_6X_{14}$ in the environment of a glove box at room temperature. Initial concentrations of $M_6X_{14}^-$ ions were 6.40 x 10^{-3} M and 1.25 x 10^{-3} M, (for $Mo_6Cl_{14}^-$ and $W_6Br_{14}^-$ ions, respectively). Reaction of the alcohol with the monoanion were initiated by addition of at least a 10-fold excess (10 µl) of benzyl alcohol, using a syringe, to the $M_6X_{14}^-$ solution in a stoppered 0.1 cm or 0.2 cm pathlength quartz cell. The cell was shaken and the progress of the reaction monitored by observing the change in absorbance of the $M_6X_{14}^-$ ions $(Mo_6Cl_{14}^-$ at 500 nm, $\varepsilon = 1,087$ M⁻¹ cm⁻¹ and $W_6Br_{14}^-$ at 565 nm, $\varepsilon = 2,800$ M⁻¹ cm⁻¹) using a Varian 2300 spectrometer. The cell was monitored spectroscopically approximately for one h or until the absorbance of the $M_6X_{14}^-$ ion decreased to less than 10% of the initial value before alcohol addition. The $M_6X_{14}^-$ solution was also monitored in the stoppered cell without alcohol, in order to ensure that $M_6X_{14}^-$ was not undergoing any side reactions.

CHAPTER III

Indirect Photo-Oxidation of Organic Substrates
By Use of Singlet Oxgyen

A. Background

Although many sources of singlet oxygen are available, the photosensitized formation of singlet oxygen remains the method of choice 158 for many applications due to the adaptability of these systems to a wide range of reaction temperatures, solvents, and sensitizers. The significance of singlet oxygen as a chemical intermediate is reflected by the large number of applications for photosensitized singlet oxygen generation, primarily in the areas of medicine and biology, the environment, and The investigation of the involvement of singlet oxygen in biochemical/medical processes is a rapidly growing area of research. Singlet oxygen reactivity has already been implicated in a variety of cellular events¹⁵⁹ such as the presence of singlet oxygen in the sensitized photooxidation and photodynamic action of biomolecules 160,161 including amino acids, proteins and enzymes, nucleic acids and membrane components. It is also involved in certain blood diseases, 161c, 162 causing blood homolysis, and phagocytosis. 163 the process by which some types of white blood cells destroy microorganisms. Aging of the skin 159 is correlated with oxidative polymerization of elastin, also a singlet oxygen mediated process. Yet, singlet oxygen chemistry plays a therapeutic role, as it has been used successfully in the destruction of cancerous tumors. 106,164-167 The malignant cells bind to the sensitizer, hematoporphyrin, to a greater extent than normal tissue; thus irradiation selectively kills the tumor cells. These examples illustrate the importance of understanding the production and fate of excited oxygen precursors, as well as the need for more efficient singlet oxygen generating molecules.

The uses for singlet oxygen chemistry in the environment are remarkably diverse. 168 In an effort to develop degradation pathways of

polychlorinated biphenyls (PCB's), ¹⁶⁹ polychlorinated dioxins (PCD's) ¹⁶⁹ and other chloroaromatics ¹⁷⁰ distributed in water and soil, a variety of studies have been prompted regarding the deactivation of these molecules using singlet oxygen chemistry. Indeed, organic matter in sewage effluent has been treated successfully using singlet oxygen ¹⁷¹ offering a new alternative for the disinfection of municipal wastewater. Preliminary studies also suggest the use of singlet oxygen as an algacide ¹⁷² and pesticide. ¹⁷³ While the production and fate of excited state oxygen is fairly well understood in these aqueous systems, the generation of singlet oxygen from atmospheric photochemical processes and the relationship of this oxidant to the biochemistry of the atmospheric environment is relatively unknown. ^{159,174}

Singlet oxygen chemistry also has numerous commercial applications. Singlet oxygen has been proposed as a useful reagent for the specific oxidation of chemical compounds in the natural products¹⁷⁵ and fragrance industries. While it is also used to treat the surfaces of plastics and rubber materials, improving self-adhesion properties, ¹⁷⁶ and in bleaching processes in the paper¹⁷⁷ and textile industries, ¹⁷⁸ singlet oxygen does exhibit some undesirable properties. It has been shown that singlet oxygen degrades synthetic polymers such as polystyrenes and polydienes via attack of singlet oxygen at sites of unsaturation, ¹⁷⁶ and causes undesirable yellowing of pulp, due to photoinduced lignin oxidation in the bleaching process. ¹⁷⁷

Because of its ubiquitous nature and inherently interesting characteristics and reactivity, singlet oxygen will continue to be studied extensively.

B. Homogeneous Reactions

B.1. Background

Reactions between O₂ and molecules in electronic excited states (sensitizers) typically proceed by energy or electron transfer to yield unique primary photoproducts of oxygen. These excited state reactions may be categorized in two major classes. ^{160,179} In Type I reactions, as classified by Gollnick^{97d} and Schenck, ^{180a} the sensitizer activates the substrate or solvent molecule directly by hydrogen atom or electron transfer. The resulting radicals further react with oxygen to yield a variety of photo-oxidation products or initiate free-radical auto-oxidation, chain engendering a variety of complex chemical processes. An example that is a benchmark of Type I chemistry is the oxidation of aromatic olefins (donor D) by electron poor aromatics such as dicyanoanthracene (DCA). This reaction proceeds by the electron transfer mechanism as follows, ¹⁸¹⁻¹⁸⁶

$$DCA + hv \longrightarrow {}^{1}DCA^{*}$$
 (103)

$$^{1}DCA^{*} + D \longrightarrow DCA^{-} + D^{+}$$
 (104)

$$DCA^{-} + O_{2}(^{3}\Sigma_{g}) \longrightarrow DCA + O_{2}^{-}$$
 (105)

$$D^{+} + O_{2}^{-} \longrightarrow DO_{2}$$
 (106)

Type I chemistry is predisposed by substrates that are readily oxidized (amines, phenols), reduced (quinones), or are prone to hydrogen atom abstraction (paraffins). In general, sensitizers of ketonic structure (ketones, quinones, quinone-type dyes) with low lying $n-\pi^*$ excited states are powerful abstractors of hydrogen from organic molecules and react accordingly. In these cases, electron transfer to a radical ion generated in

the quenching process, eq (105), has been implicated as a major route for oxygen activation. 181-186

Recently, a number of investigations have suggested the availability of an alternative pathway for photooxygenation reactions. In these studies, deactivation of the excited sensitizer (³S*) occurs by electron transfer directly to oxygen, as shown below: ¹⁸⁷⁻¹⁸⁹

$$S + hv \longrightarrow {}^{3}S^{*}$$
 (107)

$${}^{3}S^{*} + O_{2} \longrightarrow S^{+} + O_{2}^{-}$$
 (108)

Subsequent reactions include reduction of the sensitizer by substrate or reaction of substrate with superoxide. Examples of this reaction are somewhat rarer than the Type I reaction, ¹⁶⁰ as described by eq (106), although there is a great deal of interest in these reactions owing to the possible generation of singlet oxygen by back electron transfer of the products in eq (108).

The excited state sensitizer triplet may also react with oxygen via a collisional energy transfer or Type II reaction, generating excited state or singlet oxygen ($^{1}O_{2}$), usually the $^{1}\Delta_{g}$ state. There are a multitude of examples of this reaction pathway, $^{93-111,164-172,190-194}$ with applications ranging from organic synthesis to photodynamic tumor therapy. $^{164-167}$ A general example of a Type II reaction is shown in eqs (109) - (111), where A is the substrate to be oxidized.

$$S + hv \longrightarrow {}^{3}S^{*}$$
 (109)

$${}^{3}S^{*} + O_{2}({}^{3}\Sigma_{g}) \longrightarrow S + {}^{1}O_{2}({}^{1}\Delta_{g})$$
 (110)

$$^{1}O_{2}(^{1}\Delta_{g}) + A \longrightarrow AO_{2}$$
 (111)

Oxidation of substrate by $^{1}O_{2}$, a very electrophilic species, is preferred owing to greater stereospecificity (as discussed in Chapter I), as compared to the superoxide anion generated from Type I reactions. The Type II mode is the most prevalent for sensitizers with triplet excited states (fluoroscein-and phenothiazine-type dyes, aromatic hydrocarbons) and substrates that are not easily reduced or oxidized (olefins, dienes, aromatic compounds). In general, the less reactive the acceptor is toward $^{1}O_{2}$, the more significant the side-processes will be.

The significant competition, which determines whether an energy or electron transfer reaction occurs, is between the substrate and oxygen for the triplet sensitizer. Energy exchange leaves oxygen in its lowest energy singlet excited state, while transfer of a single electron from an electronic excited state results in the direct production or indirect production of O_2^- . These processes are summarized in Figure 13.

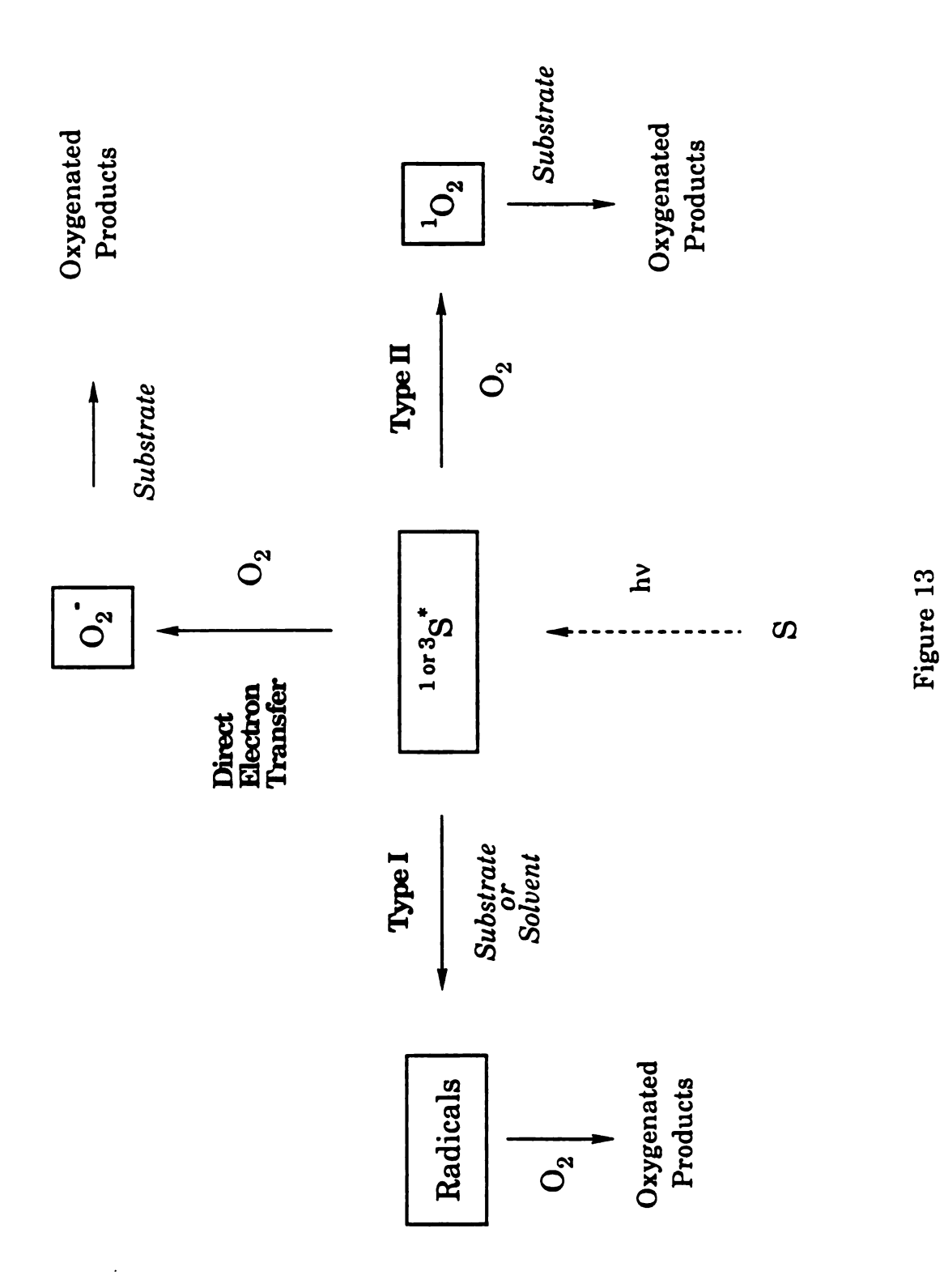
The formation of ${}^{1}O_{2}$ can be explained, alternatively, by postulating secondary reactions of photoinduced electron transfer products. Specifically, several investigations during recent years have described the formation of ${}^{1}O_{2}$ by the oxidation of ${}^{0}O_{2}$ with organic peroxides 195 and transition metal complexes. 196,197 It has been shown that the superoxide ion $(O_{2}^{\bullet -})$ will react with transition metal oxidants such as the ferrocenium radical ion $(R^{\bullet +})$ according to the electrogenerated chemiluminescence (ecl) scheme, shown below:

$$R - e^{-} \longrightarrow R^{\bullet}$$
 (112)

$${}^{3}O_{2} + e^{-} \longrightarrow O_{2}^{\bullet} -$$
 (113)

$$O_2^{\bullet-} + R^{\bullet+} \longrightarrow R + {}^{1}O_2$$
 (114)

Potential reaction pathways for reaction between excited state sensitizer (S^*) , organic substrate and oxygen.



Upon annihilation, ferrocene and $^{1}O_{2}$ are produced where R = ferrocene. Such chemiluminescence reactions may play an especially important role in photochemical $^{1}O_{2}$ schemes involving the former because the back reaction between superoxide and a one-electron photo-oxidized metal complex, produced as the primary photoproducts of electron transfer quenching, often occurs with sufficient exergonicities to directly populate the lowest energy singlet excited state ($^{1}\Delta_{g}$) of oxygen. For example, the Ru(bpy) $_{3}^{2+}$ (bpy = 2,2'-bipyridine)/ O_{2} system, has served as the prototype for transition metal sensitization of $^{1}O_{2}$, 198,199

$$\text{Ru(bpy)}_{3}^{2+} + \text{hv} \longrightarrow \text{Ru(bpy)}_{3}^{2+*}$$
 (115)

$$\text{Ru(bpy)}_{3}^{2+*} + \text{O}_{2} \longrightarrow \text{Ru(bpy)}_{3}^{2+} + \text{O}_{2}$$
 (116)

The energetics of this system are such that singlet oxygen can be formed in principle by electron transfer between $\operatorname{Ru(bpy)}_3^{2+}$ and O_2 followed by cage recombination of the primary photoproducts as shown in eqs (117) and (118), respectively.

$$\text{Ru(bpy)}_{3}^{2+*} + \text{O}_{2} \longrightarrow \text{Ru(bpy)}_{3}^{3+} + \text{O}_{2}^{-}$$
 (117)

$$\text{Ru(bpy)}_{3}^{3+} + \text{O}_{2}^{-} \longrightarrow \text{Ru(bpy)}_{3}^{2+} + \text{O}_{2}$$
 (118)

Kinetics studies employing chemical traps initially suggested the quantitative production of singlet oxygen from the $\mathrm{Ru(bpy)}_3^{3+}/\mathrm{O}_2^{-}$ back reaction eq (118). Nevertheless, the importance of chemiluminescent $^1\mathrm{O}_2$ pathways in transition metal photochemical systems has come under considerable controversy with the studies of Rodgers, et al. The failure

to directly detect infrared luminescence at 1.27 μ m, corresponding to the $^{1}O_{2} \rightarrow ^{3}O_{2}$ transition, provides strong evidence against the chemiluminescent production of singlet oxygen. That the importance of an electron transfer pathway to photosensitized $^{1}O_{2}$ production is under dispute, even for this well examined system, underscores the difficulties associated with precisely defining photochemistry of transition metal complexes with O_{2} .

Early in the studies of the excited-state reactivity of the d⁴ M₆X₈Y₆²⁻ ions (M = Mo(II), W(II); X, Y = Cl, Br, I), it was observed that the intense luminescence, which characterizes these complexes, is efficiently quenched by oxygen. The spin-triplet nature of the luminescent M₆X₈Y₆²⁻ excited-state, originally inferred from the long lifetimes of these complexes, 133,200 has been confirmed by experiments employing conventional organic energy transfer acceptors such as azulene and anthracene. 135c On this basis, O₂ quenching of $M_6X_8Y_6^{2-}$ excited states by an energy transfer mechanism is a viable reaction pathway. Additionally, M₆X₈Y₆²⁻ excited state complexes possess a rich oxidation-reduction chemistry and we have recently demonstrated the propensity of M₆X₈Y₆²⁻ ions to undergo electron transfer reactions along highly energetic chemiluminescence pathways. 134 Electrogenerated chemiluminescence has been observed from the Mo₆Cl₁₄²⁻/acceptor eq (119) and donor eq (120) systems where A is a series of neutral aromatic amines and D is a series of nitroaromatics and nitroquinones.

$$Mo_6Cl_{14}^{3-} + A^+ \longrightarrow Mo_6Cl_{14}^{2-*} + A$$
 (119)

$$Mo_6Cl_{14}^- + D^- \longrightarrow Mo_6Cl_{14}^{2-*} + D$$
 (120)

These results in conjunction with the energetics of the $M_6X_8Y_6^{2-}$ excited state suggest that electron and energy transfer are potential contributing pathways to the photo-oxygenation reactivity of this class of compounds.

Because the energy and oxidation potential of the excited state can be tuned with the ligating halides for a given metal core, the photo-oxygenation chemistry of these cluster ions has been systematically examined over a wide range of electron and energy transfer driving forces. This chapter describes a detailed kinetics analysis of the reactions of electronically excited $M_6X_8Y_6^{2-}$ ions with O_2 , which has allowed us to unequivocally answer the question of cluster photosensitized singlet oxygen production via energy and/or electron transfer pathways.

B.2. Results

The excited-state lifetimes of $M_6X_{14}^{2-}$ and $[M_6X_8]Y_6^{2-}$ cluster ions in rigorously deoxygenated acetone at 23.0 \pm 0.5 °C are listed in Table 4; all decays were exponential over four half-lives. The lifetime and luminescence intensity of the cluster ions are attenuated significantly by oxygen. The observed rate constants (k_q^{obs}) for O_2 quenching, also given in Table 4, were determined by Stern-Volmer analysis of the emission intensity and lifetime quenching data. The measured rate constants were independent of the experimental method and the rates reported in Table 4 represent the averages of a minimum of three experimental runs. The Stern-Volmer plots were linear over the O_2 concentration range $10^{-5} - 10^{-2}$ M and the intercepts were unity.

The mechanism of the quenching reaction is intimately related to the thermodynamic driving forces of the excited-state energy transfer eq (121)

Table 4

Cluster Lifetimes and Oxygen Quenching Rate

Constants

[M ₆ X ₈]Y ₆ ² - Ions	τ _ο /μs ^a	k_q^{obs} / M ⁻¹ s ⁻¹ b,c
1.	[Mo ₆ Cl ₈]Cl ₆ 2–	180	3.5×10^7
2.	$[Mo_6Cl_8]I_6^{2-}$	86	5.6×10^7
3.	$[\mathrm{Mo_6Cl_8}]\mathrm{Br_6}^{2-}$	140	3.9×10^7
4.	$[\mathrm{Mo_6Br_8}]\mathrm{Br_6}^{2-}$	120	1.2×10^8
5.	[Mo ₆ Br ₈]I ₆ 2-	71	5.0×10^7
6.	$[\mathrm{Mo_6Br_8}]\mathrm{Cl_6}^{2-}$	190	8.2×10^7
7.	$[W_6Cl_8]Cl_6^2-$	2.2	8.4×10^{7}
8.	$[W_6Cl_8]I_6^{2-}$	5.6	6.6×10^7
9.	$[\mathrm{W_6Cl_8}]\mathrm{Br_6}^{2-}$	4.4	5.9×10^7
10.	$[\mathrm{W_6Br_8}]\mathrm{Br_6}^{2-}$	15	1.4×10^8
11.	$[\mathrm{W_6Br_8}]\mathrm{Cl_6}^{2-}$	15	1.0×10^8
12.	$[W_6Br_8]I_6^{2-}$	19	1.4×10^8
13.	$[W_6I_8]I_6^{2-}$	25	2.7×10^9
14.	$[\mathrm{W_6I_8}]\mathrm{Br_6}^{2-}$	27	1.7 x 10 ⁹
15.	$[W_6I_8]Cl_6^{2-}$	16	1.9 x 10 ⁹

^a Lifetimes measured in acetone with $\lambda_{\rm exc}$ = 355 nm (Nd:YAG, fwhm = 8 ns). ^b Rate constant for the quenching of [M₆X₈]Y₆^{2-*} luminescence by oxygen. ^c±15 %.

and electron transfer eq (122) pathways. Free energies for eqs (121) and (122) depend directly on the formal reduction potential and the free energy

$$[M_6X_8]Y_6^{2-*} + O_2 \longrightarrow [M_6X_8]Y_6^{2-} + {}^1O_2$$
 (121)

$$[M_6X_8]Y_6^{2^{-*}} + O_2 \longrightarrow [M_6X_8]Y_6^{-} + O_2^{-}$$
 (122)

content of the hexanuclear cluster excited state. This latter energy is determined directly from low temperature emission spectra. Spectroscopic studies of transition metal complexes in recent years have demonstrated that the free energy content of the excited state is primarily enthalpic and possesses only a small entropic contribution. 201,202 Consequently, the excited state free energies of the hexanuclear cluster ions are approximated by the 0-0 energies of the luminescent excited state; Table 5 lists 0-0 energies which were estimated from the high energy tail of the low temperature luminescence bands of the respective cluster ions.²⁰³ From these energies, the $[M_6X_8]Y_6^{-/2}$ excited state couple can be ascertained from the simple thermodynamic relation: $E_{1/2}([M_6X_8]Y_6^{-/2-*}) = \Delta E_{0.0}$ $E_{1/2}([M_6X_8]Y_6^{-/2-})$. This expression requires explicit knowledge of the $E_{1/2}([M_6X_8]Y_6^{-/2-})$ formal reduction potential. Accordingly, cyclic voltammograms of the hexanuclear cluster ions in acetone were recorded. The clusters undergo simple one-electron oxidation, the potentials of which are shown in Table 5. Plots of anodic and cathodic peak currents ($i_{p,a}$ and $i_{p,c}$, respectively) vs. [scan rate]^{1/2} were linear with an intercept of zero and $i_{p,a}/i_{p,c}$ = 1.02 ± 0.02. Anodic to cathodic peak separations (ΔE_p) were greater than 59 mV, but were comparable to that measured for ferrocene. thereby establishing that deviations of ΔE_p from the theoretical limit are

Table 5

Electronic Origin of Lowest Energy Excited State, Reduction Potentials, and Energy and Electron Transfer Driving Forces

[]	M ₆ X ₈]Y ₆ ² – Ion	E _{0,0} /V a	E _{1/2} /V b	ΔG _{en} /V c	ΔG _{et} /V ^d
1.	[Mo ₆ Cl ₈]Cl ₆ ² -	1.79	1.46	-0.81	+0.55
2.	$[\mathrm{Mo_6Cl_8}]\mathrm{I_6^{2-}}$	1.75	1.47	-0.77	+0.60
3.	$[\mathrm{Mo_6Cl_8}]\mathrm{Br_6}^{2-}$	1.80	1.46	-0.82	+0.54
4.	$[\mathrm{Mo_6Br_8}]\mathrm{Br_6}^{2-}$	1.79	1.20	-0.81	+0.29
5.	$[\mathrm{Mo_6Br_8}]\mathrm{I_6^{2-}}$	1.70	1.23	-0.72	+0.41
6.	$[\mathrm{Mo_6Br_8}]\mathrm{Cl_6}^{2-}$	1.70	1.20	-0.72	+0.38
7.	$[W_6Cl_8]Cl_6^{2-}$	1.83	1.06	-0.85	+0.11
8.	$[\mathrm{W_6Cl_8}]\mathrm{I_6^{2-}}$	1.93	1.11	-0.95	+0.06
9.	[W ₆ Cl ₈]Br ₆ ² –	1.86	1.11	-0.88	+0.13
10.	[W ₆ Br ₈]Br ₆ ² -	1.91	0.93	-0.93	-0.10
11.	$[W_6Br_8]Cl_6^{2-}$	1.89	0.91	-0.91	-0.10
12.	$[W_6Br_8]I_6^{2-}$	1.92	0.92	-0.94	-0.12
13.	$[W_6I_8]I_6^{2-}$	2.08	0.67	-1.10	-0.53
14.	[W ₆ I ₈]Br ₆ 2-	2.07	0.71	-1.09	-0.48
15.	[W ₆ I ₈]Cl ₆ ² -	2.07	0.69	-1.09	-0.50

a Estimation of the 0-0 energy of the emissive excited state of the $[M_6X_8]Y_6^{2-}$ ions from low temperature (77 K) luminescence spectra. b As reduction potentials for the $[M_6X_8]Y_6^{-/2-}$ couple vs. SCE. c Standard free energy change for the energy transfer reaction between $[M_6X_8]Y_6^{2-*}$ and 3O_2 ; $\Delta G_{en} = -\{E_{0,0}([M_6X_8]Y_6^{2-*}) - E(^1O_2(^1\Delta_g))\}$. d Standard free energy change for the electron transfer reaction between $[M_6X_8]Y_6^{2-*}$ and 3O_2 to produce $[M_6X_8]Y_6^{-}$ and superoxide; $\Delta G_{et} = -\{E_{1/2}([M_6X_8]Y_6^{-/2-*}) - E_{1/2}(O_2/O_2^{-/2})\}$.

primarily due to uncompensated cell resistance.

2,3-Diphenyl-p-dioxene 2, undergoes a well documented 145,156 and efficient dioxetane reaction with $^{1}O_{2}$, in nonaqueous solution that yields the carbonyl containing product, 3, ethylene glycol dibenzoate at a rate of 1.5 x 107 M $^{-1}$ s $^{-1}$. 100b

2 also is a desirable substrate, in our experiments, because it does not react appreciably with the clusters in the absence of oxygen $(k_a \le 10^5 \text{ M}^{-1} \text{ s}^{-1})$.

The addition of various inhibiting reagents²⁰⁴ to solutions containing 2 is a useful method to probe the oxygenation mechanism. DABCO [1,4-diazobicyclo[2.2.2]octane] (D) acts as a powerful inhibitor of the oxidation of known reactive acceptors of ${}^{1}O_{2}$, 204,205 via a charge transfer process.

$$\mathbf{D} + {}^{1}\mathrm{O}_{2} \rightleftarrows {}^{1}[\mathbf{D}^{+}...\mathrm{O}_{2}^{-}] \rightleftarrows {}^{3}[\mathbf{D}^{+}...\mathrm{O}_{2}^{-}] \rightleftarrows \mathbf{D} + {}^{3}\mathrm{O}_{2}$$
 (124)

DABCO is only moderately effective as a $^{1}O_{2}$ quencher, $k_{q} = 5.2 \times 10^{7} \, \text{M}^{-1} \, \text{s}^{-1}$ (in MeOH), 206 but is oxidatively stable and does not absorb light of wavelengths longer than 300 nm, thereby serving as an extremely stable quencher. DABCO does not react appreciably with the cluster ions in the absence of oxygen as evidenced by extremely small quenching rate constants ($k_{q} \le 10^{4} \, \text{M}^{-1} \, \text{s}^{-1}$). Thus in the event that $^{1}O_{2}$ is the primary oxygen species produced in eq (123), there should be no appreciable

oxidation of 2 in the presence of DABCO. Table 6 reports the results of the oxidation of 2 in the absence and presence of DABCO, sensitized by $W_6Br_8Cl_6^{2-}$, $W_6I_8Br_6^{2-}$ and $W_6I_{14}^{2-}$ ions for various periods of irradiation.

Conversely, 2,6-di-tert-butyl phenol (DTBP) 4, acts as a free radical inhibitor or antioxidant that does not suppress the singlet oxygen reaction. 207 It is not completely inert to 1 O₂, but at concentrations below 0.01 M, its influence on 1 O₂ is small. 204 The products which are formed during free radical oxidations are shown below: 160

If superoxide is generated in the oxidation of 2, eq (123) should be suppressed and 5 or 6 formed. Table 7 reports the results of the oxidation of 2 in the absence and presence of 4, sensitized by $W_6Br_8Cl_6^{2-}$ and $W_6I_8Br_6^{2-}$ ions. As evidenced by extremely small quenching rate constants $(k_q(4) \le 10^5 \, \text{M}^{-1} \text{s}^{-1})$ 4 does not react with the excited state clusters.

Further mechanistic insight can be gained from product distribution studies. Generation of free $^{1}\text{O}_{2}$ or superoxide is signified by characteristic products and product distributions of substituted cyclohexenes. Reaction of 1-methylcyclohexene 7, and 1,2-dimethylcyclohexene 8, with $^{1}\text{O}_{2}$ yields products 9-13, derived from allylic hydroperoxide intermediates (ene reaction $^{209-211}$), illustrated in Figures 14 and 15. Conversely, reactions of 7 and 8 with superoxide ion yield oxygenated products corresponding to the radical auto-oxidation of the olefin. For 8, the ene products (12 and 13) are

 ${\bf Table \, 6}$ Effect of DABCO on Oxidation Reactions via $^1{\rm O}_2$

Sensitizer	[DABCO] / M a	[2] / M ^a	%2 Oxidized ^b	t/min c
W ₆ Br ₈ Cl ₆ ²⁻	0	1.49 x 10 ⁻²	35	15
W ₆ Br ₈ Cl ₆ ² -	4.41×10^{-2}	1.47×10^{-2}	0	15
	4.41×10^{-2}	1.47×10^{-2}	4	30
W ₆ I ₈ Br ₆ ²⁻	0	1.52×10^{-2}	47	12
$W_6 I_8 Br_6^{2-}$	4.82×10^{-2}	1.48×10^{-2}	0	12
$W_{6}I_{14}^{2-}$	0	1.51×10^{-2}	46	12
$W_{6}I_{14}^{2-}$	4.53×10^{-2}	1.48×10^{-2}	0	12

^a Initial concentrations. ^b Lamp intensity monitored by actinometry during experiments. ^c Time of sample irradiation.

Table 7 Effect of 2,6-Di-tert-Butyl Phenol (DTBP) on Oxidation Reactions via O_2^-

Sensitizer	[DTBP] / M ^a	[2] / M ^a	%2 Oxidized b	t/min c
	(BIBI]/ WI	(2), W		
W ₆ Br ₈ Cl ₆ ² -	0	1.49×10^{-2}	35	15
$W_6Br_8Cl_6^{2-}$	2.67×10^{-2}	1.49×10^{-2}	33	15
W ₆ I ₈ Br ₆ ²⁻	0	1.51×10^{-2}	42	15
$W_6I_8Br_6^{2-}$	4.85×10^{-2}	1.51×10^{-2}	42	15
$W_6I_8Br_6^{2-}$	1.46×10^{-1}	1.51×10^{-2}	41	15

^a Initial concentrations. ^b Lamp intensity monitored by actinometry during experiments. ^c Sample irradiation time.

Pathways for the reaction of ${}^{1}O_{2}$ with 1-methylcyclohexene 7.

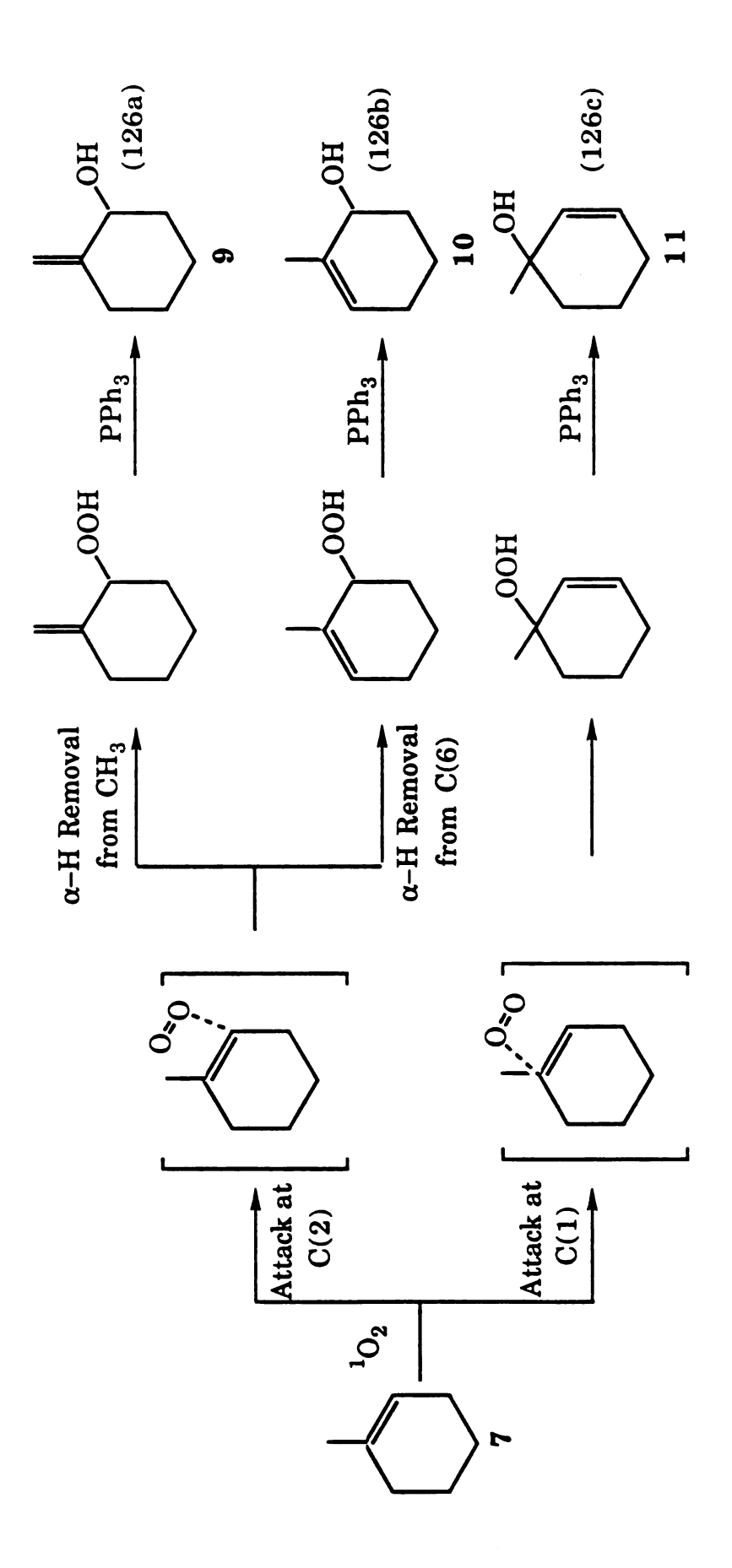


Figure 14

Pathways for the reaction of $^{1}O_{2}$ with 1,2-dimethylcyclohexene 8.

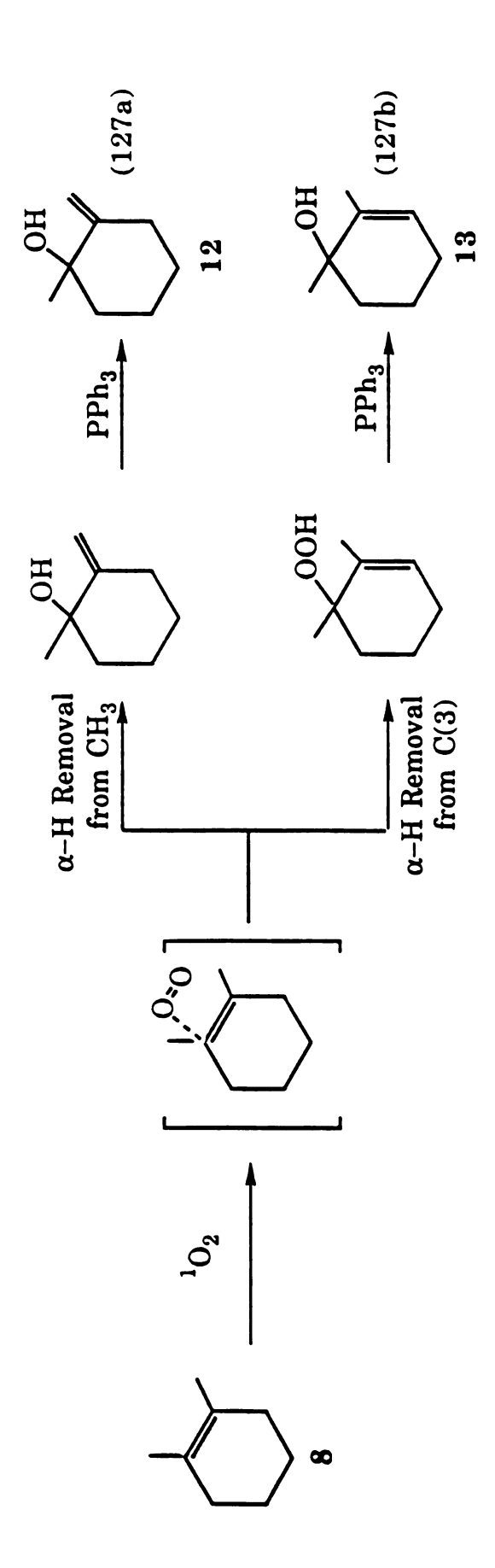


Figure 15

distinct from the product generated by radical auto-oxidation (14). Table 8

reproduces the product distributions for the photo-oxidation of 7 and 8 sensitized by Mo₆Cl₁₄²⁻, W₆I₁₄²⁻, and Rose Bengal, and also lists the previously reported product distributions measured by Foote *et al.* for the radical oxidation and Rose Bengal sensitized photo-oxidations of 7 and 8.

Efficiencies for the overall production of $^{1}O_{2}$ for cluster-sensitized photoreactions can be deduced with quantum yield measurements of substrate photo-oxidation. Quantum yield measurements were performed by employing 2,3-diphenyl-p-dioxene, 2 as a trapping substrate. The ^{1}H nmr spectra, recorded at various time intervals of a photolyzed solution containing $Mo_{6}Cl_{14}^{2-}$ (6 x 10^{-3} M) and 2 (2 x 10^{-1} M) and saturated with oxygen, is displayed in Figure 16. Inspection of these spectra reveal the quantitative conversion of 2 to 3, thereby establishing that the photo-oxidation reaction is catalytic in cluster complex. Indeed, solutions of the $Mo_{6}Cl_{14}^{2-}$ cluster ion are indefinitely stable and no appreciable diminution in photoreactivity is observed over a period of months. All of the clusters

Table 8

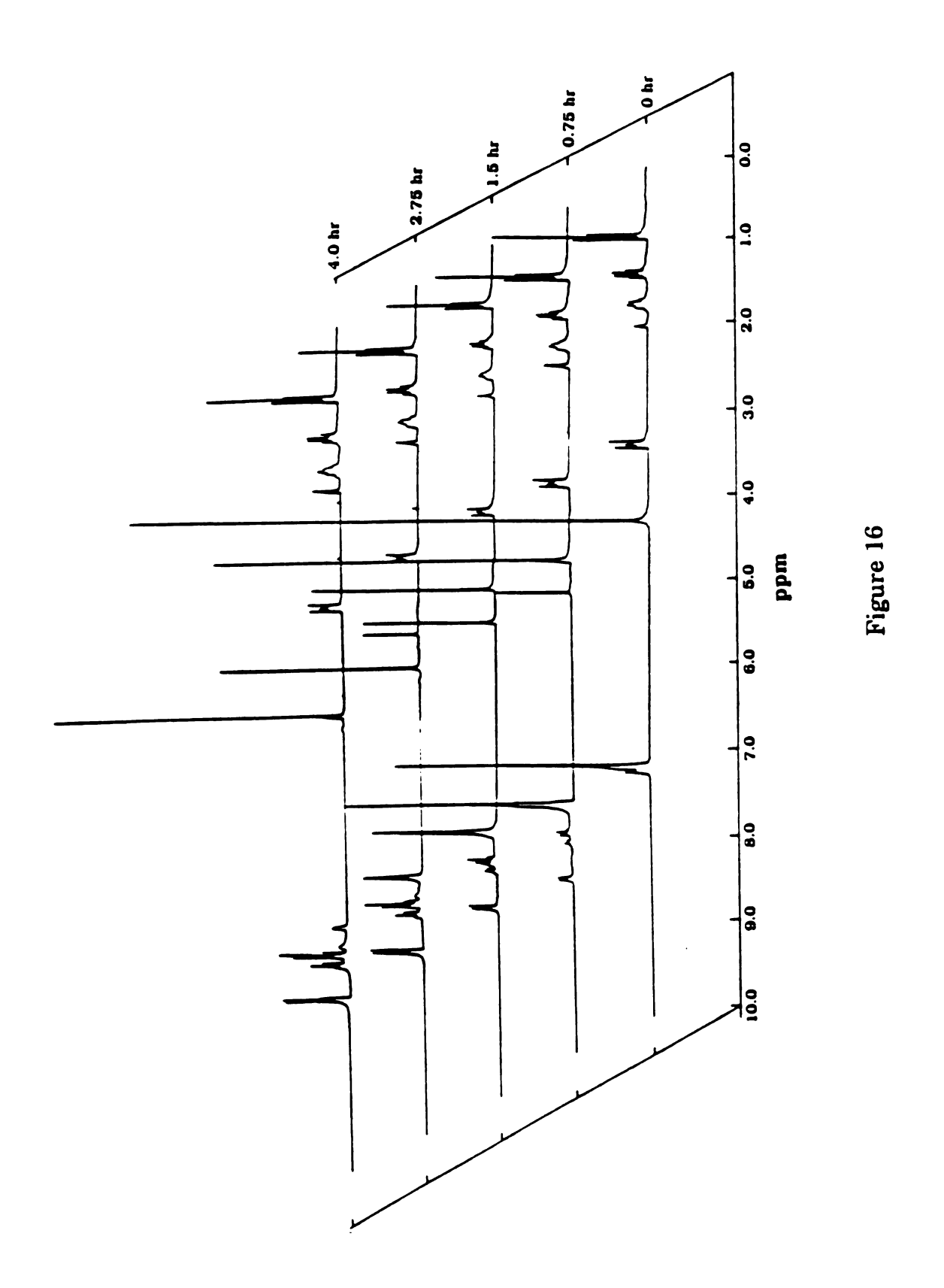
Products of Reaction of 1-Methylcyclohexene 7, and

1,2-Dimethylcyclohexene 8, with Oxygen under Photosensitized and
Radical Oxidation Conditions ^a

	Products of 7			P	roducts o	f 8
Photosensitizer	9	10	11	12	13	14
Mo ₆ Cl ₁₄ ^{2-b}	77%	23%	0%	85%	15%	0%
$W_6I_{14}^{2-c}$	64%	24%	2%	90%	10%	0%
Rose Bengal d	41%	45%	14%	89%	11%	0%
Radical Auto- oxidation e	36%	12%	40%	7%	39%	54%

^a Products designated 7-14 are defined in eqs 126 - 129. ^b Irradiated $(\lambda_{\rm exc} \ge 436 \text{ nm})$ O₂-saturated acetone solutions containing [Mo₆Cl₁₄²⁻] = 1 x 10⁻⁵ M and [olefin] = 2 x 10⁻² M. ^c Irradiated $(\lambda_{\rm exc} \ge 436 \text{ nm})$ O₂-saturated acetone solutions containing [W₆I₁₄²⁻] = 1 x 10⁻⁵ M and [olefin] = 2 x 10⁻² M. The photosensitized reaction of 7 yielded 10% unidentified products. ^d Product distributions reported in Reference 208. Radical auto-oxidation of 7 yields 12% unidentified products. ^e Product distributions reported in Reference 208.

The tetrabutylammonium salt of $Mo_6Cl_{14}^{2-}$ -photosensitized conversion of 2,3-diphenyl-p-dioxene 2, to ethylene glycol dibenzoate 3, in d_6 -acetone as monitored by 1H nmr spectroscopy at various irradiation ($\lambda_{exc} \geq 436$ nm) time intervals. Upon photosensitized reaction, the 4.4 ppm resonance of the methylene protons of 2 are shifted to 4.9 ppm for 3 and the phenyl ring proton resonance located at 7.3 ppm in 2 is split and shifted downfield in 3. Peaks arising from the tetrabutylammonium cation and the solvent lie between 0.9 and 3.5 ppm.



exhibited structural stability for the duration of the quantum yield experiments, demonstrated by constant solution absorbance at 436 nm, with the exception of the $[W_6Cl_8]Y_6^{2-}$ ions. Upon irradiation of the $[W_6Cl_8]Y_6^{2-}$ quantum yield solutions, the absorbance increased rapidly, suggesting a competing reaction pathway. Thus, the measured quantum yield for the $[M_6X_8]Y_6^{2-}$ -photosensitized oxidations of 2 (M \neq W, X \neq Cl) are summarized in Table 9.

B.3. Discussion

The product distributions of cluster-photosensitized oxidations of 7 and 8 parallel that of Rose Bengal (Table 8), which is a known efficient ¹O₂ generator. Distributions characteristic of radical auto-oxidation chemistry are not observed. For 7, addition of ${}^{1}O_{2}$ to the olefinic bond, with subsequent abstraction of the sterically accessible allylic hydrogen, produces the appropriate hydroperoxide, which undergoes ensuing decomposition to give 9 and 10 in highest yields. Owing to the steric congestion of the "ene" transition state, 11 is produced in the lowest yield. This result is noteworthy because 11 is the auto-oxidation product of 7 therefore suggesting that the photochemically generated oxidant is ${}^{1}O_{2}$ and not O_{2}^{-} . Along this line, photo-oxidation studies employing 8 as a chemical trap are even more compelling. The symmetric disposition of the methyl groups about the double bond in 8 is manifested in the generation of only two products, 12 and 13, from the ene reaction; production of 14 is unique to the radical auto-oxidation pathway. As summarized in Table 8, the products formed in the cluster photo-sensitized oxidation of 8 can exclusively be accounted for by 12 and 13, and 14 is not detected as an oxidation product. In

Table 9 Quantum Yields for the $[M_6X_8]Y_6^{2-}$ -Sensitized Photo-Oxidation of 2,3-Diphenyl-p-Dioxene 2 in Acetone

		(a) b
Photosensitizer ^a	Obsd	Pp(3) b Calcd c
[Mo ₆ Cl ₈]Cl ₆ ² -	0.80	0.91
$[\mathrm{Mo_6Cl_8}]\mathrm{I_6^{2-}}$	0.77	0.91
$[\mathrm{Mo_6Cl_8}]\mathrm{Br_6}^{2-}$	0.84	0.91
$[\mathrm{Mo_6Br_8}]\mathrm{Br_6}^{2-}$	0.79	0.91
$[\mathrm{Mo_6Cl_8}]\mathrm{I_6^{2-}}$	0.72	0.90
$[\mathrm{Mo_6Cl_8}]\mathrm{Cl_6}^{2-}$	0.84	0.91
$[\mathrm{W_6Br_8}]\mathrm{Br_6}^{2-}$	0.96	0.86
$[\mathrm{W_6Br_8}]\mathrm{Cl_6}^{2-}$	0.92	0.86
$[W_6Br_8]I_6^{2-}$	0.77	0.87
$[W_6I_8]I_6^{2-}$	0.76	0.04 ^d
$[\mathrm{W_6Br_8}]\mathrm{Br_6}^{2-}$	0.65	0.04 ^d

a The absorbance of oxygenated solutions containing $[W_6Cl_8]Y_6^{2-}$ clusters significantly increased during photolysis thereby suggesting a competing reaction pathway. Therefore, quantum yields are not reported for these complexes. ^b Quantum yield for the $[M_6X_8]Y_6^{2-}$ sensitized photoproduction of 3 from 2. ^c Evaluated from eq (133) where T_0 's are given in Table 4, k_3 's (= k_q^{obs}) are given in Table 4, $k_4 \leq 10^5$ M⁻¹ s⁻¹ for all clusters, $k_5 = 1.5 \times 10^7$ M⁻¹ s⁻¹ (Ref 100b), and $k_6 = 1.95 \times 10^4$ s⁻¹ (Ref 93, pg. 183). The oxygen concentration in acetone at saturation is 1.14 x 10⁻² M (Wilhelm, E.; Battino, R. *Chem. Rev.* 1973, 73, 1-9) and the concentration of 2 was 1.47 x 10⁻² M. ^d Calculated by using eq (135) with $k_3 = k_q^{\text{en}} = 8.1 \times 10^7$ M⁻¹ s⁻¹, $k_7 = 2.1 \times 10^9$ M⁻¹ s⁻¹, and k_8 is negligibly small.

addition, the photo-oxidation of 2 was completely inhibited by DABCO, a singlet oxygen inhibitor (Table 6), present in 3-fold excess (inhibitor/substrate). Eq (123) was unaffected, within the error of our experiment (±10%), when conducted in the presence of DTBP, a free radical inhibitor (Table 7), present in 3- and 10-fold excess.

These product distribution and inhibitor studies clearly establish that $^1\mathrm{O}_2$ is the principal oxidant generated from the reaction between electronically excited $[\mathrm{M}_6\mathrm{X}_8]\mathrm{Y}_6{}^{2-}$ cluster ions and O_2 , and that the reaction is substrate independent in our systems. The production of $^1\mathrm{O}_2$ as the photo-oxidant, though, does not necessarily imply that it is the primary photoproduct. As described above, the cluster excited states are sufficiently strong reducing agents to produce the superoxide ion. Recombination of oxidized cluster ion $[\mathrm{M}_6\mathrm{X}_8]\mathrm{Y}_6^-$ and O_2^- by electron transfer is sufficiently energetic to leave oxygen in either its $^1\mathrm{\Delta}_g$ or $^1\mathrm{\Sigma}_g$ excited states. Although the results of the free-radical inhibition studies may not appear to be consistent with this conclusion, it is possible that under our experimental conditions, the superoxide anion may actually react with DTBP, but too slowly to indicate any radical reactivity.

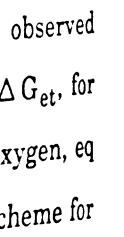
Insight into the nature of the primary photoprocess for the reaction of electronically excited $[M_6X_8]Y_6^{2-}$ ions with oxygen is provided by analysis of the free energy dependence of the quenching rate constants for eqs (121) and (122). Let us begin by considering the electron transfer pathway. The classical theory of outer-sphere electron transfer predicts that the rate of quenching of an electronically excited molecule by an oxidant or reductant, k_q^{et} , at modest free energy driving forces, ΔG_{et} , is given by the Marcus expression, 212

$$\ln k_q^{\text{et}} = \left\{ \ln \left[\frac{2H_{AB}^2}{\cancel{\pi}} \left(\frac{\pi^3}{\lambda k_B T} \right)^{1/2} \right] - \frac{\lambda}{4k_B T} \right\} - \frac{1}{2} \frac{\Delta G_{\text{et}}}{k_B T}$$
 (130)

where H_{AB} is the electronic coupling matrix element and λ is the sum of the inner and outer sphere reorganizational energies. For a homologous series of molecules, which are electronically and structurally related, H_{AB} and λ will be constant;²⁰² and eq (130) predicts that a plot of the k_BT $\ln(k_q^{\text{et}})$ vs. ΔG_{et} , Figure 17, should be linear with a slope -0.5 and an intercept given by the argument of the logarithm on the rhs of eq (130). A slope of -0.09 and a poor linear correlation of this plot (ΔG_{et} 's are given in Table 5) for the one-electron reduction of oxygen by the homologous series of $[M_6X_8]Y_6^-$ cluster ions are clearly incompatible with a quenching mechanism proceeding exclusively by electron transfer.

Conversely, the observed quenching rate constants are better correlated to the driving force for energy transfer eq (121). Ignoring the $[W_6I_8]Y_6^{2-}$ cluster ions for the moment, inspection of Figure 18 reveals that the observed quenching rates of the $[M_6X_8]Y_6^{2-}$ $[M=M_0,W;X=Cl,Br]$ clusters are relatively independent of the energy transfer driving force. Acknowledging small differences in rates among the $[M_6X_8]Y_6^{2-}$ $(M \neq W;X \neq I)$ series, which can be attributed to minor differences in the electronic structures of the $[M_6X_8]$ core, a constant value of $k_q^{obs} = 8.1(3.7) \times 10^7 \, M^{-1} \, s^{-1}$ is observed for this cluster series. This result can be understood within the context of current energy transfer theories. Specifically, Balzani and coworkers have shown²¹³ that the quenching rate constant for energy transfer, k_q^{en} , between an electronically excited donor D and acceptor A is obtained directly from

Plot of k_BT ln k_q^{obs} , where ln k_q obs is the logarithm of the observed quenching rate constant, vs. the free energy driving force, ΔG_{et} , for electron transfer from electronically excited $[M_6X_8]Y_6^{2-}$ to oxygen, eq (122). Values of ΔG_{et} are given in Table 5. The numbering scheme for different clusters is given in Tables 4 and 5.



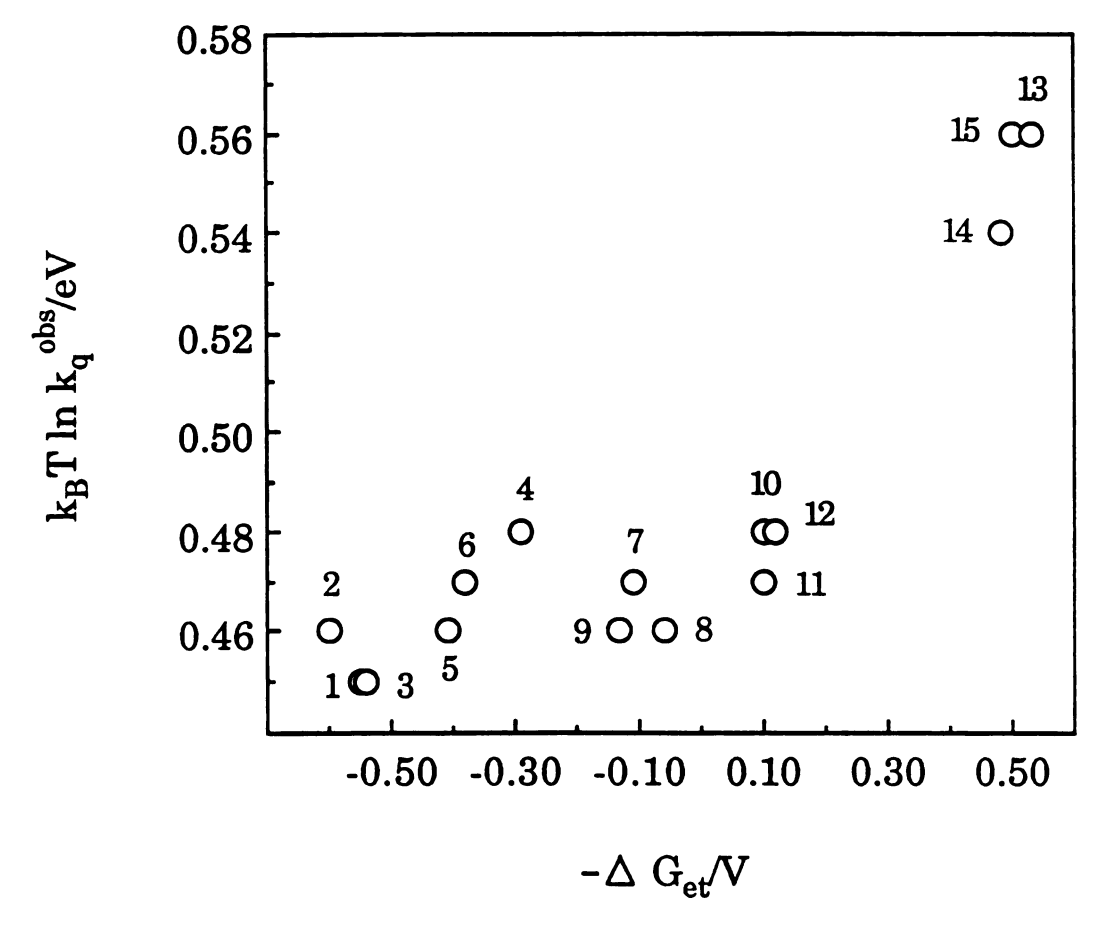


Figure 17

Plot of the logarithm of the observed quenching rate constant vs. the free energy driving force, ΔG_{en} , for energy transfer from electronically excited $[M_6X_8]Y_6^{2-}$ to oxygen, eq (121). Values of ΔG_{en} are given in Table 5. The numbering scheme for different clusters is given in Tables 4 and 5.

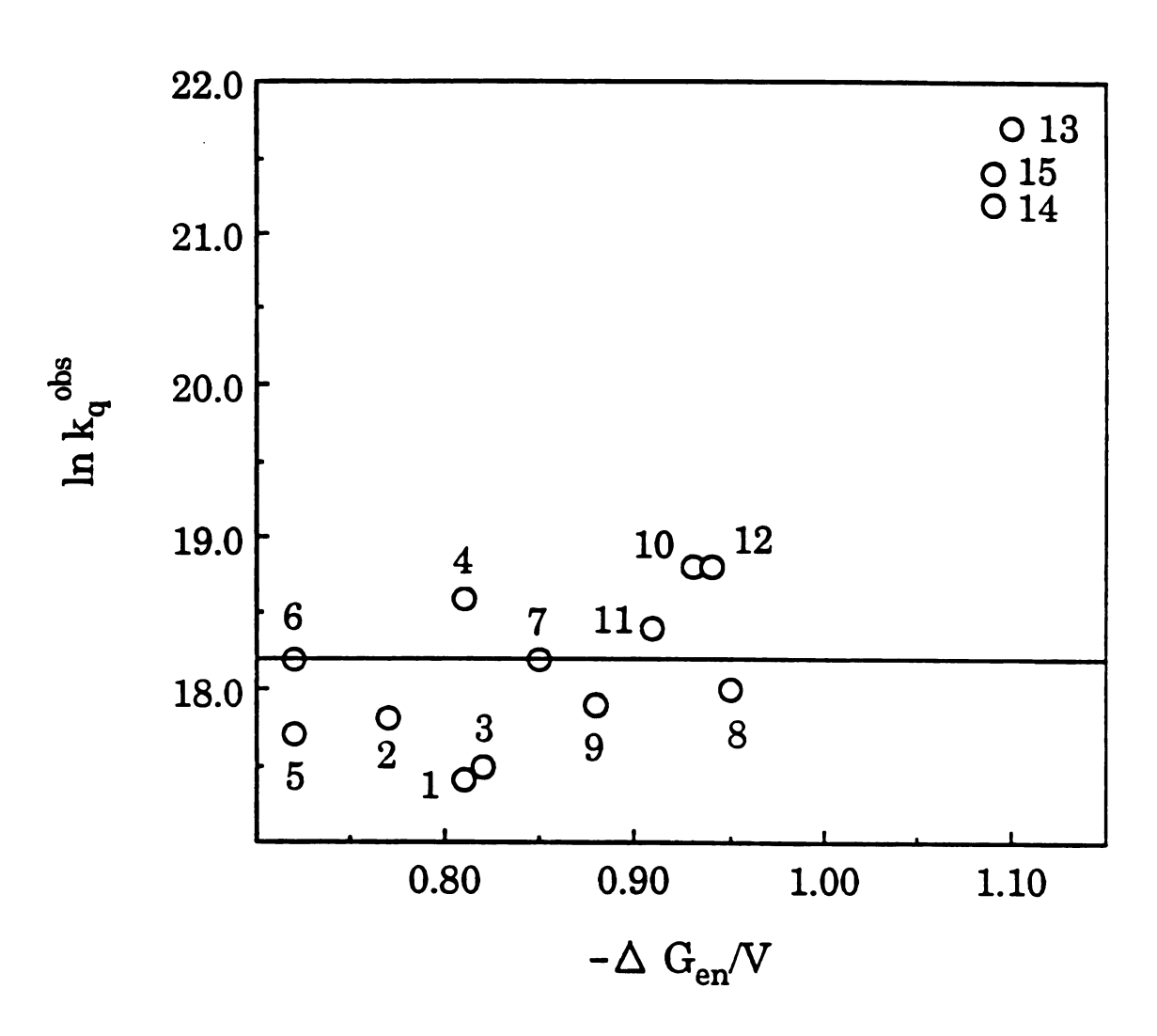


Figure 18

$$D^* + A = \frac{k_d}{k_{-d}} \quad D^* - A = \frac{k_{en}}{k_{-en}} \quad D - A^* = \frac{k_{-d}}{k_d} \quad D + A^* \quad (131)$$

coupling Agmon and Levines' free energy relationship²¹⁴ to absolute rate theory, and is given by

$$k_{q}^{en} = \frac{k_{d}}{1 + \exp\left(\frac{\Delta G_{en}}{k_{B}T}\right) + \frac{k_{-d}}{k_{en}}} \left\{ \frac{\Delta G_{en} + \frac{\Delta G_{en}^{\ddagger}(0)}{\ln 2} \ln\left[1 + \exp\left(-\frac{\Delta G_{en} \ln 2}{\Delta G_{en}^{\ddagger}(0)}\right)\right]}{k_{B}T} \right\}$$
(132)

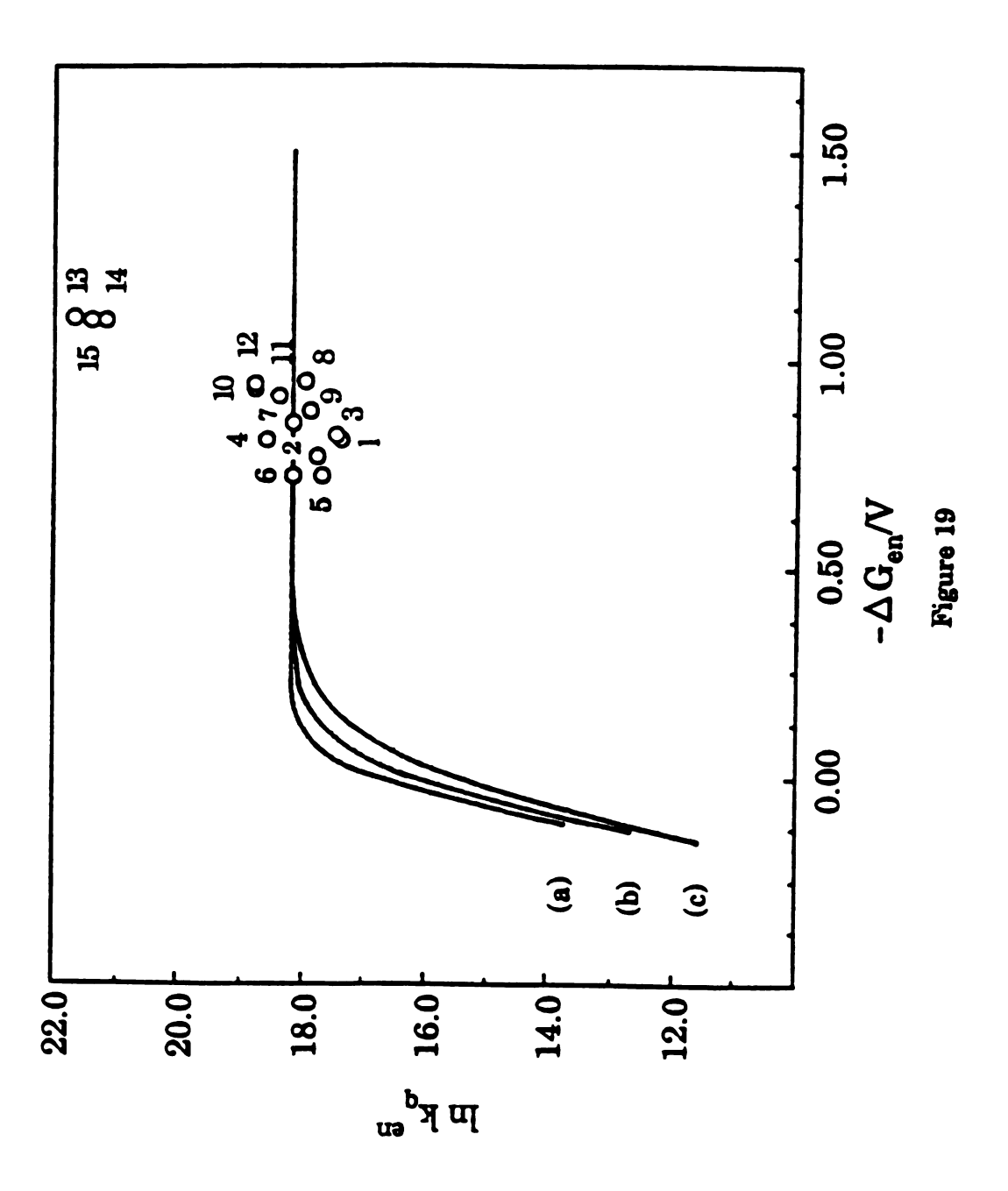
In the above expression ΔG_{en} is the free energy driving force for energy transfer, $\Delta G_{en}^{\dagger}(0)$, which is the free energy of activation for the energy transfer process with $\Delta G_{en}=0$, is the sum of the inner and outer sphere reorganizational energies associated with relaxation of D* to ground state and promotion of A to its excited state, and k_{en}° is the usual pre-exponential factor given by $k_{en}(k_BT/\pi)$ where the transmission coefficient k_{en} is the product of nuclear and electronic factors. Parallel to electron transfer kinetics schemes, k_d , k_{en}° , and $\Delta G_{en}^{\dagger}(0)$ are constant for the reaction between a quencher and a homologous series of electronically and structurally related excited states. In this case, two limiting regimes follow directly from eq (132): at large ΔG_{en} , $\ln(k_q^{en})$ will be constant and equal to either k_d for $k_{en}^{\circ} * k_d$ or equal to $k_{en}^{\circ}(k_d/k_{-d})$ for $k_{en}^{\circ} < k_{-d}$; and for small ΔG_{en} , $\ln(k_q^{en})$ will linearly increase with a slope of (1/k_BT) as ΔG_{en} increases. These two limiting regimes are interconnected by a monotonic increase of $\ln(k_q^{en})$ with ΔG_{en} as described by eq (132). This nonlinear

regime will span a larger range of ΔG_{en} with increasing $\Delta G_{en}^{\dagger}(0)$. Thus the functional dependence of the energy transfer quenching rate constant on the free energy driving force of a given system can be ascertained simply with a knowledge of $\Delta G_{en}^{\dagger}(0)$. In contrast to electron transfer reactions, the outer-sphere contribution to the activation free energy is typically negligible because the net charges of the reactants are not changed upon Consequently, $\Delta G_{en}^{\dagger}(0)$ only reflects the energy energy transfer. associated with the inner sphere reorganizations of the donor and acceptor molecules. For eq (121), inner-sphere reorganizational energies arise from the exchange of electrons among the frontier orbitals of the cluster core and oxygen. Spectroscopic 133a and theoretical 136,137 results establish that the HOMO and LUMO orbitals are primarily metal in character and possess e_g and a_{2g} molecular symmetries, respectively. In this regard, the cluster ion is brought to ground state during collisional energy transfer by the simultaneous removal of an electron from the antibonding \mathbf{a}_{2g} orbital and population of the bonding eg level. Oxygen is promoted to its lowest energy singlet state by spin-pairing the electrons residing in the p π orbital. For the latter process, the oxygen bond length increases by $< 0.01 \text{ Å}.^{215}$ For the former, crystal structure²¹⁶ and epr data^{133a} of M₆X₁₄-ions reveal few structural differences from that of the parent dianion; electron transfer measurements show an inner sphere reorganizational energy of $\leq 0.2 \text{ eV}$ for the $M_6X_{14}^{2-}/M_6X_{14}^{3-}$ exchange,²¹⁷ which involves the interchange of an electron between the a_{2g} metal-based molecular orbitals. On this basis, the upper limit for the total reorganizational energy of eq (121) is ≤ 0.2 eV and thus the free energy of activation, as is typical of most energy transfer processes involving transition metal complexes, will be small ($\Delta G_{en}^{\dagger}(0)$ ~ 1500 cm⁻¹). According to eq (132), the large free energies of eq (121) (Table 5)

as compared to this relatively small $\Delta G^{\ddagger}_{en}(0)$ will be manifested in quenching rate constants that are independent of ΔG_{en} . Indeed, this predicted behavior is observed. Figure 19 shows a plot of $\ln(k_q^{en}) \, \textit{vs.} \, \Delta \, G_{en}$ as determined from eq (132) for the homologous cluster series, for $\Delta G_{en}^{\dagger}(0)$ values of 0.10 eV, 0.15 eV, and 0.20 eV (the upper limit). The observed quenching rate constants for the $[M_6X_8]Y_6^{2-}$ cluster ions $(M \neq W, X \neq I)$ are identical within the experimental error of our Stern-Volmer measurements to the theoretical curve. The best fit of the experimental data to eq (132) yields an asymptotically limiting value of $k_q^{en} = 8.0 \times 10^7 M^{-1}$ s⁻¹. The good agreement between the observed quenching rate constants and eq (132) suggests that the primary photoprocess between oxygen and the electronically excited $[M_6X_8]Y_6^{2-}(M \neq W, X \neq I)$ cluster ions is direct energy transfer. It is important to note that the energy transfer rates of the $[M_6X_8]Y_6^{2-}$ and $[W_6I_8]Y_6^{2-}$ ions cannot be related by a unique fit to a single curve described by eq (132). If this were the case, the energy transfer rates of the [M₆X₈]Y₆²- ions would be activated. However, owing to the large driving forces of the energy transfer reactions of the $[M_6X_8]Y_6^{\,2-}$ series, activation-controlled energy transfer rates will be observed for ΔG_{en}^{\dagger} > 12,000 cm⁻¹. Because such large activation energies are without precedence in the energy transfer chemistry of transition metal complexes and more importantly entirely inconsistent with the reorganizational energies of these cluster compounds, the anomalous behavior of the $[W_6I_8]Y_6^{2-}$ series cannot reasonably be ascribed to the activated energy transfer. Thus, the order of magnitude increase in the quenching rate constant of the [W₆I₈]Y₆²⁻ ions presages either more efficient energy transfer quenching of these ions by oxygen or a contributing quenching pathway in addition to energy transfer (vide supra).

Figure 19

Free energy dependence of the rate constant for energy transfer, calculated by evaluating eq (132) with $k_d = 1.0 \times 10^{10} \, \text{M}^{-1} \, \text{s}^{-1}$, $k_{-d} = 1.2 \times 10^{10} \, \text{M}^{-1} \, \text{s}^{-1}$, $k_{en}^{\ 0} = 9.4 \times 10^7 \, \text{s}^{-1}$, $T = 298 \, \text{K}$, and $\Delta \, \text{G}^{\ddagger}_{en}(0)$ values of (a) 0.10 eV, (b) 0.15 eV, and (c) 0.20 eV. The solid line is the theoretical fit to the experimental data (O). The numbering scheme for different clusters is given in Tables 4 and 5.



isfer,

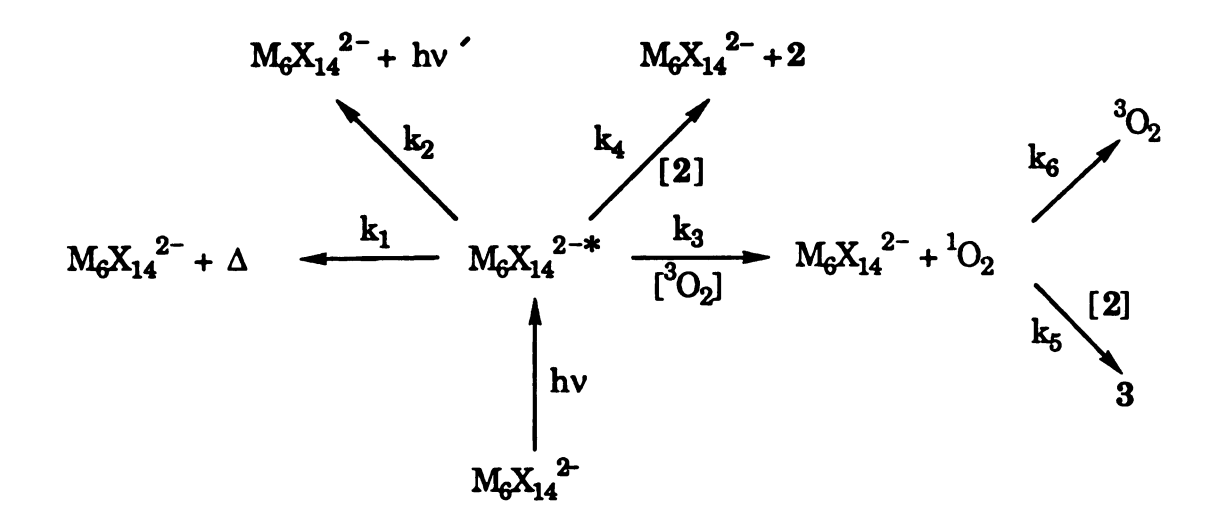
1.2 x

0.10

the

rs is

The analysis of the quenching rate constants by classical electron and energy transfer models is supported by the kinetics of cluster-sensitized photo-oxidation of olefins such as 2,3-diphenyl-p-dioxene 2. Scheme I shows the excited state decay pathways and reactions for $[M_6X_8]Y_6^{2-}$ in the presence of oxygen and 2. Internal conversion to the long-lived



Scheme I

triplet which characterizes these $[M_6X_8]Y_6^{2-}$ complexes, is fast and hence reaction from the initially prepared singlet excited state of the cluster ion need not be considered. In Scheme I, bimolecular rates for oxygen and substrate quenching, k_3 and k_4 respectively, are directly competitive with the unimolecular rates for intrinsic nonradiative (k_1) and radiative (k_2) decay. The overall kinetics for the appearance of oxidized olefin 3 will be mediated by the trapping efficiency of 2 with respect to unimolecular conversion of ${}^{1}O_2$ ground state (defined by rate constants k_5 and k_6 , respectively). By using steady-state approximations, the overall quantum yield for the cluster-sensitized production of 3, $\Phi_p(3)$, is derived to be

$$\Phi_{p}(3) = \left(\frac{k_{3}[^{3}O_{2}]}{(1/\tau_{1}) + k_{3}[^{3}O_{2}] + k_{4}[2]}\right) \left(\frac{k_{5}[2]}{(1/\tau_{2}) + k_{5}[2]}\right)$$
(133)

where $\tau_1 = (k_1 + k_2)^{-1}$ and τ_2 , equal to k_6^{-1} , is the lifetime of singlet oxygen in acetone. In the above expression, the observed quenching rate constant is defined by k_3 . Inasmuch as the rate constants in eq (133) are known, $\Phi_p(3)$ can be explicitly calculated. Table 9 lists the observed quantum yields for photosensitized production of 3 as well as the values calculated from eq (133). The observed quantum yields for $[M_6X_8]Y_6^{2-}$ -sensitized (X \neq I) reactions are in good agreement with those expected for an exclusive singlet oxygen quenching mechanism whereas the $[W_6I_8]Y_6^{2-}$ ions, parallel to Stern-Volmer quenching results, exhibit anomalous behavior.

An obvious explanation for the behavior of the $[W_6I_8]Y_6^{2-}$ system is that the quenching reaction does not proceed solely by energy transfer but also includes an additional contribution from electron transfer. In this case, Scheme I should be expanded to include electron transfer quenching of the $[W_6I_8]Y_6^{2-}$ excited state as well as the back reactions between the primary photoproducts to yield oxygen in its excited singlet (eq (134a)) and ground triplet (eq (134b)) states. Inclusion of eqs (134a) and (134b) in

$$[W_6I_8]Y_6^{2-*} + {}^3O_2 \xrightarrow{k_7} [W_6I_8]Y_6^{-} + O_2^{-} \xrightarrow{k_8} [W_6I_8]Y_6^{2-} + {}^1O_2 \quad (134a)$$

$$[W_6I_8]Y_6^{2-*} + {}^3O_2 \xrightarrow{k_7} [W_6I_8]Y_6^{-} + O_2^{-} \xrightarrow{k_9} [W_6I_8]Y_6^{2-} + {}^3O_2 \quad (134b)$$

Scheme I modifies the expression for the overall observed quantum yield as follows.

$$\Phi_{p}(3) = \left\{ \frac{k_{3}[^{3}O_{2}] + \left(\frac{k_{7}k_{8}}{k_{8} + k_{9}}\right)[^{3}O_{2}]}{(1/\tau_{1}) + (k_{3} + k_{7})[^{3}O_{2}] + k_{4}[2]} \right\} \left(\frac{k_{5}[2]}{(1/\tau_{2}) + k_{5}[2]} \right)$$
(135)

where k_q^{obs} is now equal to the sum of the energy and electron transfer rate constants $(k_3 + k_7)$. The partitioning of the back electron transfer reaction between chemiluminescent and ground state pathways (i.e. the chemiluminescence efficiency = $k_8/(k_8 + k_9)$) can be calculated directly from eq (135) with knowledge of the energy and electron transfer rate constants. Assuming for the moment that the energy transfer quenching rate constant of the $[W_6I_8]Y_6^{2-}$ clusters is the same as that for the remaining members of the homologous series (from Figure 19, k_q^{en} = 8.1 x 10⁷ M⁻¹ s⁻¹), an electron transfer rate of 2.1 x 10⁹ M⁻¹ s⁻¹ is determined from the $k_q^{obs}([W_6I_8]Y_6^{2-})$ values listed in Table 4. Solving eq (135) for $k_8/(k_8 + k_9)$ yields a chemiluminescence efficiency of 83%. On this basis, quenching is predicted to proceed predominantly by electron transfer and therefore nearly exclusive production of $[W_6I_8]Y_6^{-}$ and O_2^{-} should be observed.

Yet transient absorption experiments do not show any evidence of the $[W_6I_8]Y_6^-$ ion. The transient absorption spectrum of oxygenated solutions of $W_6I_{14}^{2-}$ is representative of those for each of the $[W_6I_8]Y_6^{2-}$ ions. Figure 20 compares the spectra of transients produced upon excitation of deoxygenated CH₃CN solutions containing $W_6I_{14}^{2-}$ and $W_6I_{14}^{2-}$ /TCNE to a CH₃CN solution of $W_6I_{14}^{2-}$ saturated with oxygen. We initially consider the transient spectrum of $W_6I_{14}^{2-}$ in the absence of oxygen. The appearance of an intense transient absorption feature at 490 nm is consistent with the expected red-shift of the lowest energy ligand-to-metal

Figure 20

Transient difference spectra for $W_6I_{14}^{2-}$ in deoxygenated CH_3CN (O), $W_6I_{14}^{2-}/TCNE$ in deoxygenated CH_3CN (\square), and $W_6I_{14}^{2-}$ in oxygenated CH_3CN (\triangle), recorded with 355-nm excitation. All difference spectra were recorded 50 ns after the excitation pulse. The concentration of $W_6I_{14}^{2-}$ in CH_3CN was 8 x 10^{-4} M and that of TCNE (tetracyanoethylene) was 4 x 10^{-3} M. Deoxygenated and oxygen saturated solutions were prepared by bubbling with N_2 and O_2 , respectively.

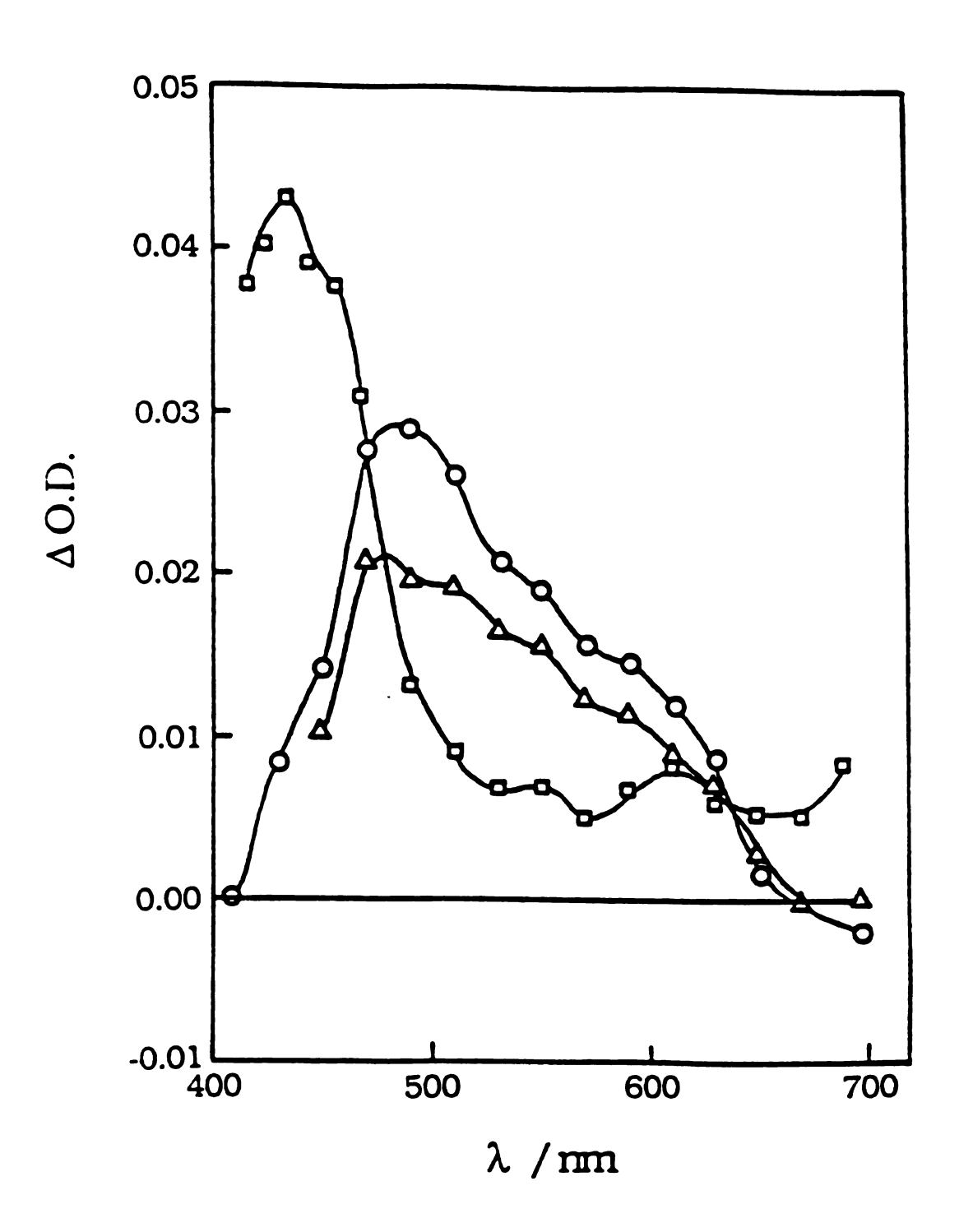


Figure 20

charge transfer transition upon excited-state production. 218 It is noteworthy that the spectrum of $W_6I_{14}^{2-}$ in its excited state is spectroscopically distinct from the transient profile produced upon electron transfer quenching of the excited state. The transient spectrum of $W_6I_{14}{}^{2-}$ in the presence of TCNE, which is known to be an efficient one-electron quencher of $[M_6X_8]Y_6^{2-}$ excited states, ^{133a} is dominated by bands at 435 and 610 nm and a shoulder at 550 nm. The 435-nm feature is characteristic of the TCNE anion $(\lambda_{max} = 435 \text{ nm} (\epsilon = 7100 \text{ M}^{-1} \text{ cm}^{-1}))^{148}$ whereas the absorptions to the red of the TCNE band are those of the W₆I₁₄ ion. The important issue of interest here is that the transient spectrum of $W_6I_{14}^{\ 2-}$ in the presence of oxygen is identical to that of $W_6 I_{14}^{\ 2-*}$, and no evidence of the electron transfer product, W₆I₁₄-, is observed. In our experiment, the relative intensity of the transient for $W_6I_{14}^{2-*}$ is such that the electron transfer contribution, if any, to the quenching pathway must be less than 30%. These transient absorption results establish that oxygen quenching proceeds primarily by energy transfer and that our assumption of similar energy transfer rates across the [M₆X₈]Y₆²⁻ series is invalid for the [W₆I₈]Y₆²⁻ cluster species, with the latter exhibiting more efficient energy transfer reactivity.

These results suggest that the quenching rates of the $[M_6X_8]Y_6^{2-}$ ions are governed by the transmission coefficient. By using $k_d = 10^{10} \, \text{M}^{-1} \, \text{s}^{-1}$, and determining $k_{-d} = 1.2 \times 10^{10} \, \text{M}^{-1} \, \text{s}^{-1}$ from the Eigen equation, 219 a value of $k_{en}^{\,\,0} = 9.4 \times 10^7 \, \text{s}^{-1}$ for the $[M_6X_8]Y_6^{\,\,2-} (X \neq I)$ cluster ions follows directly from the limiting observed quenching rate (Figure 19). This transmission coefficient is five orders of magnitude smaller than that calculated for the the adiabatic limit, $k_{en}^{\,\,0} = k_B T/A = 3.9 \times 10^{13} \, \text{s}^{-1}$. Low values of $k_{en}^{\,\,0}$ have been observed previously for both organic $^{210,220-222}$ and inorganic $^{223-225}$

energy transfer reactions; because $k_{\rm en}^{\rm o}$ directly reflects the electronic matrix coupling element, these low values of $k_{\rm en}^{\rm o}$ have been attributed to poor orbital overlap between the donor/acceptor pair. Examples of some inorganic energy transfer systems which exhibit this phenomena are shown in Table 10.

Such an explanation for the very low k_{en}^{o} of the $[M_6X_8]Y_6^{2-}$ cluster series is particularly appropriate because energy transfer involves the overlap of localized orbitals of the metal core. The aforementioned eg HOMO and a2g LUMO orbitals, which are the crucial orbitals involved in the energy transfer process, are constructed from linear combinations of d_{xy} orbitals of adjacent metal atoms. 136 As indicated by the pictorial representation in Figure 21, the molecular orbitals are confined to a cube that inscribes the octahedral metal atoms of the cluster unit. These orbitals are masked by the eight face-bridging atoms situated at the vertices of the cube and the six axial halides juxtaposed over the faces of the cube. Photophysical and spectroscopic studies of the Mo6 clusters indicate little mixing between these metal-based orbitals 133a,133c and the ligating halides and hence the HOMO and LUMO orbitals are effectively shielded from interactions with exogenous substrates. Similarly, the axial ligands of the W₆ clusters shield the metal core and insignificantly perturb the electronic However, steady-state and time-resolved emission studies indicate that the metal-based orbitals are mixed with the face-bridging ligands and that this mixing is greatest for clusters with face-bridging iodides. 135 To this end, the simultaneous overlap of the cluster's HOMO and LUMO with the oxygen acceptor orbitals will be enhanced and therefore keno will be increased. Consequently the energy transfer

Table 10

Energy Transfer Quenching Reactions of Transition Metal Complexes

which Exhibit Low Pre-Exponential Factors

Complex	Quencher	ΔG _{en} /eV ^a	Solvent	$k_q/M^{-1} s^{-1}b$	k _{en} º/s ^{-1 c}
$\overline{\left[\mathrm{Ru(bpy)}_3\right]^{2+d}}$	O_2	-1.10	Acetone	1.8 x 10 ⁹	~10 ^{9 e}
$[Ru(bpm)_3]^{2+f}$	O_2	-1.04	Acetone	4.9×10^8	~10 ^{8 e}
$[\mathrm{Ru(bpz)}_3]^{2+g}$	O_2	-1.13	Acetone	1.9×10^8	~10 ^{8 e}
Cr(CN) ₆ ²⁻ Cr(en) ₆ ³⁺	Napthalene Napthalene	-1.10 -0.78	Mixed ^h Mixed ^h	1.7×10^{8} e 6.2×10^{7} e	2.2×10^8 7.5×10^7

^a Standard free energy change for the energy transfer reaction between M* and Q; $\Delta G_{en} = -\{E_{0,o}([M]^*) - E(Q)\}$. ^b Rate constant for quenching of transition metal complex by quencher. ^c Pre-exponential factor as defined in text. ^d (bpy) = Bipyridine. ^e Reference 225. ^f (bpm) = Bipyrimidine. ^g (bpz) = Bipyrazine. ^h Mixed solvent system: 50% EtOH-Water. ⁱ Reference 223.

Figure 21

Depiction of the e_g and a_{2g} metal based cluster orbitals.

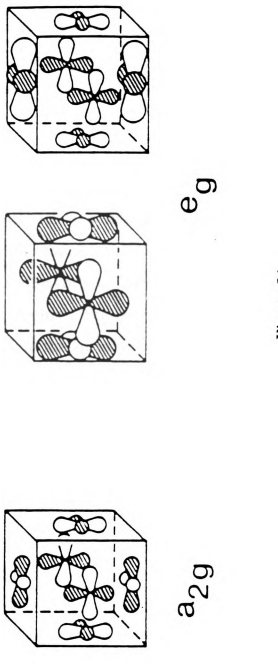


Figure 21

quenching rate constant will also increase. In agreement with previous spectroscopic studies, our quenching results suggest that this increase is most important for the tungsten clusters possessing face-bridging iodides. The enhanced energy transfer rates of the $[W_6I_8]Y_6^{2-}$ clusters can be accounted for with an increase of $k_{en}^{\,0}$ from 9.4 x 10^7 s⁻¹ for the $[M_6X_8]Y_6^{2-}$ (M \neq W and X \neq I) to 2.4 x 10^9 s⁻¹ for the $[W_6I_8]Y_6^{2-}$ species. It is noteworthy that despite this increase, $k_{en}^{\,0}$ has not attained the adiabatic limit.

B.4. Conclusion

Thus, electronically excited $[M_6X_8]Y_6^{2-}$ ions react with oxygen exclusively by energy transfer to produce singlet oxygen. Generation of singlet oxygen by electron transfer between one-electron oxidized cluster and the superoxide ion is efficiently circumvented by the competitive energy transfer process despite the high free energy driving forces associated with the former pathway. That the quenching rates of the $[M_6X_8]Y_6^{2-}(M =$ Mo,W; X = Cl, Br) ions are small and similar is entirely consistent with a highly nonadiabatic exchange resulting from poor overlap of the oxygen acceptor orbitals with the sterically shielded frontier orbitals of the cluster core. The anomalous behavior of the [W₆I₈]Y₆²⁻ clusters is in accordance with increased electronic coupling arising from mixing between the orbitals of the metal core and the face-bridging iodides. The absence of an electron transfer contribution to the [M₆X₈]Y₆²⁻-cluster photosensitized production of ${}^{1}O_{2}$ parallels the results of RuL_{3}^{2+} (L = polypyridyl) systems 112a,225 and contributes to the emerging trend that reaction of electronically excited transition metal complexes with oxygen will proceed by energy transfer even in the presence of potentially competitive exergonic electron transfer pathways.

On a less fundamental level, our studies also possess significance of a more applied nature. The results of our investigations have identified the $[M_6X_8]Y_6^{2-}$ cluster ions as excellent homogeneous 1O_2 generation catalysts. In solution the clusters are structurally robust, 1O_2 generation occurs with no detectable superoxide anion formation, and olefinic substrates are oxidized with greater than 80% efficiency. In this regard, we became interested in binding these clusters to insoluble supports and studying the reactions of these bound clusters as heterogeneous catalysts. These investigations are presented in the following section.

C. Heterogeneous Reactions

C.1. Background

Singlet oxygen chemistry has been limited in many instances by the need for reliable sources of singlet oxygen. Sensitizers must be capable of inducing reaction with visible light, possess chemical stability and good light absorption properties, exhibit solubility in water but allow easy removal from solution, and lack troublesome side reactions or complicated operating conditions. Many of these obstacles can be overcome with the development of polymer bound photosensitizers.

Photochemical catalysts have been bound to insoluble polymers by use of solid phase synthesis, resulting in the creation of "sensitizers of choice." These polymer bound photosensitizers increase the stability of the sensitizer in solution and the range of useful solvents. The sensitizer is easily removed from solution by filtration or centrifugation and can be used, in general, without loss of efficiency. An additional benefit, which is useful in systems exhibiting self-quenching, is that sensitizers bound to a polymeric backbone are site isolated and consequently decreased self-

quenching may be exhibited between sensitizer molecules. One disadvantage of these systems, though, is that some difficulty may arise in analyzing residues attached to polymeric materials versus the residue in free solution.²²⁶

Insoluble polymer supports were introduced in the mid 1960's by Merrifield²²⁷ and Letsinger²²⁸ in order to facilitate polypeptide synthesis. The methodology is based on carrying out successive chemical transformations on insoluble polymer beads. This approach was extended to photosensitizers, with the rationale that if energy transfer donors could be immobilized on insoluble polymer beads and the properties of the immobilized sensitizer were similar to those of the sensitizer in solution, then one might effect energy transfer. In the early 1970's, the first heterogeneous singlet oxygen sensitizer was prepared with polymer ester Rose Bengal (a uranine dye) or Sensitox I. Typically, this polymer is made from poly(styrene covinyl benzyl chloride) by nucleophilic displacement using the C-2' carboxylate of the dye. This work lead to development of other polymer bound organic sensitizers²²⁹⁻²³⁰ and their use in other heterogeneous media²³¹ such as membranes,²³² vesicles,²³³ micelles,²³⁴ Nafion powders.²³⁵ and zeolites.¹⁹⁹

Transition metal complexes bound to polymeric materials have since been developed. 198a-c These transition-metal-complex photosensitizers, which have been bound to many of the same heterogeneous media as their organic analogues, 198a, 199, 236 have proved quite popular for a variety of reasons. They tend to absorb and emit intensely, can be tuned over a wide range of excited state energies by small variations in the ligation coordination sphere, and above all, are robust in solution. One fundamental advantage of metallopolymer sensitizers, over the organic

analogues, is that organic sensitizers are susceptible to attack by singlet oxygen resulting in the bleaching of the sensitizer off of the polymer, whereas transition metal complexes, in general, do not bleach.

There are three general approaches to the design of polymer-based photosensitizers: 156 (1) incorporation of the sensitizer into a polymeric thin film by dissolving the sensitizer and polymer in a solvent and depositing the polymer/sensitizer solution on a flat surface; (2) immobilization of the sensitizer by absorption onto the solid support (generally silica gel); this is a convenient method, but the sensitizer is often easily eluted by polar solvents; and (3) covalent or electrostatic binding of the sensitizer to crosslinked polymer beads or specially functionalized silica gels; these polymeric sensitizers are generally prepared via chemical reaction of the sensitizer with functionalized polymer. The most frequently used insoluble polymer is polystyrene cross-linked with divinyl benzene. These are highly crosslinked or "macroreticular" copolymers with functionalities on the aromatic ring, allowing attachment of smaller reagents.

The clusters are extremely versatile sensitizers for polymer modification since the M_6X_{12} complexes contain two vacant axial sites that may be coordinated by free nucleophiles in solution, such as nitrogen, ²³⁷ phosphine, ²³⁸ and alkoxide donor ligands. ²³⁹ Either or both of these sites should be capable of binding to the nucleophilic side chain of the polymer. Also, the $[M_6X_8]Y_6^{2-}$ derivative should bind electrostatically to polymers with positively charged sites. Indeed several recent studies conducted in our laboratories have successfully shown $[M_6X_8]Y_6^{2-}$ cluster ions to be bound to methylated polyvinylpyridine, $[(PVP-Me^+)_2[M_6X_8]Y_6^{2-}]$ depicted in Figure 22.²⁴⁰ In addition, Dr. M. Newsham has attached the M_6X_{12}

Figure 22

Model depicting $Mo_6Cl_{14}^{\ 2-}$ electrostatically bound to methylated polyvinylpyridine.

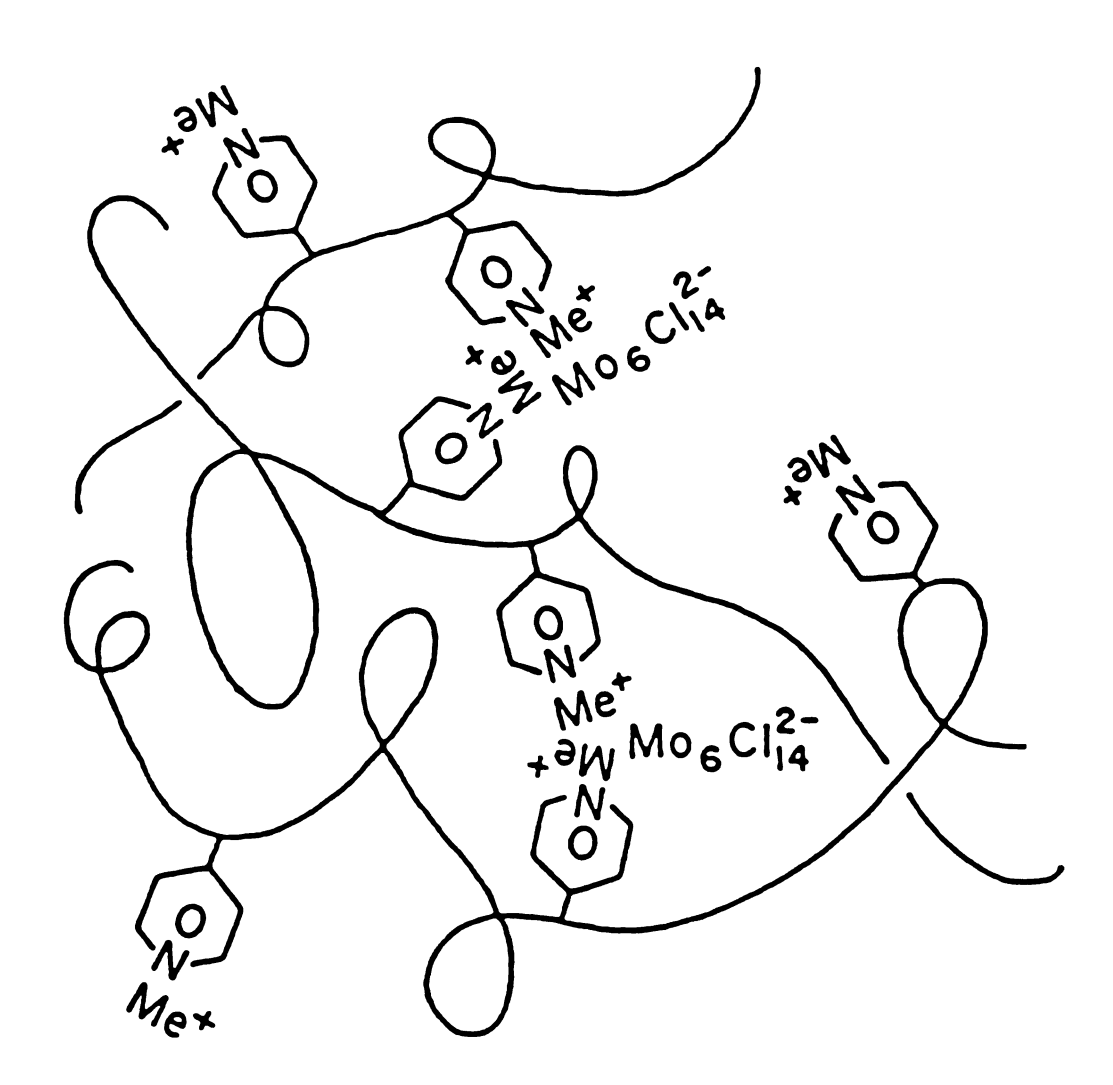


Figure 22

derivative covalently to the inorganic polymer chains of silicon oxide gels. 138

The main goals of the studies presented in this section are to prepare organic polymer beads covalently coordinated with M_6X_{12} units and to characterize the singlet oxygen energy transfer properties of the polymer bound cluster derivatives. The polymer used in these studies is Reillex 402^{TM} 15 or 4-polyvinylpyridine that is 2% crosslinked with divinylbenzene. This polymer has a high density of pyridyl binding sites (8 meq/g), which

$$\binom{n}{N}$$

15

exhibit a pK_a of ~3-4. The swelling properties of the polymer are listed in Table 11. Since this material is only 2% crosslinked, it should exhibit properties of both a gel and a macroreticular polymer. Thus, for our studies, this support is ideal because it is structurally well-defined, yet exhibits sufficient flexibility to allow oxygen to permeate the polymer and come in contact with bound cluster. A secondary goal of these studies is to probe the nature of the binding site of the immobilized sensitizer by luminescence measurements.²⁴¹

Table 11 Swelling Properties of Reillex TM 402 (Data Courtesy of Reilly Tar and Coal Company)

Solvent	% Swelling ^a	
5%HCl	100 b	
Methanol	70 - 7 5	
Water	33 - 37	
Acetone	30 - 35	
Isopropanol	13 - 17	
Toluene	8 - 12	
Ethyl Acetate	3-6	
Hexane	0	

a Percent swelling from dry state to solvent saturated state. b Percent swelling from free base to hydrochloride form, in water.

C.2. Results and Discussion

Our initial experiments were concerned with the binding of $\mathrm{Mo_6Cl_{12}}$ to polymer beads and the subsequent characterization of this material as a singlet oxygen sensitizer. The polymer was covalently modified by heating MeOH solutions of $\mathrm{Mo_6Cl_{12}}$ in the presence of Reillex 402^{TM} beads (2% crosslinked 4-polyvinylpyridine). The $\mathrm{Mo_6Cl_{12}}$ derivatized polymer was washed with copious quantities of MeOH ensuring that no free $\mathrm{Mo_6Cl_{12}}$ remained admixed with the polymer. As an added precaution, $\mathrm{Mo_6Cl_{12}}$ modified polymer was refluxed for 24 h in MeOH to ensure that the sensitizer was chemically bound to the polymer structure and not simply trapped in the polymer matrix. Electronic absorption spectra of the filtered supernatant liquid indicate a maximum binding of 3.5 x 10^{-3} moles of $\mathrm{Mo_6Cl_{12}}$ per gram of polymer is achieved. Typical experiments employed polymer $\mathrm{Mo_6Cl_{12}}$ containing 8.8 x 10^{-4} moles of $\mathrm{Mo_6Cl_{12}}$ per gram of polymer (Derivative 2). Modified polymers by this method are hereafter designated as $\mathrm{P-Mo_6Cl_{12}}$.

Photo-oxidation of 2,3-diphenyl-p-dioxene 2 with P-Mo $_6Cl_{12}$ in acetonitrile, as shown in eq (123), gave ethylene glycol dibenzoate 3 in 100% yield. Absorption spectra of the reaction solution before and after photolysis showed that no Mo $_6Cl_{12}$ had leached into the solution during reaction. Similar to the photosensitized reactions in homogeneous solution, the photo-oxidation of 2 was inhibited by DABCO, but was unaffected when conducted in the presence of the free radical inhibitor DTBP. The results of these experiments are summarized in Table 12. These trapping studies indicate that the oxidation of 2 is an authentic singlet oxygen reaction sensitized by P-Mo $_6Cl_{12}$.

Table 12 $\label{eq:photo-Oxidation} Photo-Oxidation of 2,3-Diphenyl-p-Dioxene \ 2$ with P-Mo $_6$ Cl $_{12}$ in Acetonitrile

Experiment Number	Reaction Conditions ^a	% Reaction After 2 h ^b
1	$2 (6.0 \times 10^{-3} \text{ M})$ 100 mg Reillex $402^{\text{TM c}}$	No Reaction
2	$2 (6.0 \times 10^{-3} \text{ M})$ $70 \text{ mg P-Mo}_6\text{Cl}_{12}$	30%
3	2 (6.0 x 10 ⁻³ M) 70 mg P-Mo ₆ Cl ₁₂ DABCO (2.5 x 10 ⁻² M)	2%
4	$2 (6.0 \times 10^{-3} \text{M})$ $70 \text{ mg P-Mo}_6 \text{Cl}_{12}$ DTBP $(2.2 \times 10^{-2} \text{ M})$	27%

^a Reaction mixtures were irradiated using a 436 nm cutoff filter. P- Mo_6Cl_{12} with a loading of 8.4 x 10^{-4} moles cluster/g polymer was used in all experiments. ^b \pm 5%. ^c Unbound 4-polyvinylpyridine.

As illustrated in Section III.B, another criterion for the generation of free singlet oxygen is the characteristic product distributions obtained from the photo-oxidation of 1-methylcyclohexene 7, and 1,2-dimethylcyclohexene 8. As in the homogeneous system, photo-oxidation of 7 and 8 with P- Mo_6Cl_{12} yields the characteristic ene product distributions; these are reproduced in Table 13. For purposes of comparison, the product distributions of $Mo_6Cl_{14}^{2-}$ and Rose Bengal in homogeneous solution are also shown. Not only are these product distributions independent of solution medium (homogeneous vs. heterogeneous), but in the case of 1,2-dimethylcyclohexene 8, the distribution is independent of the identity of the sensitizer.

The oxidation of 2 to 3 may also be conducted in mixed solvent systems such as 1:1 water:acetonitrile, where the water content is limited by the solubility of the organic substrate. Irradiation of a sample containing 2, P-Mo₆Cl₁₂, and acetonitrile for 4 h in a pyrex vessel, using a 1000W Hg/Xe arc lamp or sunlight with a water filter to reduce IR sample heating, showed negligible leaching of the cluster from P-Mo₆Cl₁₂ (less than 6%) and 100% oxidation of 2. In these samples, the IR filter is necessary because the cluster will leach from the polymer and develop a bright orange color owing to sample heating during photolysis. Activity from these P-Mo₆Cl₁₂ derivatives has been observed for a period of over several months. Polymers derivatized with W_6I_{12} have also been attached to the Reillex 402TM polymer beads, but despite repeated washings of P-W₆I₁₂, W₆I₁₂ leaches into solution during the course of photolysis, indicating that significant quantities of W₆I₁₂ are not bound to the polymer, but probably are entrapped in the polymer matrix.

Table 13

Products of Reaction of 1-Methylcyclohexene 7, and

1,2-Dimethylcyclohexene 8, with Oxygen under Photosensitized and

Radical Oxidation Conditions ^a using Polymer Bound Sensitizers

	Products of 7			Products of 8		
Photosensitizer	9	10	11	12	13	14
P-Mo ₆ Cl ₁₂ b	74%	17%	9%	85%	15%	0%
P -Rose Bengal ^b	45%	41%	14%	86%	14%	0%
Mo ₆ Cl ₁₄ ^{2-c}	77%	23%	0%	89%	11%	0%
Rose Bengal ^c	45%	41%	14%	86%	14%	0%
Rose Bengal ^d	41%	45%	14%	89%	11%	0%
Radical Auto- oxidation ^e	36%	12%	40%	7%	39%	54%
Reillex 402 ^{TM f}	0%	0%	0%	0%	0%	0%

^a Products designated 7-14 are defined in eqs 126-129. ^b Polymer-bound sensitizer in O_2 -saturated acetonitrile solutions containing [olefin] = 2 x 10^{-2} M. ^c Irradiated ($\lambda_{\rm exc} \ge 436$ nm) O_2 -saturated acetonitrile solutions containing [$Mo_6Cl_{14}^{2-}$] = 1 x 10^{-5} M and [olefin] = 2 x 10^{-2} M. ^d Product distributions reported in Reference 208. Radical auto-oxidation of 7 yields 12% unidentified products. ^e Product distributions reported in Reference 208. ^f Unbound 4-polyvinylpyridine.

Mo₆Cl₁₂ may be bound to other polymers containing pendant nucleophilic groups such as 2% and 20% crosslinked styrene-divinyl benzene copolymer beads with pendant triphenyl phosphine groups. These derivatives exhibit behavior similar to that shown discussed above.

Insight into the nature of the binding site can be provided with photophysical studies of the cluster moiety. The luminescence properties of P-Mo₆Cl₁₂ derivatives with four different cluster loadings under various experimental conditions are displayed in Table 14. As revealed in Table 15, the lifetime behavior of the various polymers in vacuum, air, and a pure oxygen atmosphere is independent of the manner by which the derivative was prepared or stored. These excited state properties of the different polymer derivatives are similar to the model monomer complex $Mo_6Cl_{12}py_2$ (py = pyridine) which exhibits broad, featureless emission (λ_{max} = 766 nm) with an emission decay profile that can be nicely fit by a biexponential rate law (τ_1 = 8 μ sec (39%) and τ_2 = 55 μ sec (61%)). Solutions containing these polymer bound cluster derivatives saturated with N_2 and O_2 also exhibit multiexponential luminescence decays which may be fit by a biexponential rate law, the results of which are summarized in Table 16.

There are two possible explanations for this biexponential lifetime behavior: (i) two different cluster sites may exist (one which is oxygen accessible and the other which is not), or (ii) two cluster species with different lifetimes in the polymer. We favor the latter for a number of reasons. First, the biexponential lifetimes do not arise from impurities in the Mo_6Cl_{12} starting complex. Mo_6Cl_{12} was washed with organic solvents such as CH_2Cl_2 and also recrystallized in MeOH to remove any impurities. The resulting solid state lifetime data of these purified samples, shown in Table 17, remains biexponential. Size exclusion and adsorption

Table 14
Solid State Emission Lifetimes of Cluster-Incorporated
Polyvinylpyridine Polymers

Polymer Loading a/	Lifetime		τ's (μs) ^b	
(moles cluster/g PVP)	Component	Vacuum ^c	Air ^d	O ₂ e
Derivative $1/(3.1 \times 10^{-4})$	τ_1	12(42%)	10(42%)	10(43%)
	$ au_{2}$	103(58%)	80(58%)	57(57%)
Derivative $2 / (8.4 \times 10^{-4})$	τ_1	13(42%)	8(42%)	9(43%)
	$ au_2$	95(58%)	83(58%)	65(57%)
Derivative $3 / (1.9 \times 10^{-3})$	$ au_1$	11(39%)	9(45%)	9(45%)
,	$ au_2^1$	113(61%)	84(55%)	75(55%)
Derivative 4 / (3.5×10^{-3})	${f au_1}$	12(52%)	10(76%)	10(72%)
	${f au_2}$	105(48%)	99(24%)	96(28%)

^a Synthesized by addition of cluster to pretreated polymer in MeOH. Derivatives were stored under vacuum. ^b The percentages indicate total emission decay by the given lifetime component, based on 100%. ^c Lifetimes measured at ~1 x 10^{-6} torr. ^d Lifetimes measured with sample exposed to air. ^e Lifetimes measured with sample exposed to a pure oxygen atmosphere.

Table 15

Solid State Emission Lifetimes of Cluster-Incorporated

Polyvinylpyridine Polymers Synthesized under

Different Reaction Conditions

Polymer Loading/ Lifetime Preparation τ's (μs) ^a					
(moles cluster/g PVP) Co.	mponent	t Method b	Vacuum	c Air d	O_2^{e}
Derivative $1/(3.1 \times 10^{-4})$	τ ₁	Cluster →			10(43%)
	τ_{2}	Polymer f	103(58%)	80(58%)	57(57%)
Derivative $1/(3.1 \times 10^{-4})$	τ_1	Polymer →	11(39%)	11(37%)	11(40%)
	$ au_2$	Cluster ^g	113(61%)	77(63%)	50(60%)
Derivative $1/(3.1 \times 10^{-4})$	τ_1	Polymer →	13(39%)	11(45%)	12(45%)
	$ au_{2}$	Cluster h	117(61%)	80(55%)	58(55%)
Derivative $1/(3.1 \times 10^{-4})$	τ_1	Polymer →	13(34%)	12(37%)	10(42%)
	$ au_2$	Cluster ⁱ	115(66%)	84(63%)	60(58%)
Derivative $2/(8.4 \times 10^{-4})$	τ_1	Cluster →	13(42%)	8(42%)	9(43%)
	$ au_{2}$	Polymer ^f	95(58%)	83(58%	65(57%)
Derivative 2 / (8.4 x 10 ⁻⁴)	τ_1	Polymer →	11(48%)	12(38%)	7(40%)
	$ au_{2}$	Cluster ^g	102(52%)	72(62%)	64(60%)
Derivative 2 / (8.4 x 10 ⁻⁴)	τ_1	Polymer →	17(42%)	11(43%)	11(42%)
	τ_2	Cluster h	111(58%)	76(57%)	65(58%)

^a The percentages indicate total emission decay by the given lifetime component, based on 100%. ^b All synthesis done in MeOH. ^c Lifetimes measured at ~1 x 10⁻⁶ torr. ^d Lifetimes measured with sample exposed to air. ^e Lifetimes measured with sample exposed to pure oxygen atmospheres. ^f Cluster added to pretreated polymer. Product stored under vacuum. ^g Added undried polymer to cluster, product dried in air. ^h Same as e, product dried on Schlenk line. ^u Same as e, product heated to 60 °C on Schlenk line.

Table 16

Solution Emission Lifetimes of Cluster-Incorporated

Polyvinylpyridine Polymers in Various Solvents

Polymer Loading/	Lifetime	Solvent	τ's (ן	us) ^a
(moles cluster/g PVP)	Component		N ₂ b	O ₂ c
Derivative $1/(3.1 \times 10^{-4})$	τ_1	Toluene	10(55%)	10(52%)
,	$ au_{2}^{^{1}}$		95(45%)	58(48%)
Derivative 2 / (8.4 x 10 ⁻⁴)	τ_1	Toluene	7(57%)	7(51%)
	$ au_{2}^{1}$		99(46%)	60(49%)
Derivative $3/(1.9 \times 10^{-3})$	τ_1	Toluene	8(57%)	7(63%)
	$ au_{2}^{1}$		99(43%)	62(37%)
Derivative $4/(3.5 \times 10^{-3})$	τ_1	Toluene	8(65%)	7(75%)
	$ au_{2}^{1}$		96(35%)	81(25%)
Derivative $1/(3.1 \times 10^{-4})$	τ_1	MeOH	6(51%)	5(69%)
	$ au_{2}^{1}$		69(49%)	17(31%)
Derivative 2 / (8.4 x 10 ⁻⁴)	τ_1	MeOH	6(57%)	5(74%)
,	$ au_{2}^{1}$		82(43%)	23(26%)
Derivative $3/(1.9 \times 10^{-3})$	~	MeOH	<i>C(C)(</i> ()	A (7 A 07 \
Derivative 37 (1.9 x 10°)	$rac{ au_1}{ au_2}$	MeOH	6(63%) 89(37%)	4(74%) 20(26%)
3	_			
Derivative $4/(3.5 \times 10^{-3})$	1	MeOH	6(68%)	4(70%)
	$ au_{f 2}$		47(32%)	13(30%)

^a The percentages indicate total emission decay by the given lifetime component, based on 100%. ^b Lifetimes measured with sample under a nitrogen atmosphere. ^c Lifetimes measured with sample under a pure oxygen atmosphere.

Table 17
Solid State Emission Lifetimes of Relevant
Cluster Derivatives

Cluster			•	μs) ^a
		Component	Vacuum ^b	Air ^c
Mo ₆ Cl ₁₂	Stored under	τ_1	20(48%)	20(48%)
	Vacuum	$ au_{f 2}$	113(52%)	113(52%)
$\mathrm{Mo_6Cl}_{12}$	Washed in	τ_1	7(39%)	7(36%)
	$\mathrm{CH_2Cl_2}$	$ au_{2}$	45(71%)	48(64%)
Mo_6Cl_{12}	Recryst. from	τ_1	7(33%)	7(36%)
	MeOH	$ au_{f 2}$	51(67%)	40(64%)
Mo_6Cl_{12}	Bound to	τ_1	NC d	5(62%)
•	Uncrosslinked PVI	_		55(38%)
Mo ₆ Cl ₁₄ ²⁻	Stored under	τ_1	118(100%)	118(100%)
	Air	$ au_{f 2}^-$	•••	•••
Mo ₆ Cl ₁₂ I ₂ ²⁻	Stored under	τ_1	NC ^d	10(34%)
60-12-2	Air	τ_2	NC	67(66%)
Mo ₆ Cl ₁₂ (SCN) ₂ ²	Stored under	τ_1	NC d	12(37%)
0 12 2	Air	$ au_2^{ au}$	110	90(63%)
$\mathrm{Mo_6Br_{12}Cl_2}^{2-}$	Stored under	τ_1	NC ^d	11(37%)
	Air	τ_2	NC	74(63%)

^a The percentages indicate total emission decay by the given lifetime component, based on 100%. ^b Lifetimes measured with sample under a vacuum atmosphere. ^c Lifetimes measured with sample under a pure oxygen atmosphere. ^d Data not collected since sample was stored under air. Remaining samples were stored under vacuum.

chromatography performed on Mo₆Cl₁₂ yielded one broad unresolved band, suggesting that if an impurity complex is present, then it is not easily separated from Mo₆Cl₁₂. Rather, this biexponential data is consistent with the presence of *cis* and *trans* forms of the substituted cluster in the polymer matrix.

Yamaguchi and coworkers have shown that reaction of donor ligands with Mo_6Cl_{12} leads to both the cis and trans forms of $Mo_6Cl_{12}L_2$.²⁴² Along these lines, the mixture of cis and trans isomers of Mo₆Cl₁₂(P(npropyl)3)2 in the solid state exhibits biexponential lifetime behavior with lifetimes of 11 μ sec (37%) and 86 μ sec (63%), similar to the $Mo_6Cl_{12}(py)_2$ complexes. Although the evidence is not unequivocal, it is reasonable to attribute the multicomponent decay of these polymer bound clusters and the Mo₆X₁₂Y₂²⁻ derivatives to the presence of cis and trans cluster complexes on this basis. Moreover, as presented in Table 17, solid state lifetime data of a variety of $Mo_6Cl_{12}L_2^{2-}(L = SCN^-, \Gamma)$ derivatives show biexponential behavior. It is known that it is in general difficult to separate cis and trans isomers. While Mo₆Cl₁₂(P(n-propyl)₃)₂ was prepared by the method of Yamaguchi and coworkers, 242 chromatographic separation of these cis and trans isomers was not achieved due to the retention of these complexes on the Florisil column. This is not surprising, since Yamaguchi and coworkers recovered only 18% of the material after column chromatographic separation.

Thus, it is not known at this time whether the short lifetime component is that of the cis or trans isomer. However, from the data in Tables 14 - 17, it is clear that the long lifetime component is quenched significantly and the short lifetime apparently is not. Of the quenchable long lifetime component, several trends can be explained in terms of the

polymer matrix properties. The fact that the solid polymer derivatives exhibit oxygen quenching indicates that the luminescent centers are accessible to freely diffusing oxygen in the polymer matrix. In each case, that the long lifetime component of Derivative 4 is quenched to a lesser extent (10%) than the other derivatives (35%), is consistent with greater crosslinking of the former, whose synthesis involved refluxing for at least 12 h compared to 1 h of refluxing for the other derivatives.

The attenuation of the long lifetime component of these derivatives in different solvents can be directly correlated to the swelling behavior of the polymer matrix. These data for a variety of solvents are summarized in Table 16. In toluene, all derivatives exhibit the same degree of oxygen quenching shown in the solid state (Table 14). This is not surprising, since the polymer swells only 8 - 10% from the dry state. All derivatives exhibit identical behavior in MeOH, in which the polymer swells by ~70%, relative to the dry state. Oxygen quenching increases to approximately 80%, as shown by the long lifetime component, indicating that the oxygen is diffusing more freely in the polymer swelled by MeOH, than in toluene or the solid state (Table 16). In all cases, oxygen diffusion in the P-Mo₆Cl₁₂ environment does not occur as freely as in homogeneous solution. This is manifested in the Stern-Volmer quenching rate constants for $\mathbf{P}\text{-}\mathrm{Mo_6Cl}_{12}$ and $\mathrm{Mo_6Cl_{14}}^{2-}$ in homogeneous solution. The data from Table 16 shows that MeOH exhibits the most quenching, yet the quenching rate for P-Mo₆Cl₁₂ in MeOH as calculated from two point Stern-Volmer plots (nitrogen and oxygen) is less than that of $Mo_6Cl_{14}^{\ 2-}$ in homogeneous acetone solution $(k_q(P-Mo_6Cl_{12}, O_2) = 4.1 (\pm 1.0) \times 10^6 M^{-1} s^{-1})$ (average value, Table 18) and $k_q(Mo_6Cl_{14}^{2-}, O_2) = \sim 3.5 \times 10^7 M^{-1} s^{-1}$ (Table 4)).

Table 18 ${\it Rate Date for the Quenching of P-Mo_6Cl_{12}}$ ${\it in MeOH by Molecular Oxygen}$

P-Mo ₆ Cl ₁₂ Derivative	$k_q / M^{-1} s^{-1} a$	$τ_1$ (O $_2$,Calcd)/μs $^{ m b}$	τ ₁ (O ₂ ,Obsd)/μs ^c
1	4.3 x 10 ⁶	4.6	5
2	3.1×10^6	5.0	5
3	3.8×10^6	4.8	4
4	5.5 x 10 ⁶	4.4	5

^a Calculated from long lifetime component (τ_2) , data in Table 16 using singlet point Stern-Volmer analysis. ^b Calculated using Stern-Volmer analysis where $[O_2] = 1.02 \times 10^{-2} \, \text{M}$ (Wilhelm, E; Battino, R. Chem Rev. 1973, 73, 1-9). k_q is from column 2. ^c The experimental lifetime (τ_1) of P-Mo₆Cl₁₂ in oxygen saturated MeOH, from Table 16.

The pH studies, summarized in Table 19, are equally as revealing. From pH 3-6, all cluster derivatives exhibited oxygen quenching behavior intermediate between that of toluene and methanol, as expected, since the polymer swells 33-37% in water. This behavior changes significantly at pH 1, where each of these derivatives exhibits very little oxygen quenching (16-30%) of the long lifetime component Although the polymer swells to 130% vs. the dry state in 5% HCl (~pH 1), the hydrochloride is formed with the presence of hydrophilic and hydrophobic domains in the polymer. In the presence of this "new" morphology, it is more difficult for the oxygen to freely diffuse into the polymer.

On the basis of the cis and trans model for binding of the cluster to the polymer, it is reasonable to ask why the short lifetime is not apparently undergoing any appreciable quenching by molecular oxygen. We would expect oxygen accessibility to both the cis and trans sites. The short lifetime component (τ_1) may be too short to undergo quenching by molecular oxygen in the polymer matrix. τ_1 was calculated using the Stern-Volmer quenching rate constant tabulated from τ_2 experimental data (Table 18). It is reasonable to assume that both the cis and trans isomers should be quenched at the same rates by molecular oxygen according to the quenching data for homogeneous clusters and oxygen in Table 4, which indicates that changing the terminal halide cluster ligands does not perturb the energy transfer properties of these systems. τ_1 (calculated) is within the error of τ_1 (experimental), thus, it is likely that in MeOH (and other solvents in which oxygen permeates the polymer matrix) the cluster isomer that exhibits τ_1 is quenched by oxygen at the same rate as the isomer that exhibits τ_2 , but τ_1 is too short to be reflected in a significant Stern-Volmer constant.

Table 19
pH Studies of the Solution Emission Lifetimes of Cluster-Incorporated
Polyvinylpyridine Polymers

Polymer Loading/	Lifetime pH		τ's (μs) ^a	
(moles cluster/g PVP) C	omponent		$N_2^{\ b}$	$O_2^{\ c}$
Derivative $1/(3.1 \times 10^{-4})$	τ_1	6	6(44%)	5(52%)
	$ au_{f 2}^-$		77(56%)	45(48%)
Derivative $1/(3.1 \times 10^{-4})$	τ_1	5	5(48%)	4(57%)
	$ au_{f 2}^-$		76(52%)	36(43%)
Derivative $1/(3.1 \times 10^{-4})$	τ_1	3	3(58%)	4(68%)
	$ au_{f 2}^-$		63(42%)	33(32%)
Derivative $1/(3.1 \times 10^{-4})$	τ_1	1	7(54%)	6(62%)
	$ au_{f 2}^-$		43(46%)	36(38%)
Derivative $2 / (8.4 \times 10^{-4})$	τ_1	6	6(52%)	3(52%)
	$ au_{f 2}^-$		71(48%)	45(48%)
Derivative $2/(8.4 \times 10^{-4})$	τ_1	1	6(63%)	5(64%)
	$ au_{f 2}^-$		52(37%)	43(36%)
Derivative $3/(1.9 \times 10^{-3})$	τ_1	6	6(72%)	4(76%)
	$ au_{f 2}^-$		70(28%)	32(24%)
Derivative $3/(1.9 \times 10^{-3})$	τ_1	5	5(68%)	4(74%)
	$ au_{f 2}^-$		64(32%)	29(26%)
Derivative $3/(1.9 \times 10^{-3})$	τ_1	3	4(77%)	4(70%)
	$ au_{2}^{\mathbf{-}}$		58(23%)	26(30%)
Derivative $3/(1.9 \times 10^{-3})$	τ_1	1	6(66%)	6(67%)
	$ au_2^-$		44(34%)	32(33%)
Derivative $4/(3.5 \times 10^{-3})$	τ_1	6	8(69%)	7(74%)
	$ au_{2}^{2}$		64(31%)	34(26%)
Derivative $4/(3.5 \times 10^{-3})$	τ_1	1	6(73%)	4(80%)
	$ au_{f 2}^{f r}$		39(27%)	27(20%)

^a The percentages indicate total emission decay by the given lifetime component, based on 100%. ^b Lifetimes measured with sample under a nitrogen atmosphere. ^c Lifetimes measured with sample under a pure oxygen atmosphere.

As might be expected, the relationship between polymer swelling properties and oxygen diffusion is also manifested in the singlet photo-oxygenation of a well understood substrate, 2,3-diphenyl-p-dioxene 2, in various solvents, using P-Mo₆Cl₁₂ as the sensitizer. Derivative 2 was used as the sensitizer in toluene, MeOH, and acetone as shown in Table 20. These results directly parallel the swelling pattern exhibited by the polymer matrix. During a 3 h period, the amount of 2 oxidized increases with the degree of matrix swelling. The results of the oxidations in MeOH and toluene are particularly compelling, given that the lifetime of singlet oxygen is shorter in MeOH than in toluene. These oxidation studies, shown in Table 20, are consistent with the lifetime studies shown in Tables 15-19, indicating a surface loading model wherein the quenchable clusters are covalently attached to the polymer surface and that the swelling behavior of the polymer matrix regulates the diffusion of oxygen in P-Mo₆Cl₁₂ sensitizers.

C. Conclusion

Thus, the molybdenum(II) chloride cluster Mo₆Cl₁₂ has been immobilized on 2% crosslinked 4-polyvinylpyridine and the resulting P-Mo₆Cl₁₂, as depicted in Figure 23, has retained all of the energy transfer properties of free Mo₆Cl₁₂ in solution. The quenching of excited state P-Mo₆Cl₁₂ by molecular oxygen is slower than that of the free cluster in homogeneous solution and can be attributed to the hindered ability of the oxygen to diffuse through the polymer matrix. The accessibility of the cluster can be controlled by adjusting the physical structure of the matrix using preferential solvation.

Table 20 The Photo-Sensitized Oxygenation of 2,3-Diphenyl-p-Dioxene 2, Using $\mathbf{P}\text{-}\mathrm{Mo}_6\mathrm{Cl}_{12}$ in Methanol, Acetone and Toluene

Experiment Number ^a	Solvent	% Reaction After 3 h ^b	% Polymer Swelling ^c	τ (μs) ^d ¹ O ₂
1	Methanol	72	70-75	9
2	Acetone	33	30-35	48
3	Toluene	10	8-12	27

^a All samples consisted of 10 ml solvent, 40 mg of P-Mo₆Cl₁₂ (Derivative 2) and 3.4×10^{-5} moles 2, saturated with oxygen. ^b Reaction monitored by gas chromatographic analysis of sample, error $\pm 7\%$. ^c Percent swelling from the dry state to the solvent saturated state. ^d Lifetime of singlet oxygen in the appropriate solvent, from Reference 93.

Model depicting $m Mo_6Cl_{12}$ covalently bound to 4-polyvinylpyridine (Reillex TM 402).

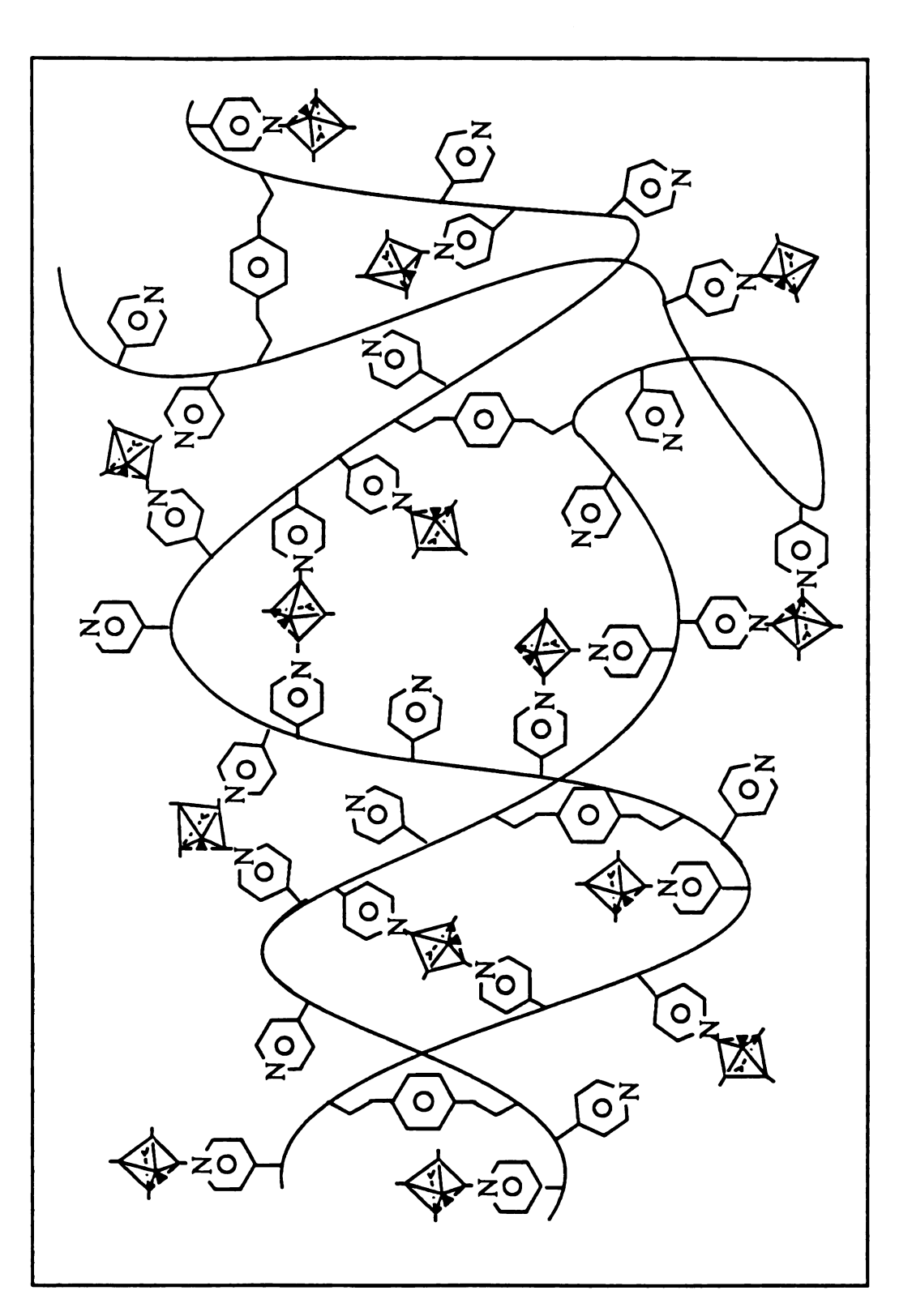


Figure 23

On a microscopic level, up to 3.5×10^{-3} moles of cluster have been bound per gram of ReillexTM 402, but the actual binding interaction between a specific polymer site and the cluster is still somewhat unclear. It is evident from the lifetime studies, that the Mo₆Cl₁₂ and $Mo_6Cl_{12}L_2/Mo_6Cl_{12}L_2^{2-}$ derivatives possess cis and trans isomers, which bind to the polymer. It is not known which isomer exhibits τ_1 (or τ_2), but it is likely that both the cis and trans isomers are comparably quenched by molecular oxygen. It is most probable that there are some cluster isomers bound to one pyridine residue in the polymer matrix, as indicated by the observation that these derivatives turn brown upon prolonged exposure to the atmosphere, indicating attack of water at the cluster vacant axial site(s)²⁴⁴ to form Mo₆Cl₁₂(OH)₂²⁻ type species. Other clusters are likely bound to two pyridine residues, since addition of Mo_6Cl_{12} to an excess of uncrosslinked 4-polyvinylpyridine in solution results in the formation of a precipitate, probably crosslinked polymer.²⁴⁵ These studies are hindered by the fact that it is extremely difficult to synthesize pure $\mathrm{Mo_6Cl_{12}L/Mo_6Cl_{12}L^-}$ or the cis and $trans\ \mathrm{Mo_6Cl_{12}L_2/Mo_6Cl_{12}L_2^{2-}}$ isomers exclusively.

In order for these $P\text{-}Mo_6Cl_{12}$ derivatives to be useful materials as oxygen sensors or solid state photocatalysts in any of the applications mentioned in the beginning of this chapter, the efficiency of singlet oxygen generation in these systems must be improved (recall $k_q(P\text{-}Mo_6Cl_{12}, O_2) = 4.1 (\pm 1.0) \times 10^6 \, \text{M}^{-1} \, \text{s}^{-1}$, in MeOH). This could be achieved easily by binding these clusters to solid supports which exhibit greater oxygen permeability than ReillexTM 402. Once these systems have been optimized, the cluster could be bound to polymers which undergo singlet oxygen degradation and thus eventually be used to study polymer degradation. Currently in the laboratories of Dow Chemical Company, these studies are being pursued.

CHAPTER IV

Direct Photo-Oxidation of Organic Substrates

A. Background

The clusters undergo clean one electron oxidation in nonaqueous deoxygenated solvents (Sec. I.C.2). It was recently noted in our group that the solution color of the electrogenerated $\mathrm{Mo_6Cl_{14}}^-$ ions changed from orange to the yellow color characteristic of $\mathrm{Mo_6Cl_{14}}^2$ —upon addition of isopropanol. This simple observation suggests that the $\mathrm{M_6X_8Y_6}^-$ ions are potent enough oxidizing agents to yield oxidized organic substrates. Given the range of potentials of the $\mathrm{M_6X_8Y_6}^-$ -couples shown in Table 21, this system has the potential to oxidize a variety of organic substrates. Moreover, because the $\mathrm{M_6X_8Y_6}^-$ ions are accessible by simple one-electron quenching routes (as indicated by the Latimer diagram in Figure 12), this observation opens the avenue for the $\mathrm{M_6X_8Y_6}^2$ -photo-oxidation of organic substrates. To this end, the clusters should serve as excellent electron transfer reagents since they possess high structural stability, undergo well understood electron transfer reactions, possess a rich synthetic chemistry, $^{139-144}$ and have potential catalytic activity. $^{133-135}$

An advantage of the $M_6X_8Y_6^{2-}$ cluster ion system is that the mechanism of substrate oxidation is accessible by electrochemical techniques, owing to the ability to generate the $M_6X_8Y_6^-$ ion at an electrode with potentials between 1.0 - 1.3 V. Thus substrates whose oxidations occur at potentials positive of +1.3 V are ideal candidates for mechanistic studies. Alcohols, in general, were chosen as the prototypic organic substrate because their reactivity is well understood, 84,126,127,246 they exhibit good solubility in nonaqueous solvents, are commercially available in fairly pure grades and their oxidation generally occurs at potentials greater than 1.3 V. In regard to photochemical studies, direct photochemical oxidation of

Table 21 Electrochemical Data of the $(NBu_4)_2M_6X_{14}$ Clusters in CH_2Cl_2

Cluster	${ m E_{1/2}(M_6X_{14}^{-/2-*})/eV^a}$	$E_{1/2}(M_6X_{14}^{-/2-})/V^{b}$
${(\mathrm{NBu_4})_2\mathrm{Mo_6Cl_{14}}}$	-0.54	1.33
$(\mathrm{NBu_4})_2\mathrm{Mo_6Br_{14}}$	-0.71	1.17
$(\mathrm{NBu_4})_2\mathrm{W_6Cl_{14}}$	-0.95	0.98
$(\mathrm{NBu_4})_2\mathrm{W_6Br_{14}}$	-1.05	0.80
$(\mathrm{NBu_4})_2\mathrm{W_6I_{14}}$	-1.11	0.58

^a Reduction potential for the $M_6X_{14}^{-/2-*}$ couple vs. SCE. ^b Reduction potential for the $M_6X_{14}^{-/2-}$ couple vs. SCE (0.1 M NBu₄PF₆).

most alcohols will not occur, since oxidation does not occur at wavelengths greater than 254 nm.²⁴⁷ Moreover, the monoanion can be photochemically generated by use of an oxidative quencher, utilizing visible and near UV radiation without competition from the uninteresting direct photo-oxidation of the alcohol.

Described in this chapter are electrochemical studies centered on the elucidation of the mechanism for the selective oxidation of alcohols by the powerfully oxidizing $M_6X_8Y_6^-$ ions. From these studies, rational pathways for the photochemical oxidation of alcohols are also presented.

B. Results and Discussion

B.1. Electrochemical Studies

Oxidation studies were conducted using primarily the ${\rm Mo_6 Cl_{14}}^{2-}$ cluster, since it possesses the most favorable ${\rm M_6X_8Y_6}^{-/2-}$ reduction potential (+1.4 V in ${\rm CH_2Cl_2}\ vs.$ SCE), and benzyl alcohol as the organic substrate (${\rm E_{1/2}} > 2$ V in ${\rm CH_3CN}\ vs.$ SCE). The solvents used in these studies were ${\rm CH_2Cl_2}$ and ${\rm C_2H_4Cl_2}$, which possess a sufficiently large window for bulk electrolysis.

Cyclic voltammograms of the hexanuclear cluster ions recorded in CH_2Cl_2 and $C_2H_4Cl_2$ reveal that all of the clusters undergo simple one electron oxidation, the potentials of which are shown in Table 21. A typical cyclic voltammogram for the $Mo_6Cl_{14}^{-2}$ couple in $C_2H_4Cl_2$ is shown in Figure 24. Plots of anodic and cathodic peak currents $(i_{p,a}, i_{p,c} \text{ respectively})$ vs. [scan rate]^{1/2} were linear with an intercept of zero and $i_{p,a}/i_{p,c} = 1.03 \pm 0.08$. Anodic to cathodic peak separations (ΔE_p) were greater than 59 mV, but were comparable to that measured for ferrocene, thereby establishing

Cyclic voltammogram of the $\rm Mo_6Cl_{14}^{-/2-}$ couple in $\rm C_2H_4Cl_2$ (0.1 M $\rm NBu_4PF_6$ at room temperature).

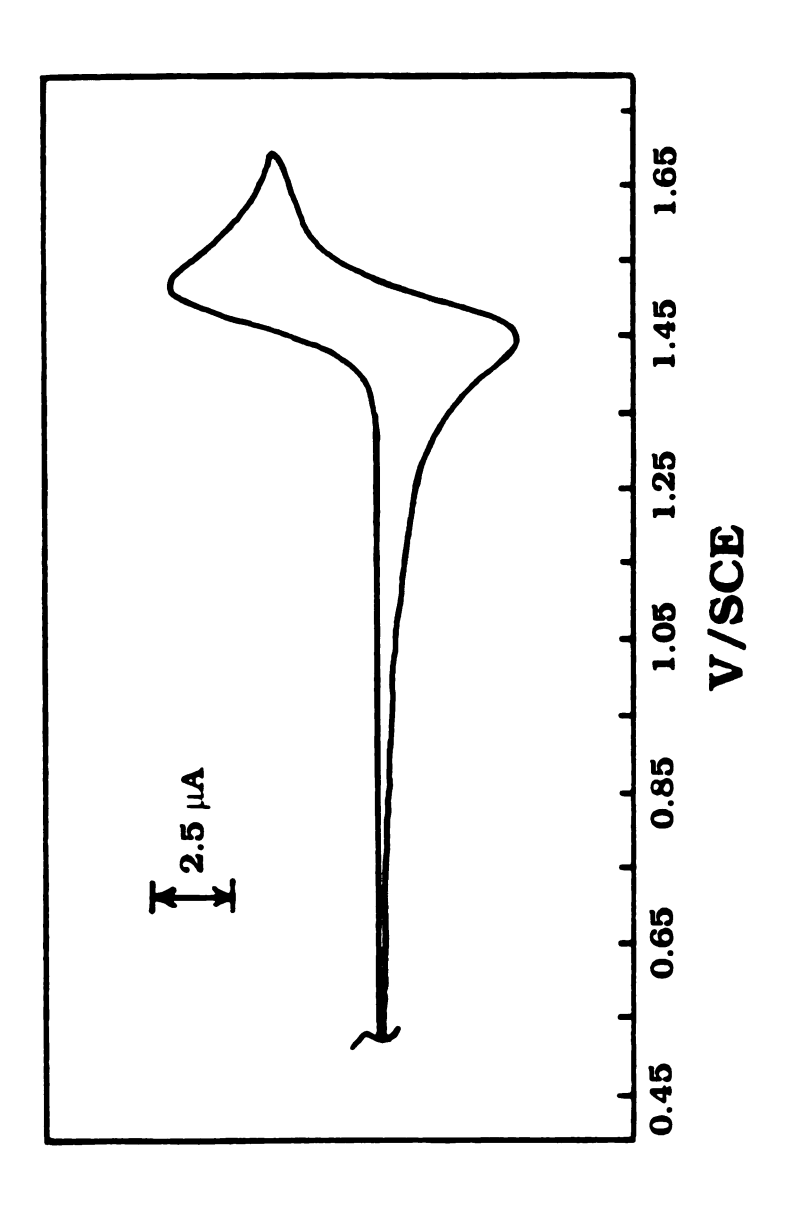


Figure 24

that deviations of ΔE_p from the theoretical limit are primarily due to uncompensated cell resistance.

Because vestiges of anodic current are observed from solutions containing benzyl alcohol at platinum electrodes poised at potentials between 1.3 - 1.4 V, the cluster monoanion was generated in the absence of alcohol by bulk electrolysis at a large area Pt electrode held at a potential 100 mV positive of the formal potential of the cluster. Upon generation of Mo₆Cl₁₄, the solution was then charged with alcohol. voltammograms recorded before and after bulk electrolysis were identical, indicating that no cluster had destroyed or no new electroactive species was formed during the electrolysis process. Upon bulk electrolysis the solution turned bright orange, the color of the monoanion. This color change, a signature of the one-electron oxidized cluster anion, is logical because the LMCT should red shift upon introduction of the hole in the cluster HOMO. Upon addition of alcohol, the yellow color of the ${\rm Mo_6Cl_{14}}^2$ solution returns over 30 - 45 min, depending upon the rate of stirring, cell geometry, etc. Analysis of the products by gas chromatography and mass spectrometry shows that the oxidation reaction between $Mo_6Cl_{14}^{}$ and benzyl alcohol produces benzaldehyde and benzyl chloride with current efficiencies of greater than 87% (Table 22). Benzyl chloride is formed with a stoichiometry of 1.8 moles of benzyl chloride to 2 moles of Mo₆Cl₁₄. A typical gas chromatogram of the Mo₆Cl₁₄⁻/ benzyl alcohol system is shown in Figure 25. The order of elution of the components of the reaction solution from the GC column is solvent (CH₂Cl₂ or C₂H₄Cl₂), benzyl chloride (peak B) and benzaldehyde (peak A), all which elute over ~12 min. Benzyl alcohol is not shown, eluting from the column after ~30 min. Typical mass spectra for the oxidation products of the Mo₆Cl₁₄-/ benzyl alcohol system are

Gas chromatogram of the oxidation products of the ${\rm Mo_6Cl_{14}}^{2-}$ / benzyl alcohol system, where peak (A) is benzaldehyde and peak (B) is benzyl chloride.

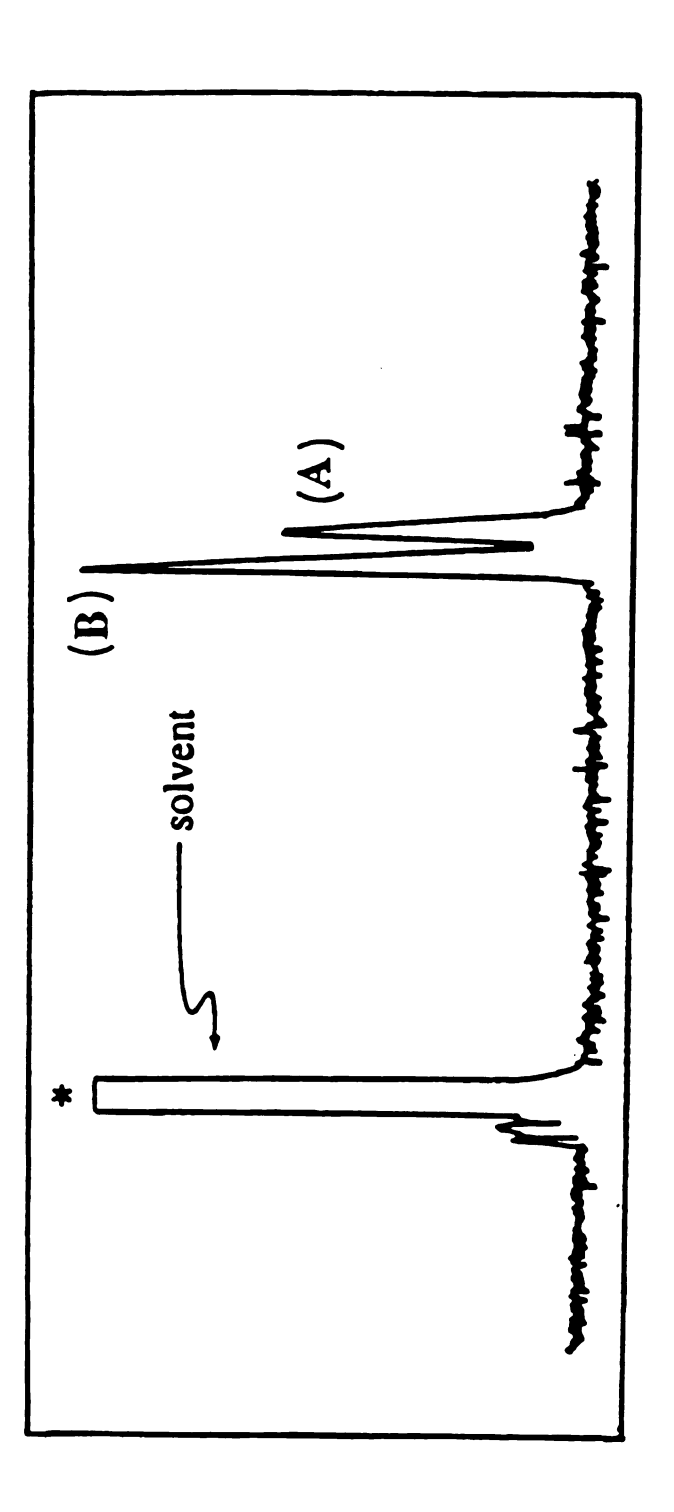


Figure 25

nzyl nzyl

nzyl

shown in Figure 26, where (A) is the spectrum for benzaldehyde and (B) is the spectrum of benzyl chloride. Production of benzaldehyde was selective with no formation of the carboxylic acid.

The oxidation reaction can also be monitored by emission spectroscopy. Upon bulk electrolysis, the emission intensity of the solution approaches zero as ${\rm Mo_6Cl_{14}}^{2-}$ is depleted, since ${\rm Mo_6Cl_{14}}^{-}$ is not luminescent. Upon addition of benzyl alcohol, the intensity of the solution emission returns; emission intensities greater than 75% of the initial value were obtained over a period of approximately 30 min.

Benzaldehyde production can be accommodated with a mechanism involving sequential hydrogen atom abstraction,

$$Mo_6Cl_{14}^{2-} \xrightarrow{-e^-} Mo_6Cl_{14}^{-}$$
 (136)

$$Mo_6Cl_{14}^- + OH \xrightarrow{k_1} Mo_6Cl_{14}^2 + OH + H^+ (137)$$

$$Mo_6Cl_{14}^- + OH \xrightarrow{k_2} Mo_6Cl_{14}^2 + OC=O+H^+$$
 (138)

Consistent with this mechanism are the following observations: (i) no reaction is observed between $\mathrm{Mo_6Cl_{14}}^-$ and alcohols such as tert-butanol which do not possess an α -hydrogen atom; and (ii) the stoichiometry of the reaction (Table 22), 2 moles of $\mathrm{Mo_6Cl_{14}}^{2-}$: 0.92 moles of benzaldehyde,

Mass spectra of the oxidation products of the $\mathrm{Mo_6Cl_{14}}^{2-}$ / benzyl alcohol system, where (A) is benzaldehyde spectrum and (B) is the benzyl chloride spectrum. ([P] denotes the parent ion peak).

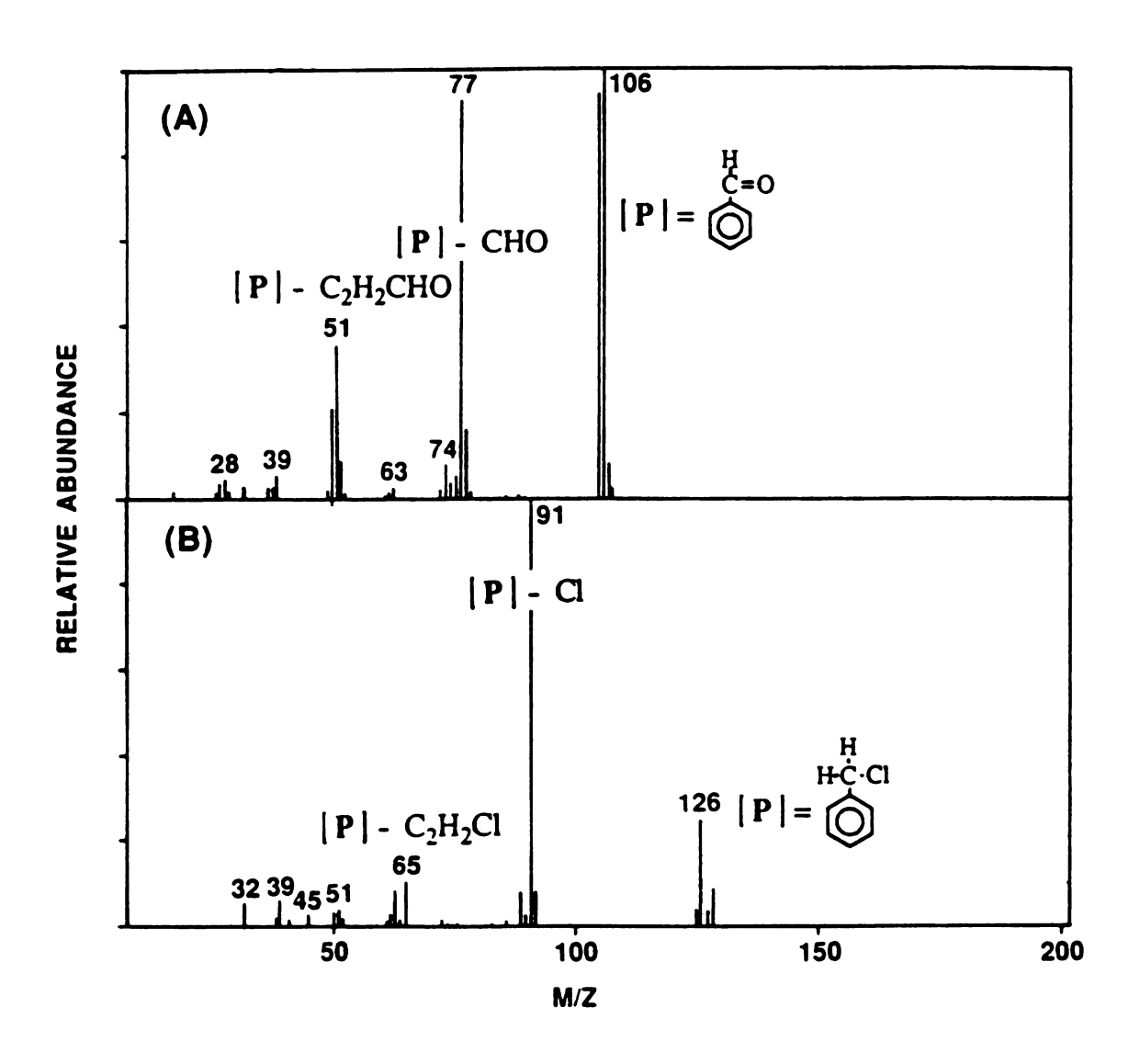


Figure 26

indicates that the oxidation of benzyl alcohol requires two equivalents of $Mo_6Cl_{14}^{-}$.

The intimate details of this mechanism remain undefined. We do not yet know if hydrogen abstraction produces a discrete transition metal hydride which then deprotonates or whether the central reaction is electron transfer to the cluster followed by proton loss. Similar α-hydrogen atom mechanisms have been postulated for [Ru(trpy)(bpy)(OH)]²⁺ (where trpy = 2,2',2"-terpyridyl and bpy = 2,2'-bipyridyl)^{84b} and trans-[Ru(TMC)OX]⁺ (where TMC = 1,4,8,11-tetramethyl-1,4,8,11-tetraazacyclotetradecane and X $^-$ = Cl $^-$, NCO $^-$, and N $_3$ $^-$) 248 which are one electron oxidants. Although it is generally accepted that the first oxidation step involves α -C-H bond activation, 84b,248,249 there is little substantial evidence for differentiating between a hydrogen atom abstraction mechanism from a proton coupled outer-sphere electron transfer mechanism, (particularly when a transition between the two can be induced by a change in solvents as observed for [Ru(trpy)(bpy)(OH)]²⁺ in CH₃CN and H₂O).^{84b} In our laboratories, investigations are currently underway probing the intimate mechanism of alcohol oxidation by the M₆X₁₄ ions. The most compelling studies should involve kinetic isotope effects using alcohols deuterated in the α-hydrogen position, since an α-hydrogen atom abstraction step should exhibit a much larger kinetic isotope effect than proton coupled outer-sphere electron transfer.84b

Of course, eqs (136) - (138) do not account for benzyl chloride formation. It is proposed that benzyl chloride results from the subsequent reaction of the protons produced in the hydrogen atom abstraction step. Because the oxidations are conducted in nonaqueous solution, the activity of H⁺ should be significant. The OH provides a site as a Lewis base and thus

is susceptible to attack by H⁺ to produce the carbocation. Benzyl chloride will form upon nucleophilic attack by the halide ion displaced from the axial coordination site of the cluster; the proposed mechanism is shown below,

Several experiments were undertaken to assess the validity of this proposed mechanism. These data are summarized in Table 22. A 2:1 benzyl halide: benzaldehyde stoichiometry is consistent with the production of two equivalents of protons liberated in eqs (136) - (138). Because protons generated from benzyl alcohol oxidation (2 equiv / mole of alcohol oxidized) have been observed to protonate electrocatalysts such as trans-Os(η^4 -CHBA-Et)(py)₂²⁴⁹ (H₄CHBA-Et = 1,2-bis(3,5-dichloro-2-hydroxybenzamido)ethane), we decided to perform the oxidation reaction in the presence of a proton scavenger or base. The data for the Mo₆Cl₁₄-/ benzyl alcohol system in the presence of Na₂CO₃ in Table 22 shows a significant reduction in the benzyl halide: benzaldehyde stoichiometry from 2:1 (no base) to 1:1 (15-fold excess Na₂CO₃). The pathway for benzyl halide formation is not completely shut down most likely because Na₂CO₃ is a heterogeneous base in these chlorinated solvents^{246b-c,249} and hence is a relatively inefficient trap of H⁺.

Table 22 Product Characterization for the Oxidation of Benzyl Alcohol by Electrogenerated ${\rm M_6X_{14}}^-$

		Benzyl Alcohol Products ^a			
Cluster Ion	Solvent	Benzyl Chloride	Benz- aldehyde	Benzyl Bromide	Current b Efficiency(%)
Mo ₆ Cl ₁₄	$C_2H_4Cl_2$	1.8 ± 0.5	0.92 ± 0.33	0	87 ± 5
Mo ₆ Cl ₁₄ ⁻ / Na ₂ CO ₃	$C_2H_4Cl_2$	0.96 ± 0.30	1.0 ± 0.1	0	95 ± 5
W ₆ Br ₁₄ -	$\mathrm{C_2H_4Cl_2}$	0.44 ± 0.11	1.04 ± 0.04	1.5 ± 0.6	103 ± 3
W ₆ Br ₁₄ -	$\mathrm{CH_2Cl_2}$	0.59 ± 0.10	1.08 ± 0.07	1.6 ± 0.7	101 ± 2

^a Moles of product per two moles of M₆X₁₄⁻ ion. ^b Method of calculation of current efficiency is discussed in eq (94).

Unfortunately, most common homogeneous bases such as pyridines or alkyl/aryl amines either react with Mo₆Cl₁₄ or do not possess sufficiently positive oxidation potentials to be inert to our electrochemical conditions and hence are precluded for our study.

In order to determine if the mechanism postulated in eq (139) and (140) possesses any free radical character, cumene (a free radical scavenger)²⁵⁰ was added to solutions of Mo₆Cl₁₄ in lieu of benzyl alcohol. If chlorine radicals are present as a result of bulk electrolysis, the following reactions are expected to occur,²⁵⁰

The reaction of the chlorine radical with cumene is diffusion controlled (k_f = 6.9 x 10⁹ M⁻¹ s⁻¹)²⁵⁰ as well as the rate of cumyl radical recombination (k_c = 8.0 x 10⁹ M⁻¹ s⁻¹).²⁵⁰ The disproportionation of dicumene is negligible (k_d/k_c = 0.05).²⁵⁰ Gas chromatographic analysis of the Mo₆Cl₁₄^{-/}/ cumene solution showed no formation of dicumene, indicating no free radical Clactivity and hence formation of the benzyl halide most likely results from the addition of Cl⁻ to the carbocation.

There are two possible sources for Cl⁻: the solvent and the cluster. Conducting bulk electrolysis in a nonchlorinated polar organic solvent stable to at least 1.7 V is nontrivial. Most solvents such as acetone, acetonitrile, or propylene carbonate either do not possess a sufficiently large

potential range or possess such a high boiling point that they are impractical to manipulate in a glove box or on a vacuum line. Thus, the cluster was varied. Since the stability of $Mo_6Br_{14}^{\ 2-}$ and any other molybdenum clusters with axial bromide ligands toward oxidation is questionable (losing Br^-), $^{133a}W_6Br_{14}^{\ 2-}$ was the cluster of choice. Addition of benzyl alcohol to a solution of $W_6Br_{14}^{\ 2-}$ produced by bulk electrolysis in CH_2Cl_2 yielded 0.44 moles of benzyl chloride: 1.04 moles of benzaldehyde: 1.5 moles of benzyl bromide per two moles of the $W_6Br_{14}^{\ -}$ ion (Table 22). A similar product distribution is also obtained in $C_2H_4Cl_2$. These results indicate that the majority of halide ions present in the halogenated products come from the cluster ions. The source of chloride present in the $W_6Br_{14}^{\ -}$ system is somewhat uncertain, but may be due to solvent impurities or Cl^- left from cleaning the cells with aqua regia.

The kinetics for the reaction between $M_6X_{14}^-$ and alcohol can be analyzed on the basis of an EC mechanism embodied by eq (136) - (138). Hydrogen atom abstraction from the alcohol is much slower than abstraction from the corresponding radical or $k_1 << k_2$. $^{246a-b,84b}$ According to eq (137), the reaction is predicted to be second order. Thus, RRDE in principle can be used to determine the rate constant k_1 (quasi first order) and the reaction order. Unfortunately, the overlap of current for $Mo_6Cl_{14}^{\ \ 2-}$ oxidation and prewave benzyl alcohol effects made determination of the current efficiency of the cluster in the presence of alcohol N_k eq (99) difficult.

The oxidation of isopropanol (which has a higher oxidation potential than benzyl alcohol) was studied and similar results were obtained. RRDE experiments were performed with $W_6 Br_{14}^{\ 2-}$, which has a lower oxidation potential than $Mo_6 Cl_{14}^{\ 2-}$. The reaction between $W_6 Br_{14}^{\ -}$ and isopropanol

(as well as benzyl alcohol) is so slow that the collection coefficient is unperturbed in the presence of alcohol (N = N_k). Thus the κ value in eq (101) must be smaller than 0.03 and the pseudo first order rate constant under these experimental conditions can be estimated to possess an upper limit of 0.3 sec⁻¹. ^{157b}

In order to determine these rate constants explicitly, spectroscopic methods were employed. Preliminary qualitative rate measurements indicate that the rate of Mo₆Cl₁₄ oxidation of benzyl alcohol is faster than that for W₆Br₁₄⁻, which is not surprising since the latter cluster is a weaker oxidant (Table 21). Rate data can be compelling evidence in determination of the mechanism of alcohol oxidation by single electron transfer transition metal complexes. As indicated in Table 23, the rate constants measured for trans-[Ru(TMC)O(Cl)]+248 are about 50% larger than those for trans-[Ru(TMC)O(NCO)]+,248 which is not surprising since the latter complex is also a somewhat weaker oxidant. Extrapolation of this trend to trans-[Ru(TMC)O(N₃)]^{+ 248} would lead to an expected rate constant only two-fold smaller than that of the monochloro catalyst, rather than the hundred-fold decrease observed. This coupled with the fact that trans- $[Ru(TMC)Cl_2]^{2+248}$ is a stronger oxidant than trans- $[Ru(TMC)O(Cl)]^+$ for the electro-oxidation of both isopropyl and benzyl alcohols, indicates that the oxidizing strength of these complexes is not the primary factor involved in determining their relative oxidative activities, and thus argues against an outer-sphere mechanism for these reactions. It is likely that the oxo ligand facilitates the transfer of a proton and an electron (or a hydrogen atom) from the alcohol by assisting the stabilization of the departing proton. The same type of discussion may be made for the [Ru(trpy)(bpy)(OH)]²⁺

Table 23

Rates for the Oxidation of Alcohols by

Transition Metal Complexes

Complex	Solvent	E/V a	$k_q / M^{-1} s^{-1}$	Alcohol
[Ru(trpy)(bpy)(OH)] ^{2+/+ b}	H ₂ O	0.49 ^c	6 x 10 ⁻⁵	Isopropanol
$[Ru(trpy)(bpy)(OH)]^{2+/+b}$	CH ₃ CN	0.49 ^c	8 x 10 ⁻⁴	Isopropanol
trans-[Ru(TMC)O(Cl)]+/o d	CH ₃ CN	1.36 ^e	2.6×10^2	Benzyl Alcohol
trans-[Ru(TMC)O(NCO)]+/o d	CH ₃ CN	1.20 ^e	1.3×10^2	Benzyl Alcohol
trans-[Ru(TMC)O(N ₃)] ^{+/o} d	CH ₃ CN	1.03 ^e	<1	Benzyl Alcohol
trans-[Ru(TMC)Cl ₂] ^{2+/+ d}	CH ₃ CN	1.46 ^e	$<2.6 \times 10^{2} \mathrm{f}$	Benzyl Alcohol

^a Reduction potential vs. SCE in CH₃CN, unless otherwise noted. ^b Reference 84b, terpy = 2,2',2"-terpyridyl and bpy = 2,2'-bipyridyl. ^c Reduction potential, pH 7. ^d Reference 248, TMC=1,4,8,11-tetramethyl-1,4,8,11-tetraazacyclotetradecane. ^e Formal reduction potential. ^f k_q of trans-[Ru(TMC)Cl₂]^{2+/+} is smaller than trans-[Ru(TMC)O(Cl)]^{+/o}, unpublished results in Reference 248.

Ru(trpy)(bpy)(OH)]²⁺ systems reflects the change from an outer sphere mechanism in water to an inner sphere mechanism in CH₃CN. A noteworthy difference between the oxo complexes and the clusters however is the lack of a basic site on the transition metal clusters. Particular care must be given to the influence of solvent on the overall oxidation mechanism with the cluster systems. The rate data for the M₆X₁₄-/benzyl alcohol systems should reveal a great deal about the oxidation mechanism, particularly since the cluster systems possess driving forces comparable to those for most of the complexes in Table 23.

B.2. Photochemical Studies

The M₆X₁₄⁻ ions are not only generated electrochemically, but can be photochemically produced as well by simple oxidative quenching. The quenching of the cluster luminescence by various known electron transfer quenchers was monitored using emission spectroscopy and the Stern-Volmer method of luminescence intensities. The rate constants for the quenching of Mo₆Cl₁₄^{2-*} luminescence by various electron acceptors are shown in Table 24, while Table 25 presents Stern-Volmer quenching rate constants for the quenching of other clusters by acceptors of appropriate potential. These studies indicate that the cluster luminescence is significantly attenuated by these quenchers at a rate which parallels the driving force of the cluster/acceptor reaction consistent with electron transfer pathways. On this basis, the photochemical cycle proposed in Figure 27 can be constructed. The cycle in Figure 27 was assembled using cluster, electron accepting molecules and alcohols of the appropriate

Table 24 Quenching Rate Data for $Mo_6Cl_{14}^{\ \ 2^{-*}}$ with Various Electron Transfer Quenchers

Quencher	E _{1/2} /V ^a	$k_q / M^{-1} s^{-1} b$	△G _{et} /V °
Chloranil ^d	-0.02	1.1 x 10 ⁸	-0.52
TCNE e	-0.24	2.5×10^9	-0.30
$SiW_{12}O_{40}^{4-f}$	-0.27	2.3×10^7	-0.27
4-Cyano-N-Benzyl Pyridinium ⁺ PF ₆ ^{-g}	-0.69	5.9×10^6	+0.15
4-Cyano-N-Methyl Pyridinium ⁺ PF ₆ ^{-g}	-0.74	4.4×10^5	+0.20
p-Dinitrobenzene	-0.75	1.1×10^6	+0.04
o-Dinitrobenzene	-0.91	7.9×10^3	+0.20

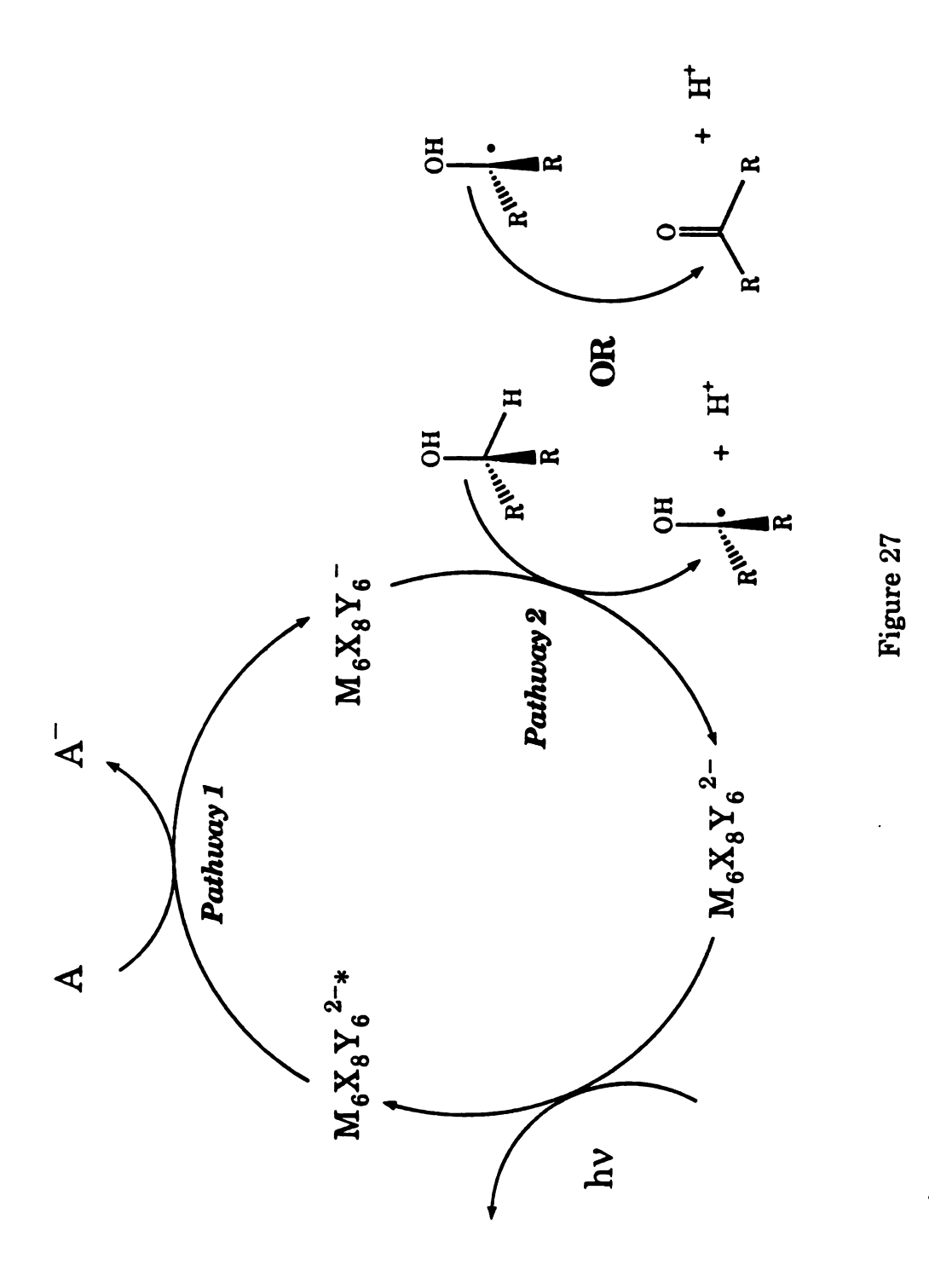
^a Reduction potentials for $A^{0/-}$ couples in CH_3CN vs. SCE. ^b Rate constant for the quenching of $Mo_6Cl_{14}^{2-}$ luminescence by various electron acceptors. ^c Standard free energy change for the electron transfer reaction between $Mo_6Cl_{14}^{2-*}$ and A; $\Delta G_{et} = -\{E_{1/2}(Mo_6Cl_{14}^{-/2-*}) - E_{1/2}(A^{0/-})\}$. ^d Chloranil = tetrachloro-1,4-benzoquinone. ^e TCNE = tetracyanoethylene. ^f Tetrabutylammonium salt. ^g PF₆ = the hexafluorophosphate anion.

Table 25 Quenching Rate Data for $Mo_6Br_{14}^{\ 2-*}$ and $W_6Cl_{14}^{\ 2-*}$ with Various Electron Transfer Quenchers

Cluster	Quencher	E _{1/2} /V ^a	k _q /M ⁻¹ s ^{-1 b}	△G _{et} /V ^c
Mo ₆ Br ₁₄ ²⁻	4-Cyano-N-Benzyl Pyridinium+ PF ₆ -0	-0.69	2.6 x 10 ⁹	-0.02
Mo ₆ Br ₁₄ ²⁻	4-Cyano-N-Methyl Pyridinium ⁺ PF ₆	-0.74 i	2.9 x 10 ⁸	+0.03
Mo ₆ Br ₁₄ ²⁻	p-Dinitrobenzene	-0.75	5.6×10^6	+0.04
$W_6Cl_{14}^{2-}$	4-Cyano-N-Benzyl	-0.74	1.5×10^{10}	-0.31
	Pyridinium ⁺ PF ₆	i 		

^a Reduction potentials for $A^{0/-}$ couples in CH_3CN vs. SCE. ^b Rate constant for the quenching of $M_6X_{14}^{2-}$ luminescence by various electron acceptors. ^c Standard free energy change for the electron transfer reaction between $M_06Cl_{14}^{2-*}$ and A; $\Delta G_{et} = -\{E_{1/2}(M_6X_{14}^{-/2-*}) - E_{1/2}(A^{0/-})\}$.

Proposed photochemical pathway for the oxidation of organic substrates $\mbox{by use of the } M_6 X_{14}{}^{2-} \mbox{ clusters}.$



potential, as summarized in Table 26. In Figure 27, upon excitation of the cluster, the excited state is formed which undergoes electron transfer with an electron accepting or quencher molecule A, yielding A⁻ and oxidized cluster, $M_6X_8Y_6^-$ (pathway I). If a renewable quencher is used, this scheme would be catalytic in both quencher and cluster. Parallel to the electrochemical results, once formed, the monoanion may undergo electron or atom transfer with substrate (as indicated in the discussion in Sec. I.C.2), resulting in formation of $M_6X_8Y_6^{-2}$ and an alcohol radical, via pathway II. The alcohol radical may then react with another molecule of $M_6X_8Y_6^{-2}$ to give $M_6X_8Y_6^{-2}$ and the two electron oxidized organic product. The two alcohols used in these experiments were benzyl alcohol and isopropanol. Although most of the electrochemical studies were conducted with benzyl alcohol, isopropanol was used in these experiments mainly due to its lower molecular weight, which facilitates sample preparation and product analysis.

A variety of quenchers were utilized for this photochemical system. Cationic quenchers such as N-methyl-4-cyanopyridinium⁺ PF_6^- ion paired with the cluster, thereby leading to precipitation. Thus studies were limited to neutral quenchers or those quenchers which are anionically charged. Moreover, since the duration of these experiments was somewhat long (>20 h), the dark reaction of the quenchers, as well as the photochemical side reactions of the quencher and the alcohol (no cluster) was observed. In the case of chloranil, direct reaction of isopropanol to acetone was slightly more efficient than the reaction promoted by $Mo_6Cl_{14}^{\ \ 2-}$. TCNE exhibited a relatively insignificant dark reaction with isopropanol in the absence of cluster. Reaction of these quenchers with

Table 26

Photochemical Systems for the Oxidation of Alcohols in CH₃CN

[Cluster]/M	[Quencher] / M	[Alcohol] / M	Irradation Time	[Oxidized Alcohol] / M
$Mo_6Cl_{14}^{2-}$ (6.42×10^{-3})	TCNE a (6.56 x 10^{-2})	Isopropanol (5M)	24 h	Acetone ~9.1 x 10 ^{-4 b}
$Mo_6Cl_{14}^{2-}$ (6.42×10^{-3})	TCNE ^a (4.00×10^{-2})	Benzyl Alcohol (5M)	20 h	Benzaldehyde ~2.0 x 10 ^{-4 c}
$Mo_6Cl_{14}^{2-}$ (6.42 x 10^{-3})	Chloranil d (4.07 x 10^{-2})	Isopropanol (5M)	20 h	Acetone ~0 e
V 11	N-Methyl-4-Cyano Pyridinium ⁺ PF_6^- (1.05 x 10^{-1})	Isopropanol (5M)	 、	Salt ^f Precipitated
$Mo_6Br_{14}^{2-}$ (5.73 x 10^{-3})	p -Dinitrobenzene (7.65 x 10^{-2})	Isopropanol (5M)	20 h	Acetone ~2.0 x 10 ^{-4 c}
$W_6Cl_{14}^{2-}$ (1.56 x 10 ⁻³)	p -Dinitrobenzene (1.03 x 10^{-1})	Isopropanol (5M)	5 h	No reaction
$Mo_6Cl_{13}^{-g}$ (1.56 x 10^{-3})	TCNE ^a (3.91 x 10 ⁻²)	Benzyl Alcohol (1M)	24 h	No reaction

^a TCNE = Tetracyanoethylene. ^b Approximate because TCNE undergoes a dark reaction with isopropanol, thus photological sample was adjusted for contents of blank. ^c At the limit of detection, using gas chromatography. ^d Chloranil = Tetrachloro-1,4-benzoquinone. ^e Substracting blank from photolyzed sample resulted in negative value. ^f Due to ion pairing, contents of solution precipitated. ^g Produced in situ by reaction of one equivalent of silver tosylate with $Mo_6Cl_{14}^{2-}$.

organic substrates has recently been cited in the literature. 251,252

As is evident from Table 26, this photochemical cycle produces oxidized alcohol (benzaldehyde or acetone) in very low yields (6-28%, assuming no catalytic activity by the cluster). These low yields for benzaldehyde and acetone production are most likely a result of very efficient back electron transfer between the cluster monoanion and reduced acceptor eq (144a). Back electron transfer between ${\rm Mo_6Cl_{14}}^-$ and ${\rm TCNE}^-$ /chloranil $^-$ have been observed to proceed near the diffusion controlled limit. 133a Thus, the hydrogen abstraction required for alcohol oxidation eq (144b) is efficiently circumvented because ${\rm k_2} >> {\rm k_3}$. As long as ${\rm k_2} >> {\rm k_3}$,

$$Mo_6Cl_{14}^- + H\dot{C}(Ph)OH \xrightarrow{k_4} Mo_6Cl_{14}^{2-} + (Ph)C=O + H^+$$
 (145)

there will be almost exclusive reaction of Mo₆Cl₁₄ with TCNE and little substrate oxidation.

Back electron transfer historically has been a problem which has plagued photochemically sensitized electron transfer reactions, including solar energy reactions.²⁵³ Traditional solutions to this problem involve charge separation of the donor and acceptor including: (1) the use of the coulombic effects;²⁵³ (2) the use of interfacial reaction systems such as micelles, vesicles, membranes, colloid particles, etc. to separate the oxidation and reduction sites;²⁵³ and (3) the use of sacrificial oxidants or

reductants to prevent back electron transfer.²⁵³ One unique approach that these clusters offer to circumvent this back electron transfer problem is the coordination of the alcohol directly to the cluster core illustrated below.

In this manner, the α -hydrogen is situated over the face of the metal octahedron and thus predisposed for abstraction. To this end, the kinetics for abstraction should be enhanced relative to the kinetics of the bimolecular back reaction. Alcohol derivatives of these clusters have been previously reported in the literature. Thus, these studies should be undertaken in the near future. Comprehensive kinetics studies for back electron transfer vs. α -hydrogen abstraction must be defined as a function of R and R', and the cluster excited state potential. From these studies, an efficient cycle for photochemical oxidation should begin to emerge.

C. Conclusion

Thus, the $M_6X_{14}^-$ ions are promising electro and photochemical oxidation catalysts. The ability to modify the cluster core with the substitution of a variety of ligands at its axial coordination sites, while

maintaining the clusters' electrochemical and photochemical properties permits these species to be specially tailored to oxidation reactions. The $M_6X_{14}^-$ ions can be produced photochemically and possess sufficient energy to oxidize organic substrates, particularly isopropyl and benzyl alcohol. The efficiency of alcohol oxidation is quite low due to back electron transfer between $M_6X_{14}^-$ and the reduced electron acceptor A^- , indicating that the photochemical utility of this system may lie in unimolecular reactions achieved by directly binding the substrate to the M_6X_{12} cluster.

CHAPTER V

References

REFERENCES

- (a) Milas, N. A. Chem. Rev. 1932, 10, 295-364. (b) Moureu, C.;
 DuFraisse, C. Chem. Rev. 1926, 3, 113-162.
- 2. Sheldon, R. A.; Kochi, J. K. Metal Catalyzed Oxidation of Organic Compounds; Academic Press: New York, 1981.
- (a) Smidt, J.; Hafner, W.; Jira, R; Sedlmeier, J.; Sabel, A. Angew.
 Chem. Int. Ed. 1962, 1, 80-88. (b) Smidt, J. J. Chem. Ind.(London)
 1962, 54-61. (c) Smidt, J.; Hafner, W.; Jira, R.; Sedlmeier, J.; Siever,
 R.; Ruttinger, R.; Kojer, H. Angew. Chem. 1959, 71, 176-182.
- 4. Waddams, A. L. Chemicals from Petroleum, 4th Edition; John Murray: London; 1978.
- (a) Wulff, H. P. U.S. Patent 3,923,843 (1975) to Shell Oil. (b) Kollar, J.
 U.S. Patents 3,625,981 (1971); 3,507,809 (1970); and 3,350,422 (1967) to
 Halcon International.
- 6. Meyer, T. J. in Fundamental Research in Homogeneous Catalysis; Tsutsui, M., Ed.; Plenum: New York; 1976, pg. 169-181.
- 7. Masters, C. in Homogeneous Transition-Metal Catalysis; Chapman and Hall: London, England; 1981, pg. 1-35; 172-196.
- (a) Bateman, L. Q. Rev., Chem. Soc. 1954, 8, 147-167. (b) Bolland, J.
 L. Q. Rev. Chem. Soc. 1949, 3, 1-21. (c) Backstrom, H. L. J. J. Am.
 Chem. Soc. 1927, 49, 1460-1472.
- 9. Carlsson, D. J.; Robb, J. C. Trans. Faraday Soc. 1966, 62, 3403-3415.
- Bromberg, A.; Muszkat, K. A. J. Am. Chem. Soc. 1969, 91, 2860-2866.
- 11. Weiss, J. Adv. Cat. 1952, 4, 343-365.

- (a) Ingold, K. U. Accts. Chem. Res. 1969, 2, 1-9. (b) Ingold. K. U.
 Pure Appl. Chem. 1967, 15, 49-67.
- Bennett, J. E.; Brown, D. M.; Mile, B. Trans. Faraday Soc. 1970,
 66, 386-396; pg. 397-405.
- (a) Howard, J. A. Adv. Free-Radical Chem. 1972, 4, 49-173. (b)
 Bartlett, P. D.; Traylor, T. G. J. Am. Chem. Soc. 1963, 85, 2407-2411; pg. 2411-2413.
- (a) Kochi, J. K. Accts. Chem. Res. 1974, 7, 351-360. (b) Kochi, J. K.
 Free Radicals; Wiley: New York, 1973; Vol. 1, pg. 591-685. (c) Kochi,
 J. K. Prog. Rec. Chem. 1966, 27, 207-250.
- 16. Kochi, J. K. Pure Appl. Chem. 1980, 52, 571-605.
- (a) Wells, C. F.; Husain, M. Trans. Faraday, Soc. 1971, 760-767.
 (b) Wells, C. F.; Mays, D. Inorg. Nucl. Chem. Lett. 1969, 5, 9-12.
 (c) Wells, C. F.; Mays, D. Inorg. Nucl. Chem. Lett., 1968, 4, 43-45.
 (d) Sigel, H.; Flierl, C.; Griesser, R. J. Am. Chem. Soc. 1969, 91, 1061-1064.
 (f) Baer, S.; Stein, G. J. Chem. Soc. 1953, 3176-3179.
- (a) Rawlinson, D. J.; Sosnowsky, G. Synthesis 1972, 1-28. (b)
 Boguslavskaya, L. S. Russ. Chem. Rev. 1965, 34, 503-515.
- (a) Uri, J. Chem. Rev. 1952, 50, 375-454. (b) Baxendale, J. H. Adv.
 Catal. 1952, 4, 31-86.
- 20. Fenton, H. J. H. J. Chem. Soc. 1894, 65, 899-910.
- (a) Walling, C. Accts. Chem. Res. 1975, 8, 125-131 and references therein.
 (b) Snook, M. E.; Hamilton, G. A. J. Am. Chem. Soc. 1974, 96, 860-869 and references therein.
 (c) Haber, F.; Weiss, J. Proc. Roy. Chem. Soc. (London) 1934, A147, 332.
 (d) Haber, F. Weiss, J. Naturwissenschaften 1932, 20, 948.

- 22. Sosnovsky, G.; Rawlinson D. J. in *Organic Peroxides*; Swern, D., Ed.: Wiley: New York, 1971; Vol. 2, pg. 269-336.
- 23. (a) Bartlett, P. D.; Guaraldi, G. J. Am. Chem. Soc. 1967, 89, 4799-4801. (b) Criegee, R. in Oxidations in Organic Chemistry; Wiberg, K., Ed.; Academic: New York, 1965; pg. 302-305.
- 24. Dixon, W. T.; Norman, R. O. C. Nature (London) 1962, 196, 891-892.
- 25. (a) Lyons, J. E. Adv. Chem. Series 1974, 132, 64-89. (b)
 Arzoumanian, H.; Blanc, A. A.; Metzger, J.; Vincent, J. E. J.
 Organometal. Chem. 1974, 82, 261-270.
- 26. (a) Scott, E. J. Y. J. Phys. Chem. 1970, 74, 1174-1182. (b) Richardson,
 W. H. J. Am. Chem. Soc. 1965, 87, 247-253 and references therein.
- 27. Denisov, E. T.; Emanuel, J. M. Russ. Chem. Rev. 1960, 29, 645-662.
- 28. (a) Sosnovsky, G.; Rawlinson, D. J. in *Organic Peroxides*; Swern,
 D., Ed.; Wiley: New York, 1971: Vol. 2, pg. 153-268. (b) Kharasch,
 M.S.: Fono, A. J. Org. Chem. 1959, 4, 72-78.
- 29. Connor, J. A.; Ebsworth, E. A. V. Adv. Inorg. Radiochem. 1964, 6, 279-381.
- 30. (a) Jorgensen, K. A. Chem Rev. 1989, 89, 431-459, and references herein. (b) Shyrne, T. M.; Kim, L. U. S. Patent 4,024,165(1977) to Shell.
- 31. Sheldon, R. A. J. Mol. Cat. 1980, 7, 107-126.
- 32. Matucci, A. M.; Perrotti, E.; Santambrogio, A. J. Chem. Soc., Chem. Comm. 1970, 1198-1199.
- (a) Landau, R.; Sullivan, G. A.; Brown, D. Chem. Tech, 1979, 602-607.
 (b) Indictor, J.; Brill, W. F. J. Org. Chem. 1964, 29, 710-713.
- 34. Baker, T. N.; Mains, G. J.; Sheng, M. N.; Zajacek, J. G.; J. Org. Chem. 1973, 38, 1145-1148.

- 35. Chong, A. O.; Sharpless, K. B. J. Org. Chem. 1977, 42, 1587-1590.
- (a) Sheldon, R. A.; van Doorn, J. A.; Schram, C. W. A.; DeJong, A.
 J. J. Cat. 1973, 31, 427-437. (b) Ibid, pg. 438-443.
- (a) Sheldon, R. A. Rec. Trav. Chim. Pay-Bas. 1973, 92, 253-266.
 (b) Ibid, pg. 367-373.
- 38. Mimoum, H. J. Mol. Catal. 1980, 7, 1-29.
- 39. di Fura, F.; Modena, G. Rev. of Chem. Intermed. 1985, 6, 51-76.
- Drago, R. S.; Zurich, A.; Nyberg, E. D. J. Am. Chem. Soc. 1985, 107, 2898-2903.
- (a) Baciocchi, E.; Mandolini, L.; Rol, C. Inorg. Chem. 1980, 45, 3906-3910.
 (b) Onopchenko, A.; Schulz, J. G. D.; Seekircher, R. J. Chem. Soc, Chem. Commun. 1971, 939-940.
 (c) Onopchenko, A.; Schulz, J. G. D.; Seekircher, R. J. Org. Chem. 1972, 37, 1414-1417.
- 42. (a) Shcherbina, F. F.; Lysukho, T. V. Kinet. Catal. 1978, 19, 872-873. (b) Kamiya, Y. J. Catal. 1974, 33, 480-485. (c) Kamiya, Y. Adv. Chem. Ser. 1968, 76, 193-206.
- 43. Chester, A. W.; Landis, P. S.; Scott, E. J. Y. Chemtech. 1978, 366-371.
- (a) Schulz, J. G. D.; Onopchenko, A. J. Org. Chem. 1980, 45, 3716-3719.
 (b) Onopchenko, A.; Schulz, J. G. D. J. Org. Chem. 1978, 38, 909-912.
 (c) Ibid, pg. 3729-3733.
 (d) Parshall, G. W. J. Mol. Catal. 1978, 4, 243-270.
- 45. Tang, R. T.; Kochi, J. K. J. Inorg. Nucl. Chem. 1973, 35, 3845-3856.
- 46. de Klein, W. J. Recl. Trav. Chim. Pays-Bas. 1975, 94, 151-153.
- Moriarty, R. M. in Selective Organic Transformations;
 Thyagarajan, B. S., Ed.; Wiley (Interscience): New York, 1972; pg. 183-237.

- 48. (a) Belgian Patent 853,864 (1976) to Halcon International. (b) Kitching, W. Organometal. React. 1972, 3, 319-400.
- (a) Johnson, R. A. U. S. Patent 4,192,814 (1980). (b) Brill, W.F. U. S.
 Patent 4,115,420 (1978) to Halcon Res. and Dev. Corp.
- 50. Allen, G. C.; Aguilo, A. Adv. Chem. Ser. 1968, 76, 363-381.
- 51. Nonhebel, D. C.; Walton, J. C. in *Free Radical Chemistry*; Cambridge Univ. Press: London and New York, 1974.
- 52. Stewart, R. in Oxidation in Organic Chemistry; Wiberg, K. B., Ed.;
 Academic Press: New York, 1965: Part A, pg. 2-68.
- 53. Wiberg, K. B. in Oxidation in Organic Chemistry; Academic Press: New York, 1965; Part A, pg. 69-185.
- 54. (a) Rabjohn, N. Org. React. (N.Y.) 1978, 24, 261-415. (b) Jerussi,
 R. A. in Selective Organic Transformations; Thyagarajan, B. S.,
 Ed.; Wiley (Interscience): New York, 1970; Vol. 1, pg. 301-325.
- 55. Schroeder, M. Chem. Rev. 1980, 80, 187-213.
- (a) Carlsen, H. J.; Katsuki, T.; Martin, V. S.; Sharpless, K. B. J. Org. Chem. 1981, 46, 3936-3938. (b) Lee, D. G.; van der Engh, M. in Oxidation in Organic Chemistry; Trahanovsky, W. S., Ed.; Academic Press: New York, 1978; Part B, Chapter 4. (c) Courtney, J. L.; Swansborough, K. F. Rev. Pure Appl. Chem. 1972, 22, 47-54.
- 57. (a) Fatiadi, A. J. Synthesis 1976, 65-167. (b) Pizey, J. S. in Synthetic Reagents; Wiley: New York, 1974; Vol. 2, pg. 143-174.
- Sharpless, K. B.; Teranishi, A. Y.; Backvall, J. E. J. Am. Chem.
 Soc. 1977, 99, 3120-3128, and references therein.

- (a) Jensen, H. P.; Sharpless, K. B. J. Org. Chem. 1975, 40, 264-265.
 (b) Arigoni, D.; Vasella, A.; Sharpless, K. B.; Jensen, H. P. J. Am. Chem. Soc. 1973, 95, 7917-7919. (c) Sharpless, K. B.; Lauer, R. F. J. Am. Chem. Soc. 1972, 94, 7154-7155.
- 60. Chung, S. K. Tetrahedron Lett. 1978, 3211-3214.
- (a) Muller, J.; Holzinger, W. Angew. Chem. Int. Ed. 1975, 14, 760-761.
 (b) Mowat, W.; Wilkinson, G. J. Organometal. Chem. 1972, 38, C35-C36.
- 62. Schrock, R. R. Accts. Chem. Res. 1979, 12, 98-104.
- 63. Mowat, W.; Shortland, A.; Yagupsky, G.; Hill, N. J.; Yagupsky, M.; Wilkinson, G. J. Chem. Soc., Dalton Trans. 1972, 533-542.
- 64. (a) Mertis, K.; Williamson, D. H.; Wilkinson, G. J. Chem. Soc.,
 Dalton Trans. 1975, 607-611. (b) Galyer, L.; Mertis, K.; Wilkinson,
 G. J. Organometal. Chem. 1975, 85, C37-C38.
- 65. Nugent, W. A. J. Org. Chem. 1980, 45, 4533-4534.
- (a) Groves, J. T. in Metal Ion Activation of Dioxygen; Spiro, T. G.,
 Ed.; Wiley-Interscience: New York, 1980; pg. 125-162. (b) Chang, C.
 K.; Dolphin, D. in Bioorganic Chemistry; van Talen, E., Ed.;
 Academic Press: New York, 1978; Vol.4, pg. 37-80.
- (a) Ullrich, V. J. Mol. Cat. 1980, 7, 159-177. (b) Groves, J. T.;
 Nemo, T. E.; Myers, R. S. J. Am. Chem. Soc. 1979, 101, 1032-1033.
- 68. Nordblom, G. D.; White, R. E.; Coon, M. J. Arch. Biochem. Biophys. 1976, 175, 524-533.
- (a) Garrison, J. M.; Ostovic, D.; Bruice, T. C. J. Am. Chem. Soc.
 1989, 111, 4960-4966. (b) Groves, J. T.; Krupper, W. J., Jr. J. Am.
 Chem. Soc. 1979, 101, 7613-7615.

- (a) Traylor, T. G.; Miksztal, A. R. J. Am. Chem. Soc. 1989, 111, 7443-7448.
 (b) Sheldon, R. A. J. Mol. Cat. 1983, 20, 1-26.
 (c) Groves, J. T.; Krupper, W. J., Jr.; Haushalter, R. C. J. Am. Chem. Soc. 1980, 102, 6375-6377.
 (d) Willner, J. W.; Otvos, J. W.; Calvin, M. J. Chem. Soc.; Chem. Commun. 1980, 964-965.
 (e) Hill, C. L.; Schardt, B. C. J. Am. Chem. Soc. 1980, 102, 6374-6375.
- (a) Labeque, R.; Marnett, L. J. J. Am. Chem. Soc. 1989, 111, 6621-6627.
 (b) Groves, J. T.; Viski, P. J. Am. Chem. Soc. 1989, 111, 8537-8538.
- 72. (a) Weber, W. P.; Gokel, G. W. Phase Transfer Catalysis in Organic Synthesis; Springer-Verlag: Berlin and New York, 1977. (b) Starks,
 C. M.; Liotta, C. Phase Transfer Catalysis: Principles and Techniques; Academic Press: New York, 1978.
- (a) Santaniello, E.; Manzocchi, A.; Farachi, C. Synthesis 1980, 563-565.
 (b) Schmidt, H. J.; Schaefer, H. J. Angew. Chem. Int. Ed. 1979, 18, 69-70.
 (c) Atherton, M. J.; Holloway, J. H. J. Chem. Soc., Chem. Commun. 1978, 254-255.
- 74. (a) Santaniello, E.; Ferraboschi, P. Synthesis 1980, 10, 75-81. (b) Pletcher, D.; Tait, S. J. D. Tetrahedron Lett. 1978, 1601-1602.
- 75. (a) Landini, D.; Montanari, F.; Rolla, F. Synthesis 1979, 134-136. (b) Cacchi, S.; LaTorre, F.; Misiti, D. Synthesis 1979, 356-359.

- (a) Toth, J. E.; Anson, F. C. J. Am. Chem. Soc. 1989, 111, 2444-2451.
 (b) Wong, K.; Anson, F. C. J. Electroanal. Chem. 1987, 237, 69-79. (c)
 Torii, S.; Inokuchi, T.; Sugiura, T. J. Org. Chem. 1986, 51, 155-161.
 (d) Che, C. M.; Wong, K.; Mak, T. C. W. J. Chem. Soc., Chem.
 Commun. 1985, 988-990. (e) McHalton, R. C.; Anson, F. C. Inorg.
 Chem. 1984, 23, 3935-3942. (f) Meyer, T. J. J. Electrochem. Soc. 1984, 131, 221C-228C.
- (a) Eberson, L.; Nyberg, K. Accts. Chem. Res. 1973, 6, 106-112. (b)
 Baizer, M. M. Organic Electrochemistry; Dekker: New York, 1973.
 (c) Fry, A. J. Synthetic Organic Electrochemistry; Harper: New York, 1973.
- 78. (a) Che, C. M.; Lai, T. F.; Wong, K. Y. Inorg. Chem. 1987, 26, 2289-2299. (b) Che, C. M.; Wong, K. Y.; Mak, T. C. W. J. Chem. Soc., Chem. Comm. 1985, 24, 1797-1800. (c) Che, C. M.; Wong, K. Y.; Poon, C. K. Inorg. Chem. 1985, 24, 1797-1800. (d) Dobson, J. C.; Takeuchik, K. J.; Pipes, D. W.; Geselowitz, D. A.; Meyer, T. J. Inorg. Chem. 1986, 25, 2357-2365. (e) Takeuchi, K. J.; Thompson, M. S.; Pipes, D. W.; Meyer, T. J. Inorg. Chem. 1984, 23, 1845-1851.
- Roecker, L.; Dobson, J. C.; Vining, W. J.; Meyer, T. J. Inorg. Chem.
 1987, 26, 779-781.
- 80. (a) Seok, W. K.; Meyer, T. J. J. Am. Chem. Soc. 1988, 110, 7358-7367.
 (b) Seok, W. K.; Dobson, J. C.; Meyer, T. J. Inorg. Chem. 1988, 27, 3-5.
- 81. Dobson, J. C.; Seok, W. K.; Meyer, T. J. Inorg. Chem. 1986, 25, 1514-1516.
- 82. Roecker, L.; Meyer, T. J. J. Am. Chem. Soc. 1986, 108, 4066-4073.

- 83. Gilbert, J. A.; Gersten, S. W.; Meyer, T. J. J. Am. Chem. Soc. 1982, 104, 6872-6873.
- 84. (a) Roecker, L.; Meyer, T. J. J. Am. Chem. Soc. 1987, 109, 746-754.
 (b) Thompson, M. S.; Meyer, T. J. J. Am. Chem. Soc. 1982, 104, 4106-4115.
- 85. Moyer, B. A.; Meyer, T. J. J. Am. Chem. Soc. 1978, 100, 3601-3603.
- 86. Thompson, M. S.; Meyer, T. J. J. Am. Chem. Soc. 1982, 104, 5070-5076.
- Moyer, B. A.; Thompson, M. S.; Meyer, T. J. J. Am. Chem. Soc.
 1980, 102, 2310-2312.
- 88. Phillips, F. C. Amer. Chem. J. 1894, 16, 255-277.
- 89. (a) Backwall, J. E.; Akermark, B.; Ljunggren, S. O. J. Am. Chem. Soc. 1979, 101, 2411-2416. (b) Stille, J. K.; Divakaruni, R. J. Organometal. Chem. 1979, 169, 239-248. (c) Henry, P. M. Adv. Organometal. Chem. 1975, 13, 363-452. (d) Henry, P. M. Accts. Chem. Res. 1973, 6, 16-24.
- 90. Henry, P. M. Adv. Chem. Series 1968, 70, 126-154.
- 91. Jira, R.; Freiesleben, W. Organometal. React. 1972, 3, 1-190.
- 92. (a) Hartley, F. R. J. Chem. Ed. 1973, 50, 263-267. (b) Hartley, F. R. Chem. Rev. 1969, 69, 799-844.
- 93. Monroe, B. M. in *Singlet Oxygen*; Frimer, A. A., Ed.; CRC: Boca Raton, FL, 1985; Vol. 1, pg. 178-224.
- 94. Rosenthal, I. in Singlet Oxygen; Frimer, A. A., Ed.; CRC: Boca Raton, FL, 1985; Vol. 1, pg. 13-38.
- 95. (a) Frimer, A. A.; Stephenson, L. M. in Singlet Oxygen; Frimer, A.
 A., Ed.; CRC: Boca Raton, FL, 1985; Vol. 2, pg. 68-87. (b) Hoffman,
 H. M. R. Angew. Chem. Ed. Eng. 1969, 8, 556-577.

- 96. (a) Jefford, C. W.; Rimbault, G. C. J. Am. Chem. Soc. 1972, 94, 2894-2895. (b) Rubottom, G. M.; Lopez Nieves, M. I. Tetrahedron Lett.
 1972, 2423-2425.
- 97. (a) Stephenson, L. M.; Grdina, M. J.; Organopoulos, M. Acc. Chem. Res. 1980, 13, 419-425. (b) Litt, F. A.; Nickon, A. Adv. Chem. Ser. 1968, 77, 118-132. (c) Ohloff, G. Pure Appl. Chem. 1975, 43, 481-502.
 (d) Gollnick, K. Adv. Photochem. 1968, 6, 1-122.
- 98. (a) Ashford, R. D.; Orgryzlo, E. A. J. Am. Chem. Soc. 1975, 97, 3604-3607. (b) Koch, E. Tetrahedron 1968, 24, 6295-6318.
- 99. Paquette, L. A.; Liotta, D. C.; Baker, A. D. Tetrahedron Lett. 1976, 2681-2684.
- 100. (a) Baumstark, A. L. in Singlet Oxygen; Frimer, A. A., Ed.; CRC: Boca Raton, FL, 1985; Vol. 1, pg. 1-35. (b) Schaap, A. P.; Zaklika, K. A. in Singlet Oxygen; Wasserman, H. H.; Murray, R. W., Eds.; Academic: New York, 1979; pg. 173-238.
- 101. Bartlett, P. D.; Landis, M. E. in Singlet Oxygen; Wasserman, H. H.; Murray, R. W., Eds.; Academic: New York, 1979; pg. 224-283.
- 102. (a) Adam. W. Adv. Heterocycl. Chem. 1977, 21, 436-481. (b) Horn, K.
 A.; Koo, J.; Schmidt, S. P.; Schuster, G. B. Mol. Photochem. 1978-9,
 9, 1-37.
- (a) Bloodworth, A. J.; Eggelte, H. J. in Singlet Oxygen; Frimer, A. A., Ed.; CRC: Boca Raton, FL, 1985; Vol. 2, pg. 93-188. (b) Saito, I.; Matsuura, T. in Singlet Oxygen; Wasserman, H. H.; Murray, R. W., Eds.; Academic: New York, 1979; Chap. 10. (c) Gollnick, K.; Schenck, G. O. in 1,4 Cycloaddition Reactions; Hamer, J.; Ed.; Academic Press: New York, 1967; Chap. 10.
- 104. Porter, G. B. J. Chem. Ed. 1983, 60, 785-790.

- 106. (a) Demas, J. N.; Harris, E. W.; McBride, R. P. J. Am. Chem. Soc.
 1977, 99, 3547-3551. (b) Demas, J. N.; Harris, E. W.; Flynn, C. M.,
 Jr.; Diemente, D. J. Am. Chem. Soc. 1975, 97, 3838-3839.
- Demas, J. N.; DeGraff, B. A. J. Macromol. Sci., Chem. 1988, A(25),
 1189-1214.

Particulation of the second

- (a) Kirk, A. D.; Namasivayam, C.; Riske, W.; Ristic-Petrovic, D.
 Inorg. Chem. 1989, 28, 972-974. (b) Pfeil, A. J. Am. Chem. Soc. 1971, 93, 5395-5398.
- 109. (a) Harriman, A.; Maiya, B. G.; Murai, T.; Hemmi, G.; Sessler, J.
 L.; Mallouk, T. E. J. Chem. Soc., Chem. Comm. 1989, 314-316. (b)
 Reddi, E.; Jori, G. Rev. of Chem. Int. 1988, 10, 241-268.
- (a) Shukla, S.; Kamath, S. S.; Srivastava, T.S. J. Photochem.
 Photobiol., A: Chem. 1988, 44, 143-152. (b) Peterson, J. R.; 1985, 89, 2486-2492.
- 111. Puthraya, K. H; Srivastava, T. S. Polyhedron 1985, 4, 1579-1584.
- 112. (a) Mulazzani, Q. G.; Ciano, M.; D'Angelantonio, M.; Venturi, M.;
 Rodgers, M. A. J. J. Am. Chem. Soc. 1988, 110, 2451-2457. (b) Miller,
 S. S.; Zahir, K.; Haim, A. Inorg. Chem 1985, 24, 3978-3980.
- 113. Moggi, L.; Juris, A.; Sandrini, D.; Manfrin, M. F. Rev. Chem. Int.1981, 4, 171-223.
- 114. (a) Balzani, V.; Sabbatini, N.; Scandola, F. Chem. Rev. 1986, 69, 319-337. (b) Balzani, V.; Bolletta, F.; Gandolfi, M. T.; Maestri, M. Top. Curr. Chem. 1978, 75, 1-64.

- 116. (a) Graetzel, M. Accts. Chem. Res. 1981, 14, 376-384. (b) Maverick,
 A. W.; Gray, H. B. Pure Appl. Chem. 1980, 52, 2339-2348. (c) Kirch,
 M.; Lehn, J. M.; Sauvage, J. P. Helvetica Chimica Acta 1979, 61,
 1345-1384. (d) Bolton, J. R. Science, 1978, 202, 705-711.
- 117. Roundhill, D. M.; Gray, H. B.; Che, C. M. Accts. Chem. Res. 1989, 22, 55-61.

Alking and a series of the last

- (a) Roundhill, D. M.; Shen, Z. P.; King, C.; Atherton, S. J. J. Phys. Chem. 1988, 92, 4088-4094. (b) Roundhill, D. M.; Atherton, S. J.; Shen, Z. P. J. Am. Chem. Soc. 1987, 109, 6076-6079. (c) Vlcek, A.; Gray, H. B. J. Am. Chem. Soc. 1987, 109, 286-287.
- 119. Roundhill, D. M. J. Am. Chem. Soc. 1985, 107, 4354-4356.
- 120. Harvey, P. D.; Gray, H. B. New. J. Chem. 1987, 11, 595-596.
- 121. Che, C. M.; Lee, W. M. J. Chem. Soc., Chem. Commun. 1986, 512-513.
- 122. (a) Pope, M. T. Heteropoly and Isopoly Oxometallates; Springer-Verlag: Berlin, 1983. (b) Day, V. W.; Klemperer, W. G. Science
 1985, 228, 533-545. (c) Tsigdinos, G. Top. Curr. Chem. 1978, 76, 1-64.
- 123. Papaconstantinou, E. Chem. Soc. Rev. 1989, 18, 1-31.
- 124. (a) Misono, M. Catal. Rev.-Sci. Eng. 1987, 29, 269-321. (b) Misono,
 M. Chem. Uses Molybdenum, Proc. Int. Conf., 4th, 1982, 289-295.
- 125. Mateev, K. I.; Kozhevnikov, I. V. Kinet. Katal. 1980, 21, 855-863, and references therein.
- 126. (a) Argitis, P.; Papaconstantinou, E. Inorg. Chem. 1986, 25, 4386-4389. (b) Ioannidis, A.; Papaconstantinou, E. Inorg. Chem. 1985, 24, 439-441, and references therein.

- (a) Akid, R.; Darwent, J. R. J. Chem. Soc., Dalton Trans. 1985,
 395-399. (b) Darwent, J. R. J. Chem. Soc., Chem. Commun. 1982,
 798-799.
- 128. Yamase, T.; Usami, T. J. Chem. Soc., Dalton Trans. 1988, 183-190.
- (a) Rennecke, R. F.; Hill, C. L. J. Am. Chem. Soc. 1988, 110, 5461-5470.
 (b) Rennecke, R. F.; Hill, C. L. N. J. Chem. 1987, 11, 763-767.
 (c) Rennecke, R. F.; Hill, C. L. J. Am. Chem. Soc. 1986, 108, 3528-3529.
- Fox, M. A.; Cardona, R.; Gaillard, E. J. Am. Chem. Soc. 1987, 109, 6347-6354.

- 131. Hill, C. L.: Bouchard, D. A. J. Am. Chem. Soc. 1985, 107, 5148-5157.
- 132. Hill, C. L.; Bouchard, D. A.; Kadkhodayan, M.; Williamson, M. M.; Schmidt, J. A.; Hilinski, E. F. J. Am. Chem. Soc. 1988, 110, 5471-5479.
- 133. (a) Maverick, A. W.; Najdzionek, J. S.; MacKenzie, D.; Nocera, D. G.; Gray, H. B. J. Am. Chem. Soc. 1983, 105, 1878-1882. (b)
 Maverick, A. W.; Gray, H. B. J. Am. Chem. Soc. 1981, 103, 1298-1290. (c) Newsham, M. D.; Nocera, D. G., to be published.
- 134. (a) Mussell, R. D.; Nocera, D. G. Polyhedron 1986, 5, 47-50. (b)
 Mussell, R. D.; Nocera, D. G. J. Am. Chem. Soc. 1988, 110, 2764-2772. (c) Nocera, D. G.; Gray, H. B. J. Am. Chem. Soc. 1984, 106, 824-825.
- 135. (a) Zietlow, T. C.; Schaefer, W. P.; Sadeghi, B.; Hua, N.; Gray, H. B. Inorg. Chem. 1986, 25, 2195-2198. (b) Zietlow, T. C.; Nocera, D. G.; Gray, H. B. Inorg. Chem. 1986, 25, 351-1353. (c) Zietlow, T. C.; Hopkins, M. D.; Gray, H. B. J. Sol. State Chem. 1985, 57, 112-119.

- 136. Hughbanks, T.; Hoffmann, R. J. Am. Chem. Soc. 1983, 105, 1150-1162.
- 137. Seifert, G.; Grossman, G.; Mueller, H. J. Mol. Struct. 1980, 64, 93-102.
- Newsham, M. D.; Cerreta, M. K.; Berglund, K. A.; Nocera, D. G.
 Material Res. Soc. Proc. 1988, 121, 133-136.
- 139. Dorman, W. C.; McCarley, R. E.; Inorg. Chem. 1974, 13, 491-493.
- 140. Sheldon, J. C. J. Chem. Soc. 1960, 1007-1014.
- 141. Sheldon, J. C. J. Chem. Soc. 1962, 410-415.
- 142. Mussell, R. D. Ph.D. Dissertation, Michigan State University, 1988.
- 143. King, R. D. Ph.D. Dissertation, Michigan State University, 1989.
- 144. Hogue, R. D. McCarley, R.E. Inorg. Chem. 1970, 9, 1354-1359.
- 145. Blossey, E. C.; Neckers, D. C.; Thayer, A. L.; Schaap, A. P. J. Am. Chem. Soc. 1973, 95, 5820-5822.
- 146. Summerbell, R. K.; Berger, D. R. J. Am. Chem. Soc. 1959, 81, 633-639.
- Bourne, E. J.; Stacey, M.; Tatlow, J. C.; Tedder, J. M. J. Chem. Soc.
 1949, 2976-2979.
- Webster, O. W.; Mahler, W.; Benson, R. E. J. Am. Chem. Soc. 1962, 84, 3678-3684.
- 149. Balzani, V.; Moggi, L.; Manfrin, M. F.; Bolletta, F. Coord. Chem. Rev. 1975, 15, 321-433.
- Newsham, M. D.; Gianellis, E. P.; Pinnavaia, T. J.; Nocera, D. G. J.
 Am. Chem. Soc. 1988, 110, 3885-3891.
- 151. Battino, R.; Clever, H. L.; Young, C. L. IUPAC Solubility Data

 Series, Volume 7, Oxygen and Ozone; Pergamon: New York, 1981;
 pg. xi-xviii.

- 152. de Mayo, P.; Shizuka, H. Creation and Detection of the Excited State Vol.4; Dekker: New York, 1976; pg. 140-206.
- 153. Calvert, J. G.; Pitts, J. N. Jr. Photochemistry; Wiley: New York, 1966.
- Hatchard, C. G.; Parker, C. A. Proc. Roy. Soc. London, Ser. A 1956, 235, 518-536.
- 155. Rabek, J. F. Experimental Methods in Photochemistry and Photophysics, Part 2; Wiley: New York, 1982; pg. 937-961.
- Packowski, J.; Neckers, D.C. ACS Symposium Ser. 1985, 278, 222-242.
- 157. (a) Bard, A. J.; Falkner, L. R. Electrochemical Methods; John Wiley: New York, 1980; pg. 701. (b) Ibid, Chapter 11. (c) Ibid, Chapter 8.
- Schapp, A. P.; Thayer, A. L.; Blossey, E. C.; Neckers, D. C. J. Am.
 Chem. Soc. 1975, 97, 3741-3745.
- 159 Bland, J. J. Chem. Ed. 1976, 53, 274-279.
- 160. Foote, C. S. Free Radicals in Biology 1976, 2, 85-133.
- (a) Spikes, J. D.; Straight, R. C. ACS Symp. Ser. 1987, 339, 98-108.
 (b) Straight, R. D.; Spikes, R.D. in Singlet Oxygen; Frimer, A. Ed.;
 CRC: Boca Raton, FL, 1985; Vol. IV, pg. 91-143. (c) Krinsky, N.I. in Singlet Oxygen; Wasserman, H. H., Murray, R. W., Eds.;
 Academic: New York, 1979; pg. 597-641.
- 162. Valenzo, D. P.; Trudgen, J.; Hutzenbahler, A.; Milne, M. Photochem. Photobiol. 1987, 46, 985-990.

- 163. (a) Allen, R. C. in The Role of Oxygen in Chemistry and
 Biochemistry; Ando, W.; Moro-Oka, Y., Eds.; Elsevier: New York,
 1988; pg. 425-434. (b) Sonoda, M.; Krishna, C. M.; Riesz, P.
 Photochem. Photobiol. 1987, 45, 625-631.
- 164. Bennett, L. E.; Ghiggino, K. P.; Henderson, R. W. J. Photochem.

 Photobiol. B: Biology 1989, 3, 81-89.
- 165. (a) Firey, P. A.; Ford, W. E.; Sounik, J. R.; Kenney, M. E.; Rodgers, M. A. J. J. Am. Chem. Soc. 1988, 110, 7626-7630. (b) Gorman, A. A.; Hamblett, I.; Rodgers, M. A. J. Photochem. Photobiol. 1987, 45, 215-221.
- 166. Gottfried, V.; Peled, D.; Winkelman, J. W.; Kimel, S. Photochem. Photobiol. 1988, 48, 157-163.
- 167. Valduga, G.; Nonell, S.; Reddi, E.; Jori, G.; Braslavsky, S. E. *Photochem. Photobiol.* 1988, 48, 1-5.
- (a) Podoll, R. T.; Jaber, H. M.; Mill, T. Environ. Sci. Technol. 1986,
 20, 490-492. (b) Haag, W. R.; Hoigne, J. Environ. Sci. Technol. 1986,
 20, 341-348. (c) Haag, W.; Hoigne, J. in Water Chlorination:
 Chem., Environ. Impact, Health Eff., Proceeding 5th Conf. 1984,
 Lewis, R.L. Ed.; Jolley: Lansing, MI, 1985; pg. 1011-1020.
- (a) Dunlin, D.; Drossman, H.; Mill, T. Environ. Sci. Technol. 1986,
 20, 72-77. (b) Karasek, F. W.; Hutzinger, O. Anal. Chem. 1986, 58,
 633A-642A.
- 170. Draper, W. Chemosphere 1985, 14, 1195-1203.
- 171. (a) Savino, A.; Angeli, G. Water Research 1984, 18, 1465-1469. (b)Acher, A. J.; Rosenthal, I. Water Research 1977, 11, 557-562.
- 172. Sakurai, H., Heitz, J. R. Environ. Entomol. 1982, 11, 467-470.
- 173. Acher, A. J.; Elgavish, A. Water Research 1980, 14, 539-543.

- 174. Czuczwa, J. M.; Hites, R. A. Environ. Sci. Technol. 1986, 20, 195-200.
- 175. Fieser, L. S. The Chemistry of Natural Products Related to Phenanthrene; Reinhold: New York, 1936.
- (a) Allen, N. S. Chem. Soc. Rev. 1986, 15, 373-404. (b) Rabek, J. F. in Singlet Oxygen; Frimer, A. Ed.; CRC: Boca Raton, FL, 1985; Vol. IV, pg. 1-90. (c) Kaplan, M. L.; Trozzolo, A. M. in Singlet Oxygen; Wasserman, H. H., Murray, R. W., Eds.; Academic: New York, 1979; pg. 575-595. (d) Ranby, B.; Rabek, J. F.; Eds. in Singlet Oxygen-Reactions with Organic Compounds and Polymers; Wiley: New York, 1978; Chap. 21-30.
- (a) Forsskahl, K.; Olkkonen, C.; Tylli, H. J. Photochem. Photobiol.
 A: Chemistry 1988, 43, 337-344. (b) Tylli, H.; Forsskahl, I.;
 Olkkonen, C. J. Photochem. Photobiol. A: Chemistry, 1988, 43, 345-356. (c) Brunow, G.; Forsskahl, I.; Gronlund, A. C.; Lundstrom, G.; Nyberg, K. in Singlet Oxygen-Reactions with Organic Compounds and Polymers; Ranby, B.; Rabeck, J. F., Eds., Wiley: New York, 1978; pg. 311-315.
- 178. Korobov, V. E., Chibisov, A. K. Russ. Chem. Rev. 1983, 52, 43-71.
- 179. Foote, C. S. ACS Symp. Ser. 1987, 339, 22-38.
- (a) Gollnick, K.; Schenk, G. O. Pure Appl. Chem 1964, 9, 507-525.
 (b) Kearns, D. R. Chem. Rev. 1971, 71, 395-427. (c) Foote, C. S. Acc. Chem. Res. 1968, 1, 104-110.
- 181. Foote, C. S. Tetrahedron 1985, 41, 2221-2227.
- 182. (a) Mattes, S. L.; Farid, S. Science 1984, 226, 917-921. (b) Mattes, S.
 L.; Farid, S. J. Am. Chem. Soc. 1982, 104, 1454-1456.

- 183. Gollnick, K.; Schnatterer, A. Photochem. Photobiol. 1986, 43, 365-378.
- 184. Shim, S. C.; Lee, H. J. J. Photochem. Photobiol. A: Chemistry 1989, 46, 59-75.
- 185. Cao, Y.; Zhang, B. W.; Ming, Y. F.; Chen, J. X. J. Photochem. 1987, 38, 131-144.
- (a) Schaap, A. P.; Siddiqui, S.; Balakrishnan, P.; Lopez, L.;
 Gagnon, S. D. *Isr. J. Chem.* 1983, 23, 415-419. (b) Schaap, A. P.;
 Siddiqui, S.; Gagnon, S. D.; Lopez. L. *J. Am. Chem. Soc.* 1983, 105, 5149-5150.
- (a) Whitten, D. G. Acc. Chem. Res. 1980, 13, 83-90. (b) Cox, G. S.;
 Whitten, D. G.; Giannotti, C. Chem. Phys. Lett. 1979, 67, 511-515.
- 188. Navarro, J. A.; Roncel, M.; de La Rosa, F. F.; de La Rosa, M. A. J. Photochem. Photobiol. A: Chemistry 1987, 40, 279-293.
- 189. Kagan, J.; Bazin, M.; Santus, R. J. Photochem. Photobiol. B: Biology 1989, 3, 165-174.
- (a) Linden, S. M.; Neckers, D. C. Photochem. Photobiol. 1988, 47, 543-550.
 (b) Paczkowska, B.; Paczkowski, J.; Neckers, D. C. Macromolecules 1986, 19, 863-870.
 (c) Neckers, D. C.; Paczkowski, J. J. Am. Chem Soc. 1986, 108, 291-292.
 (d) Lamberts, J. J. M.; Neckers, D. C. Tetrahedron 1985, 41, 2183-2190.
 (e) Paczkowski, J.; Neckers, D. C. Macromolecules 1985, 18, 1245-1253; pg. 2412-2418.
- 191. Shukla, S.; Kamath, S. S.; Srivastava, T. S. J. Photochem. Photobiol. A: Chemistry 1988, 44, 143-152.
- 192. Scaiano, J. C.; MacEachern, A.; Arnason, J. T.; Morand, P; Weir, D., Photochem. Photobiol. 1987, 46, 193-199.

- 193. Blan, Q. A.; Grossweiner, L. I., *Photochem. Photobiol.* **1987**, *45*, 177-183.
- Kumar, C. V.; Davis, H. F.; Das, P. K. Chem. Phys.. Lett. 1984, 109, 184-189.
- 195. Danen, W. C.; Arudi, R. L. J. Am. Chem. Soc. 1978, 100, 3944-3945.
- (a) Roberts, J. L., Jr.; Sawyer, D. T. Isr. J. Chem. 1983, 23, 430-438, and references therein. (b) Nanni, E. J., Jr.; Birge, R. R.; Hubbard, L. M.; Morrison, M. M.; Sawyer, D. T. Inorg. Chem. 1981, 20, 737-741.
- 197. Mayeda, E. A.; Bard, A. J. J. Am. Chem. Soc. 1973, 95, 6223-6227.
- (a) Demas, J. N.; DeGraff, B. A. J. Macromol. Sci., Chem. 1988,
 A25, 1189-1214. (b) Bacon, J. R.; Demas, J. N. Anal. Chem. 1987, 59,
 2780-2785. (c) Buell, S. L.; Demas, J. N. J. Phys. Chem. 1983, 87,
 4675-4681. (d) Demas, J. N.; McBride, R. P.; Harris, E. W. J.
 Phys. Chem. 1976, 80, 2248-2253. (e) Demas, J. N.; Harris, E. W.;
 McBride, R. P. J. Am. Chem. Soc. 1977, 99, 3547-3551. (f) Demas, J.
 N.; Diemente, D.; Harris, E. W. J. Am. Chem. Soc. 1973, 95, 6864-6865.
- 199. Pettit, T. L.; Fox, M. A. J. Phys. Chem. 1986, 90, 1353-1354.
- 200. (a) Saito, Y.; Tanaka, H. K.; Sasaki, Y.; Azumi, T. J. Phys. Chem.
 1985, 89, 4413-4415. (b) Azumi, T.; Saito, Y. J. Phys. Chem. 1988, 92, 1715-1721.
- 201. Kavarnos, G. J.; Turro, N. J. Chem. Rev. 1986, 86, 401-449.
- Bock, C. R.; Connor, J. A.; Gutierrez, A. R.; Meyer, T. J.;
 Whitten, D. G.; Sullivan, B. P.; Nagle, J. K. J. Am. Chem. Soc.
 1979, 101, 4815-4824.
- 203. Adamson, A. W. J. Chem. Ed. 1983, 60, 797-802.

- 204. (a) Foote, C. S. in Singlet Oxygen; Wasserman, H. H., Murray, R.
 W., Eds.; Academic: New York, 1979; pg. 139-173. (b) Bellus, D. in
 Singlet Oxygen-Reactions with Organic Compounds and Polymers;
 Ranby, B., Rabeck, J. F., Eds.; Wiley: New York, 1978; pg. 60-110.
- 205. Ouannes, C.; Wilson, T. J. Am. Chem. Soc. 1968, 90, 6528-6529.
- 206. (a) Monroe, B. M. J. Phys. Chem. 1977, 81, 1861-1864. (b) Foote, C.
 S.; Peterson, E. R.; Lee, K.-W. J. Am. Chem. Soc. 1972, 94, 1032-1033.
- 207. Foote, C. S.; Wexler, S.; Ando, W. Tetrahedron Letters 1965, 4111-4118.
- 208. Araki, Y.; Dobrowolski, D. C.; Goyne, T. E.; Hanson, D. C.; Jiang,
 Z. Q.; Lee, K. J.; Foote, C. S. J. Am. Chem Soc. 1984, 106, 4570-4575.
- 209. Frimer, A. A. Chem. Rev. 1979, 79, 359-387.
- 210. Turro, N. J. Modern Molecular Photochemistry;Benjamin/Cummings: Menlo Park, CA; 1978; Chapter 14.
- Gollnick, K.; Kuhn, H. J. in Singlet Oxygen; Wasserman, H. H.,Murray, R. W., Eds; Academic: New York, 1979; Chapter 8.
- (a) Marcus, R. A. Int. J. Chem. Kinet. 1981, 13, 865-872. (b)
 Marcus, R. A.; Sutin, N. Biochim. Biophys. Acta 1985, 811, 265-322.
- 213. Balzani, V.; Bolletta, F.; Scandola, F. J. Am. Chem. Soc. 1980, 102, 2152-2163.
- (a) Agmon, N.; Levine, R. D. Isr. J. Chem. 1980, 19, 330-336. (b)
 Agmon, N. J. Chem. Soc., Faraday Trans. 2 1978, 74, 388-404. (c)
 Agmon, N.; Levine, R. D. Chem. Phys. Lett. 1977, 52, 197-201.
- 215. Hertzberg, G. Molecular Spectra and Molecular Structure. I.

 Spectra of Diatomic Molecules, 2nd ed; van Nostrand Reinhold:

 New York, 1950; pg. 560.

- Zietlow, T. C.; Schaefer, W. P.; Sadeghi, B.; Nocera, D. G.; Gray, H.
 B. Inorg. Chem. 1986, 25, 2198-2201.
- 217. Mussell, R. D.; Nocera, D. G., submitted for publication.
- 218. The lowest energy LMCT transitions of the cluster ions in their ground state formally involve the promotion of electrons from ligand-based orbitals to the a_{2g} LUMO. Because excitation promotes an electron from the e_g HOMO to the a_{2g} LUMO, the LMCT's of the hexanuclear clusters in their lowest-energy excited state will shift to the red owing to transitions corresponding to the promotion of electrons from ligand-based orbitals to the depopulated e_g level.
- 219. Eigen, M. Z. Phys. Chem. (Frankfurt am Main) 1954, 1, 176-250.
- 220. Dexter, D. L. J. Chem. Phys. 1953, 21, 836-850.
- Turro, N. J. Modern Molecular Photochemistry;Benjamin/Cummings: Menlo Park, CA; 1978; Chapter 9.
- 222. (a) Wagner, P. J.; Leventis, N. J. Am. Chem. Soc. 1987, 109, 2188-2190. (b) Scaiano, J. C.; Leigh, W. J.; Meador, M. A.; Wagner, P. J. J. Am. Chem. Soc. 1985, 107, 5806-5807.
- Balzani, V.; Indelli, M. T.; Maestri, M.; Sandrini, D.; Scandola, F.J. Phys. Chem. 1980, 84, 852-855 and references therein.
- (a) Endicott, J. F. Acc. Chem. Res. 1988, 21, 59-66. (b) Endicott, J.;
 Tamilarasan, R.; Brubaker, G. R. J. Am. Chem. Soc. 1986, 108,
 5193-5201. (c) Endicott, J. F.; Ramasami, T.; Gaswick, D. C.;
 Tamilarasan, R.; Heeg, M. J.; Brubaker, G. R.; Pyke, S. C. J. Am.
 Chem. Soc. 1983, 105, 5301-5310. (d) Endicott, J. F.; Heeg, M. J.;
 Gaswick, C.; Pyke, S. C. J. Phys. Chem. 1981, 85, 1777-1779.

- 225. Timpson, C. J.; Carter, C. C.; Olmsted, J., III J. Phys. Chem. 1989, 93, 4116-4120.
- 226. Neckers, D. C. Chemtech 1978, 8, 108-116.
- 227. Merrifield, R. B. Science 1965, 150, 178-185.
- Letsinger, R. L.; Kornet, M. J.; Mahederon, V.; Jetina, D. M. J.
 Am. Chem. Soc. 1964, 86, 5163-5165.
- 229. Kamat, P. V.; Foxe, M. A. J. Phys. Chem. 1984, 88, 2297-2302.
- 230. Turro, N. J.; Chow, M.-F.; Blaustein, M. J. Phys. Chem. 1981, 85, 3014-3018.
- (a) Krishna, C. M.; Lion, Y.; Riesz, P. Photochem. Photobiol. 1987,
 45, 1-6. (b) Midden, W. R.; Wang, S. Y. J. Am. Chem. Soc. 1983,
 105, 4129-4135.
- (a) Valenzeno. D. P. ACS Symp. Ser. 1987, 339, 39-57. (b)
 Valenzeno, D. P. Photochem. Photobiol. 1987, 46, 147-160.
- 233. Encinas, M. V.; Lemp, E.; Lissi, E. A. J. *Photochem. Photobiol.*, B: Biology 1989, 3, 113-122.
- 234. (a) Hoebeke, E.; Gandin, E.; Decuyper, J.; Van de Vorst, A. J. Photochem. 1986, 35, 245-250. (c) Rodgers, M. A. J.; Lee, P. C. J. Phys. Chem. 1984, 88, 3480-3484.
- 235. Kee, P. C.; Rodgers, M. A. J. J. Phys. Chem. 1984, 88, 4385-4389.
- 236. DeWilde, W.; Peeters, G.; Lunsford, J. H. J. Phys. Chem. 1980, 84, 2306-2310.
- 237. Carmicheal, W. M.; Edwards, D. A. J. *Inorg. Nucl. Chem.* **1967**, 29, 1535-1538.
- 238. Hamer, A. D.; Smith, T. J.; Walton, R. A. Inorg. Chem. 1976, 15, 1014-1017.
- 239. Nannelli, P.; Block, B. P. Inorg. Chem. 1968, 7, 2423-2426.

- 240. King, R. D.; Mussell, R. D.; Nocera, D. G. to be published.
- (a) Winnick, M. A. ACS Symp. Series 1987, 358, 8-17. (b)
 Winnick, M. A., Ed. in Photophysical and Photochemical Tools in Polymer Science; D. Reidel: Dordrecht, Netherlands, 1987; pg. 611-627. (c) Guillet, J. E. in Photophysical and Photochemical Tools in Polymer Science; Winnick, M. A., Ed.; D. Reidel: Dordrecht, Netherlands, 1987; pg. 467-494.
- 242. Saito, T.; Nishida, M.; Yamagata, T.; Yamata, Y.; Yamaguchi, Y. *Inorg. Chem.* 1986, 25, 1111-1117.
- 243. Muller, G. in *Polyelectrolytes;* Selegny, E., Ed.; D. Reidel: Dordrecht, Netherlands; 1974; pg. 195-205.
- 244. Sheldon, J. C. Nature 1959, 84, 1210-1213.
- 245. Agnew, N. H. J. Polym. Sci., Polym. Chem. Ed. 1976, 14, 2819-2830.
- 246. (a) Parker, V. D.; Sundholm, G.; Ronlan, A.; Svanholm, U.; Hammerich, O. in Encyclopedia of Electrochemistry of the Elements; Bard, A. J.; Lund, H., Eds.; Marcel Dekker, Inc.: New York, 1978; Vol. XI, pg. 182-328. (b) Mayeda, E. A.; Miller, L. L.; Wolfe, J. F. J. Am. Chem. Soc. 1972, 94, 6812-6816. (c) Brown, O. R.; Chandra, S.; Harrison, J. A. Electroanal. Chem. and Interfac. Electrochem. 1972, 38, 185-190.
- 247. von Sonntag, C.; Schuhmann, H. P. Adv. Photochem. 1977, 10, 59-145.
- 248. Wong, K. Y.; Che, C. M.; Anson, F. C. *Inorg. Chem.* 1987, 26, 737-741.
- Anson, F. C.; Collins, T. J.; Gipson, S. C.; Krafft, T. E. Inorg.Chem. 1987, 26, 731-736.

- 250. (a) Ingold, K. E. in Free Radicals; Kochi, J. C. Ed.; Wiley-Interscience: New York, 1973; 37-156. (b) Koenig, T.; Fischer, H. in Free Radicals; Kochi, J. C. Ed.; Wiley-Interscience: New York, 1973; 170-180.
- 251. (a) Ci, X.; da Silva, R. S.; Nicodem, D.; Whitten, D. G. J. Am. Chem. Soc. 1989, 111, 1337-1343. (b) Jones, G., III; Haney, W. A.; Phan, X. T. J. Am. Chem. Soc. 1988, 110, 1922-1929.
- 252. Miyashi, T.; Kamata, M.; Mukai, T. J. Am. Chem. Soc. 1987, 109, 2780-2788.
- 253. (a) Fox, M. A. Adv. Photochem. 1986, 13, 237-337. (b) Tazuke, S.;
 Kitamura, N.; Kawaniski, Y. J. Photochem. 1985, 29,123-138.
- 254. Lindner, K.; Haller, E.; Helwig, H. A. Anorg. Chem. 1923, 130, 209-228.

MICHIGAN STATE UNIV. LIBRARIES
31293005856053